Electronic Supplementary Information

Substitution-pattern- and counteranion-dependent ion-pairing assemblies of heteroporphyrin-based π-electronic cations

Masaki Fujita, Yohei Haketa, Shu Seki and Hiromitsu Maeda*

Department of Applied Chemistry, College of Life Sciences, Ritsumeikan University, Kusatsu 525–8577, Japan, Fax: +81 77 561 2659; Tel: +81 77 561 5969; E-mail: maedahir@ph.ritsumei.ac.jp and Department of Molecular Engineering, Graduate School of Engineering, Kyoto University, Kyoto 615–8510, Japan

Table of Contents

1. Synthetic procedures and spectroscopic data

General procedures. Starting materials were purchased from FUJIFILM Wako Pure Chemical Industries Ltd., Nacalai Tesque Inc., Tokyo Chemical Industry Co., Ltd., and Sigma-Aldrich Co., and were used without further purification unless otherwise stated. 5,10,15,20-Tetraphenyl-21-thiaporphyrin **1**,[S1] Pd^{II} complex **1pd**$^+$ as a Cl^- ion pair (**1pd**$^+$-Cl^-),[S2] and 10,15-bis(pentafluorophenyl)-5,20-diphenyl-21-thiaporphyrin **2**[S3] were prepared according to the literature procedures. NMR spectra used in the characterization of products were recorded on a JEOL ECA-600 600 MHz spectrometer. All NMR spectra were referenced to solvent. UV-visible absorption spectra were recorded on a Hitachi U-3500 spectrometer. High-resolution (HR) electrospray ionization mass spectrometry (ESI-MS) was recorded on a BRUKER microTOF using ESI-TOF method. TLC analyses were carried out on aluminum sheets coated with silica gel 60 (Merck 5554). Column chromatography was performed on Sumitomo alumina KCG-1525 and Wakogel C-300.

Pd^{II} complex of 5,10,15,20-tetraphenyl-21-thiaporphyrin as a BF_4^- ion pair, 1pd$^+$-BF_4^-. To a MeOH solution (20 mL) of **1pd**$^+$-Cl^-[S2] (13.7 mg, 17.7 μmol) was added $AgBF_4$ (3.44 mg, 17.7 μmol), and the reaction mixture was stirred at r.t. for 30 min, followed by filtration and evaporation to dryness. The residue was purified by silica gel column chromatography (Wakogel C-300; eluent: 5% MeOH/CH_2Cl_2) and was recrystallized from CH_2Cl_2/*n*-hexane to afford **1pd**$^+$-BF_4^- (9.20 mg, 11.2 μmol, 63%) as a green solid. R_f = 0.46 (10% MeOH/CH_2Cl_2). ^{1}H NMR (600 MHz, $CDCl_3$, –60 °C, not fully detected): δ (ppm) 9.83 (s, 2H, β-CH), 9.12 (d, J = 7.2 Hz, 2H, Ph-H), 9.05–9.02 (m, 4H, β-CH), 8.82 (s, 2H, β-CH), 8.21 (d, J = 7.2 Hz, 2H, Ph-H), 8.17 (d, J = 6.6 Hz, 2H, Ph-H), 8.11 (t, J = 7.2 Hz, 2H, Ph-H), 7.93–7.88 (m, 4H, Ph-H), 7.86–7.81 (m, 6H, Ph-H), 7.64 (d, J = 7.2 Hz, 2H, Ph-H). ^{13}C{^{1}H} NMR (151 MHz, $CDCl_3$, –60 °C): δ (ppm) 212.56, 152.03, 145.30, 143.53, 141.46, 139.46, 139.36, 139.07, 137.27, 136.45, 134.71, 134.69, 134.62, 134.28, 134.02, 131.42, 130.50, 129.32, 129.16, 129.07, 127.41. ^{19}F NMR (564 MHz, $CDCl_3$, 20 °C): δ (ppm) –157.45 (s, $^{10}BF_4^-$), –157.50 (s, $^{11}BF_4^-$). UV/vis (CH_2Cl_2, λ_{max}[nm] (ε, 10^5 $M^{-1}cm^{-1}$)): 418 (0.49), 470 (0.71), 558 (0.074), 630 (0.067). HRMS (ESI-TOF): *m/z*: calcd for $C_{44}H_{28}N_3PdS$ ([M – BF_4]$^+$): 736.1033; found 736.1033. Calcd for BF_4 ([M – $C_{44}H_{28}N_3PdS$]$^-$): 87.0035; found 87.0035. This compound was further characterized by single-crystal X-ray analysis.

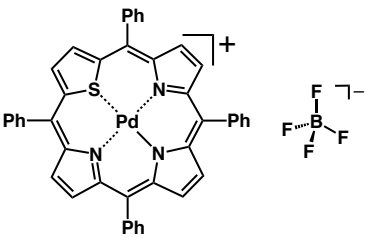

Pd^{II} complex of 5,10,15,20-tetraphenyl-21-thiaporphyrin as a PF_6^- ion pair, 1pd$^+$-PF_6^-. To a MeOH solution (20 mL) of **1pd**$^+$-Cl^-[S2] (12.4 mg, 16.0 μmol) was added $AgPF_6$ (4.22 mg, 16.7 μmol) and the reaction mixture was stirred at r.t. for 30 min, followed by filtration and evaporation to dryness. The residue was purified by silica gel column chromatography (Wakogel C-300; eluent: 5% MeOH/CH_2Cl_2) and was recrystallized from CH_2Cl_2/*n*-hexane to afford **1pd**$^+$-PF_6^- (9.17 mg, 10.4 μmol, 65%) as a green solid. R_f = 0.57 (10% MeOH/CH_2Cl_2). ^{1}H NMR (600 MHz, $CDCl_3$, –60 °C): δ (ppm) 9.82 (s, 2H, β-CH), 9.12 (d, J = 7.2 Hz, 2H, Ph-H), 9.04–9.02 (m, 4H, β-CH), 8.82 (s, 2H, β-CH), 8.21 (d, J = 6.6 Hz, 2H, Ph-H), 8.17 (d, J = 6.6 Hz, 2H, Ph-H), 8.11 (t, J = 7.5 Hz, 2H, Ph-H), 7.93–7.88 (m, 4H, Ph-H), 7.86–7.80 (m, 6H, Ph-H), 7.63 (d, J = 7.2 Hz, 2H, Ph-H). ^{13}C{^{1}H} NMR (151 MHz, $CDCl_3$, –60 °C): δ (ppm) 152.07, 145.32, 143.54, 141.51, 139.49, 139.37, 139.11, 137.29, 137.28, 136.45, 134.74, 134.69, 134.65, 134.31, 134.30, 134.02, 131.40, 130.51, 129.33, 129.21, 129.06, 127.42. ^{19}F NMR (564 MHz, $CDCl_3$, 20 °C): δ (ppm) –77.31 (d, J = 712 Hz, 6F). UV/vis (CH_2Cl_2, λ_{max}[nm] (ε, 10^5 $M^{-1}cm^{-1}$)): 417 (0.54), 470 (0.77), 560 (0.081), 632 (0.073). HRMS (ESI-TOF): *m/z*: calcd for $C_{44}H_{28}N_3PdS$ ([M – F_6P]$^+$): 736.1033; found 736.1033. Calcd for F_6P ([M – $C_{44}H_{28}N_3PdS$]$^-$): 144.9647; found 144.9650. This compound was further characterized by single-crystal X-ray analysis.

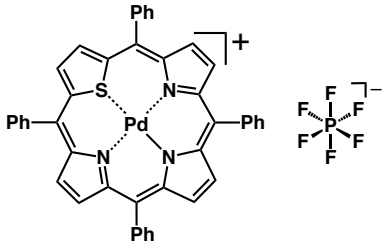

Pd^{II} complex of 5,10,15,20-tetraphenyl-21-thiaporphyrin as a $B(C_6F_5)_4^-$ ion pair, 1pd$^+$-$B(C_6F_5)_4^-$. To a MeOH solution (20 mL) of **1pd**$^+$-Cl^-[S2] (10.0 mg, 12.9 μmol) was added Li^+ salt of tetrakis(pentafluorophenyl)borate ($LiB(C_6F_5)_4$) (9.70 mg, 14.1 μmol), and the reaction mixture was stirred at r.t. for 20 min, followed by filtration and evaporation to dryness. The residue was purified by silica gel column chromatography (Wakogel C-300; eluent: 5% MeOH/CH_2Cl_2) and was recrystallized from acetone/*n*-hexane to afford **1pd**$^+$-$B(C_6F_5)_4^-$ (15.3 mg, 10.8 μmol, 84%) as a green solid. R_f = 0.77 (10% MeOH/CH_2Cl_2). ^{1}H NMR (600 MHz, $CDCl_3$, –60 °C): δ (ppm) 9.76 (s, 2H, β-CH), 9.05 (s, 4H, β-CH), 9.02 (d, J = 7.2 Hz, 2H, Ph-H), 8.83 (s, 2H, β-CH), 8.20 (d, J = 6.6 Hz, 2H, Ph-H), 8.15 (d, J = 6.0 Hz, 2H, Ph-H), 8.07 (t, J = 7.2 Hz, 2H, Ph-H), 7.93–7.88 (m, 4H, Ph-H), 7.84–7.81 (m, 6H, Ph-H), 7.62 (d, J = 6.6 Hz, 2H, Ph-H). ^{13}C{^{1}H} NMR (151 MHz, $CDCl_3$, –60 °C): δ (ppm) 212.50, 152.07, 147.60

(dm, $J_{13C–19F}$ = 240 Hz), 145.42, 143.66, 141.22, 139.42, 139.01, 138.96, 137.66 (dm, $J_{13C–19F}$ = 246Hz), 137.20, 135.84 (dm, $J_{13C–19F}$ = 260 Hz), 136.00, 134.73, 134.65, 134.60, 134.25, 134.09, 133.91, 131.67, 130.58, 129.38, 129.13, 129.07, 127.43, 123.24. ^{19}F NMR (564 MHz, $CDCl_3$, 20 °C): δ (ppm) –135.84 (s, 8F, Ar-F), –166.47 (t, J = 20.3 Hz, 4F, Ar-F), –170.09 (m, 8F, Ar-F). UV/vis (CH_2Cl_2, λ_{max}[nm] (ε, 10^5 $M^{-1}cm^{-1}$)): 418 (0.56), 470 (0.80), 559 (0.086), 631 (0.077). HRMS (ESI-TOF): *m/z*: calcd for $C_{44}H_{28}N_3PdS$ ([M – $C_{24}BF_{20}$]$^+$): 736.1033; found 736.1034. Calcd for $C_{24}BF_{20}$ ([M – $C_{44}H_{28}N_3PdS$]$^-$): 678.9779; found 678.9777.

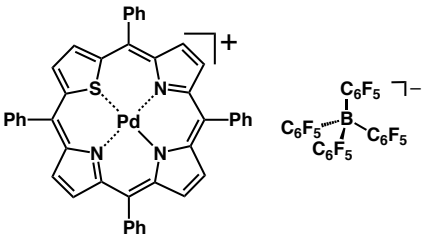

Pd^{II} complex of 5,10,15,20-tetraphenyl-21-thiaporphyrin as a PCCp$^-$ ion pair, 1pd$^+$-PCCp$^-$. To a MeOH solution (20 mL) of **1pd**$^+$-Cl$^-$[S2] (10.3 mg, 13.3 μmol) was added sodium pentacyanocyclopentadienide (NaPCCp)[S4] (2.90 mg, 13.6 μmol), and the reaction mixture was stirred at r.t. for 1 h, followed by filtration and evaporation to dryness. The residue was purified by silica gel column chromatography (Wakogel C-300; eluent: 5% MeOH/CH_2Cl_2) and was recrystallized from CH_2Cl_2/*n*-hexane to afford **1pd**$^+$-PCCp$^-$ (8.78 mg, 9.47 μmol, 71%) as a green solid. R_f = 0.53 (10% MeOH/CH_2Cl_2). ^{1}H NMR (600 MHz, $CDCl_3$, 20 °C): δ (ppm) 9.82 (s, 2H, β-CH), 9.06 (d, J = 4.8 Hz, 2H, β-CH), 9.05 (d, J = 5.4 Hz, 2H, β-CH), 8.89 (s, 2H, β-CH), 8.45 (br, Ph-H), 8.32 (d, J = 6.0 Hz, Ph-H), 7.96–7.82 (m, Ph-H) (The integrals of Ph-H were not consistent with the actual number due to broadening). ^{13}C{^{1}H} NMR (151 MHz, $CDCl_3$, 20 °C, not fully detected): δ (ppm) 152.45, 145.96, 144.11, 140.77, 140.03, 139.52, 139.47, 136.73, 135.75, 135.01, 134.60, 134.36, 131.99, 129.40, 129.02, 127.42, 111.18, 99.59. UV/vis (CH_2Cl_2, λ_{max}[nm] (ε, 10^5 $M^{-1}cm^{-1}$)): 417 (0.54), 470 (0.78), 559 (0.080), 630 (0.072). HRMS (ESI-TOF): *m/z*: calcd for $C_{44}H_{28}N_3PdS$ ([M – $C_{10}N_5$]$^+$): 736.1033; found 736.1033. Calcd for $C_{10}N_5$ ([M – $C_{44}H_{28}N_3PdS$]$^-$): 190.0159; found 190.0161. This compound was further characterized by single-crystal X-ray analysis.

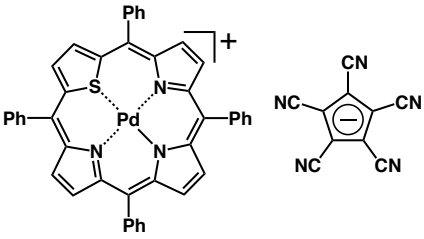

Pd^{II} complex of 10,15-bis(pentafluorophenyl)-5,20-diphenyl-21-thiaporphyrin as a Cl$^-$ ion pair, 2pd$^+$-Cl$^-$. To a $CHCl_3$/MeOH solution (40 mL/60 mL) of **2**[S3] (42.0 mg, 51.7 μmol) was added $PdCl_2$ (51.3 mg, 0.266 μmol). The reaction mixture was heated to reflux and was stirred under air for 10 h, followed by filtration and evaporation to dryness. The residue was purified by silica gel column chromatography (Wakogel C-300; eluent: CH_2Cl_2 to 10% MeOH/CH_2Cl_2) and was recrystallized from CH_2Cl_2/*n*-hexane to afford **2pd**$^+$-Cl$^-$ (44.8 mg, 47.0 μmol, 91%) as a green solid. R_f = 0.45 (10% MeOH/CH_2Cl_2). ^{1}H NMR (600 MHz, $CDCl_3$, –60 °C): δ (ppm) 10.16 (s, 2H, β-CH), 9.58 (d, J = 5.4 Hz, 2H, Ph-H), 9.21 (d, J = 4.2 Hz, 2H, β-CH), 8.98 (d, J = 4.2 Hz, 2H, β-CH), 8.92 (s, 2H, β-CH), 8.12 (t, J = 6.9 Hz, 2H, Ph-H), 7.84 (t, J = 7.2 Hz, 2H, Ph-H), 7.76 (t, J = 6.9 Hz, 2H, Ph-H), 7.62 (d, J = 6.6 Hz, 2H, Ph-H). ^{13}C{^{1}H} NMR (151 MHz, $CDCl_3$, –60 °C): δ (ppm) 212.44, 209.01, 152.05, 146.08 (dm, $J_{13C–19F}$ = 208 Hz), 145.85, 145.52, 142.54 (dm, $J_{13C–19F}$ = 259 Hz), 142.61, 142.26, 139.18, 137.49 (dm, $J_{13C–19F}$ = 253 Hz), 137.64, 137.23, 136.35, 136.22, 133.68, 133.05, 130.63, 129.70, 128.63, 121.40, 112.63, 110.05. ^{19}F NMR (564 MHz, $CDCl_3$, –60 °C): δ (ppm) –138.92 (s, 8F, Ar-F), –152.26 (s, 4F, Ar-F), –163.09 (s, 8F, Ar-F). UV/vis (CH_2Cl_2, λ_{max}[nm] (ε, 10^5 $M^{-1}cm^{-1}$)): 413 (0.43), 469 (0.78), 552 (0.089), 624 (0.055), 667 (0.050). HRMS (ESI-TOF): *m/z*: calcd for $C_{44}H_{18}F_{10}N_3PdS$ ([M – Cl]$^+$): 916.0091; found 916.0088.

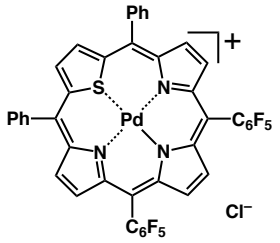

Pd^{II} complex of 10,15-bis(pentafluorophenyl)-5,20-diphenyl-21-thiaporphyrin as a BF_4^- ion pair, 2pd$^+$-BF_4^-. A CH_2Cl_2/MeOH solution (10 mL/20 mL) of **2pd**$^+$-Cl$^-$ (15.1 mg, 15.8 μmol) and $AgBF_4$ (3.70 mg, 19.0 μmol) was stirred at r.t. for 30 min, followed by filtration and evaporation to dryness. The residue was purified by silica gel column chromatography (Wakogel C-300; eluent: 10% MeOH/CH_2Cl_2) and was recrystallized from CH_2Cl_2/*n*-hexane to afford **2pd**$^+$-BF_4^- (9.42 mg, 9.38 μmol, 59%) as a green solid. R_f = 0.46 (10% MeOH/CH_2Cl_2). ^{1}H NMR (600 MHz, $CDCl_3$, 20 °C): δ (ppm) 9.95 (s, 2H, β-CH), 9.23–9.00 (m, 8H, β-CH and Ph-H), 8.12 (s, 2H, Ph-H), 7.95 (t, J = 6.9 Hz, 2H, Ph-H), 7.86 (t, J = 6.6 Hz, 2H, Ph-H), 7.71 (s, 2H, Ph-H). ^{13}C{^{1}H} NMR (151 MHz, $CDCl_3$, –60 °C): δ (ppm) 179.70, 152.20, 146.04 (dm, $J_{13C–19F}$ = 227 Hz), 145.82, 145.52, 145.29, 142.74 (dm, $J_{13C–19F}$ = 250 Hz), 143.02, 142.99, 139.18, 137.60 (dm, $J_{13C–19F}$ = 260 Hz) 137.98, 137.37, 136.30, 134.18, 133.57, 131.06, 129.81, 129.18, 113.48 (m), 110.56 (the signals of C_6F_5 units are overlapped). ^{19}F NMR (564 MHz, $CDCl_3$, 20 °C): δ (ppm) –138.37 (br, Ar-F (**2pd**$^+$)), –151.71 (t, J = 20.6 Hz, Ar-F (**2pd**$^+$)), –157.00 (s, $^{10}BF_4^-$), –157.06 (s, $^{11}BF_4^-$), –162.80 (t, J = –18.3 Hz, Ar-F (**2pd**$^+$)). UV/vis (CH_2Cl_2, λ_{max}[nm] (ε, 10^5 $M^{-1}cm^{-1}$)): 412 (0.45), 468 (0.75), 551 (0.087), 627 (0.058), 665 (0.050). HRMS (ESI-TOF):

m/z: calcd for $C_{44}H_{18}F_{10}N_3PdS$ ([M – BF_4]$^+$): 916.0091; found 916.0091. Calcd for BF_4 ([M – $C_{44}H_{18}F_{10}N_3PdS$]$^-$): 87.0035; found 87.0035.

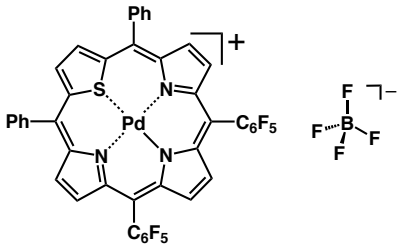

Pd^{II} complex of 10,15-bis(pentafluorophenyl)-5,20-diphenyl-21-thiaporphyrin as a PF_6^- ion pair, 2pd$^+$-PF_6^-. A CH_2Cl_2/MeOH solution (10 mL/20 mL) of **2pd**$^+$-Cl^- (16.1 mg, 16.9 μmol) and $AgPF_6$ (4.50 mg, 17.8 μmol) was stirred at r.t. for 30 min, followed by filtration and evaporation to dryness. The residue was purified by silica gel column chromatography (Wakogel C-300; eluent: 5% MeOH/CH_2Cl_2) and was recrystallized from CH_2Cl_2/*n*-hexane to afford **2pd**$^+$-PF_6^- (10.8 mg, 10.1 μmol, 60%) as a green solid. R_f = 0.54 (10% MeOH/CH_2Cl_2). ^{1}H NMR (600 MHz, $CDCl_3$, 20 °C): δ (ppm) 9.92 (s, 2H, β-CH), 9.24 (s, 2H, β-CH), 9.18 (d, J = 6.0 Hz, 2H, Ph-H), 9.06 (s, 2H, β-CH), 9.01 (s, 2H, β-CH), 8.11–8.09 (m, 2H, Ph-H), 7.93 (t, J = 6.9 Hz, 2H, Ph-H), 7.84 (t, J = 6.9 Hz, 2H, Ph-H), 7.68 (d, J = 6.0 Hz, 2H, Ph-H). ^{13}C{^{1}H} NMR (151 MHz, $CDCl_3$, –60 °C): δ (ppm) 152.04, 145.91 (dm, $J_{13C–19F}$ = 273 Hz), 146.76, 145.88, 145.86, 144.37 (dm, $J_{13C–19F}$ = 240 Hz), 144.86, 143.18, 141.91, 140.92, 139.13, 138.49 (dm, $J_{13C–19F}$ = 258 Hz), 136.93 (dm, $J_{13C–19F}$ = 240 Hz), 137.21, 136.78, 135.20, 134.25 (m), 133.70, 130.94, 129.45, 129.11, 113.25 (m), 110.74 (the signals of C_6F_5 units are overlapped). ^{19}F NMR (564 MHz, $CDCl_3$, 20 °C): δ (ppm) –76.98 (d, J = 716 Hz, 6F, PF_6^-), –139.36 (brs, 4F, Ar-F (**2pd**$^+$)), –151.68 (t, J = 19.5 Hz, 2F, Ar-F (**2pd**$^+$)) –162.78 (s, 4F, Ar-F (**2pd**$^+$)). UV/vis (CH_2Cl_2, λ_{max}[nm] (ε, 10^5 $M^{-1}cm^{-1}$)): 412 (0.46), 468 (0.76), 550 (0.093), 626 (0.064), 663 (0.060). HRMS (ESI-TOF): *m/z*: calcd for $C_{44}H_{18}F_{10}N_3PdS$ ([M – F_6P]$^+$): 916.0091; found 916.0091. Calcd for F_6P ([M – $C_{44}H_{18}F_{10}N_3PdS$]$^-$): 144.9647; found 144.9647. This compound was further characterized by single-crystal X-ray analysis.

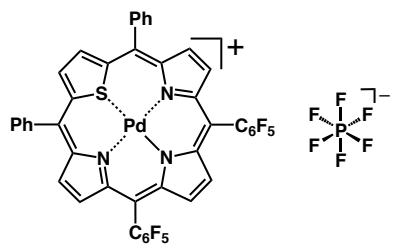

Pd^{II} complex of 10,15-bis(pentafluorophenyl)-5,20-diphenyl-21-thiaporphyrin as a $B(C_6F_5)_4^-$ ion pair, 2pd$^+$-$B(C_6F_5)_4^-$. A CH_2Cl_2/MeOH solution (10 mL/20 mL) of **2pd**$^+$-Cl^- (20.4 mg, 21.4 μmol) and $LiB(C_6F_5)_4$ (15.3 mg, 22.3 μmol) was stirred at r.t. for 1 h, followed by filtration and evaporation to dryness. The residue was purified by silica gel column chromatography (Wakogel C-300; eluent: 10% MeOH/CH_2Cl_2) and was recrystallized from acetone/*n*-hexane to afford **2pd**$^+$-$B(C_6F_5)_4^-$ (16.4 mg, 10.3 μmol, 48%) as a green solid. R_f = 0.74 (10% MeOH/CH_2Cl_2). ^{1}H NMR (600 MHz, $CDCl_3$, –60 °C): δ (ppm) 9.87 (s, 2H, β-CH), 9.24 (d, J = 4.8 Hz, 2H, β-CH), 9.06–9.04 (m, 4H, β-CH and Ph-H), 8.96 (s, 2H, β-CH), 8.09 (t, J = 6.9 Hz, 2H, Ph-H), 7.96 (t, J = 7.5 Hz, 2H, Ph-H), 7.84 (t, J = 7.5 Hz, 2H, Ph-H), 7.65 (d, J = 7.2 Hz, 2H, Ph-H). ^{13}C{^{1}H} NMR (151 MHz, $CDCl_3$, 20 °C): δ (ppm) 152.48, 148.02 (dm, $J_{13C–19F}$ = 247 Hz), 146.48, 145.54 (m), 143.293 (dm, $J_{13C–19F}$ = 260 Hz), 143.75, 140.33, 139.12, 138.83 (m), 137.29, 136.41 (dm, $J_{13C–19F}$ = 236 Hz), 136.09 (dm, $J_{13C–19F}$ = 236 Hz), 136.51, 134.47, 133.70, 131.36, 129.37, 123.68, 113.54 (m), 111.66 (the signals of C_6F_5 units are overlapped). ^{19}F NMR (564 MHz, $CDCl_3$, 20 °C): δ (ppm) –135.91 (s, 8F, $B(C_6F_5)_4^-$), –139.46 (s, 4F, Ar-F (**2pd**$^+$)), –151.11 (t, J = 20.6 Hz, 2F, Ar-F (**2pd**$^+$)), –162.47 (s, 4H, Ar-F (**2pd**$^+$)), –166.39 (t, J = 20.6 Hz, 4F, $B(C_6F_5)_4^-$), –170.10 (s, 8F, $B(C_6F_5)_4^-$). UV/vis (CH_2Cl_2, λ_{max}[nm] (ε, 10^5 $M^{-1}cm^{-1}$)): 412 (0.49), 468 (0.82), 549 (0.095), 625 (0.063), 660 (0.054). HRMS (ESI-TOF): *m/z*: calcd for $C_{44}H_{18}F_{10}N_3PdS$ ([M – $C_{24}BF_{20}$]$^+$): 916.0091; found 916.0091. Calcd for $C_{24}BF_{20}$ ([M – $C_{44}H_{18}F_{10}N_3PdS$]$^-$): 678.9779; found 678.9778.

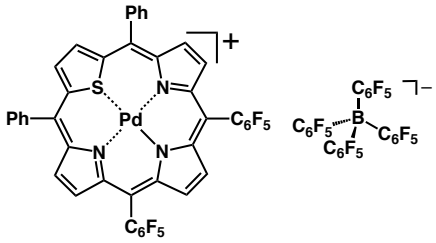

Pd^{II} complex of 10,15-bis(pentafluorophenyl)-5,20-diphenyl-21-thiaporphyrin as a $PCCp^-$ ion pair, 2pd$^+$-$PCCp^-$. A CH_2Cl_2/MeOH solution (10 mL/20 mL) of **2pd**$^+$-Cl^- (13.4 mg, 14.1 μmol) and NaPCCp[S4] (3.21 mg, 15.1 μmol) was stirred at r.t. for 30 min, followed by filtration and evaporation to dryness. The residue was purified by silica gel column chromatography (Wakogel C-300; eluent: 10% MeOH/CH_2Cl_2) and was recrystallized from CH_2Cl_2/*n*-hexane to afford **2pd**$^+$-$PCCp^-$ (11.1 mg, 10.0 μmol, 71%) as a green solid. R_f = 0.64 (10% MeOH/CH_2Cl_2). ^{1}H NMR (600 MHz, $CDCl_3$, 20 °C): δ (ppm) 9.94 (s, 2H, β-CH), 9.23 (d, J = 5.4 Hz, 2H, β-CH), 9.07 (d, J = 5.4 Hz, 2H, β-CH), 9.00 (s, 2H, β-CH), 8.47 (br, Ph-H), 8.01–7.97 (m, Ph-H) (The integrals of Ph-H were not consistent with the actual number due to broadening). ^{13}C{^{1}H} NMR (151 MHz, $CDCl_3$, 20 °C): δ (ppm) 152.62, 146.36 (dm, $J_{13C–19F}$ = 247 Hz), 146.56, 143.91, 143.59, 141.12, 139.48, 137.94 (dm, $J_{13C–19F}$ = 265 Hz), 137.21, 136.38, 136.25 (m), 134.61, 134.03, 131.16, 129.29, 113.70, 111.63, 111.24, 99.92 (the signals of C_6F_5 units are overlapped). UV/vis (CH_2Cl_2, λ_{max}[nm] (ε, 10^5 $M^{-1}cm^{-1}$)): 414 (0.47), 468 (0.79), 550 (0.092), 624 (0.061), 664 (0.052). ^{19}F NMR (564 MHz, $CDCl_3$, 20 °C): δ (ppm) –137.48 (s, Ar-F (**2pd**$^+$)), –151.56 (s, 4F, Ar-F (**2pd**$^+$)), –162.72 (s, 8F, Ar-F (**2pd**$^+$)). HRMS (ESI-TOF): *m/z*: calcd for $C_{44}H_{18}F_{10}N_3PdS$ ([M –

$C_{10}N_5]^+$): 916.0091; found 916.0094. Calcd for $C_{10}N_5$ ($[M - C_{44}H_{18}F_{10}N_3PdS]^-$): 190.0159; found 190.0159.

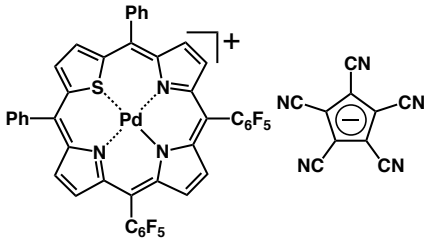

[S1] L. Latos-Grażyński, J. Lisowski, M. M. Olmstead and A. L. Balch, *Inorg. Chem.*, 1989, **28**, 1183–1188.

[S2] L. Latos-Grażyński, J. Lisowski, J. P. Chmielewski, M. Grzeszczuk, M. M. Olmstead and A. L. Balch, *Inorg. Chem.*, 1994, **33**, 192–197.

[S3] H. Mori, J.-M. Lim, D. Kim and A. Osuka, *Angew. Chem. Int. Ed.*, 2013, **52**, 12997–13001.

[S4] (a) O. W. Webster, *J. Am. Chem. Soc.*, 1965, **87**, 1820–1821; (b) T. Sakai, S. Seo, J. Matsuoka and Y. Mori, *J. Org. Chem.*, 2013, **78**, 10978–10985.

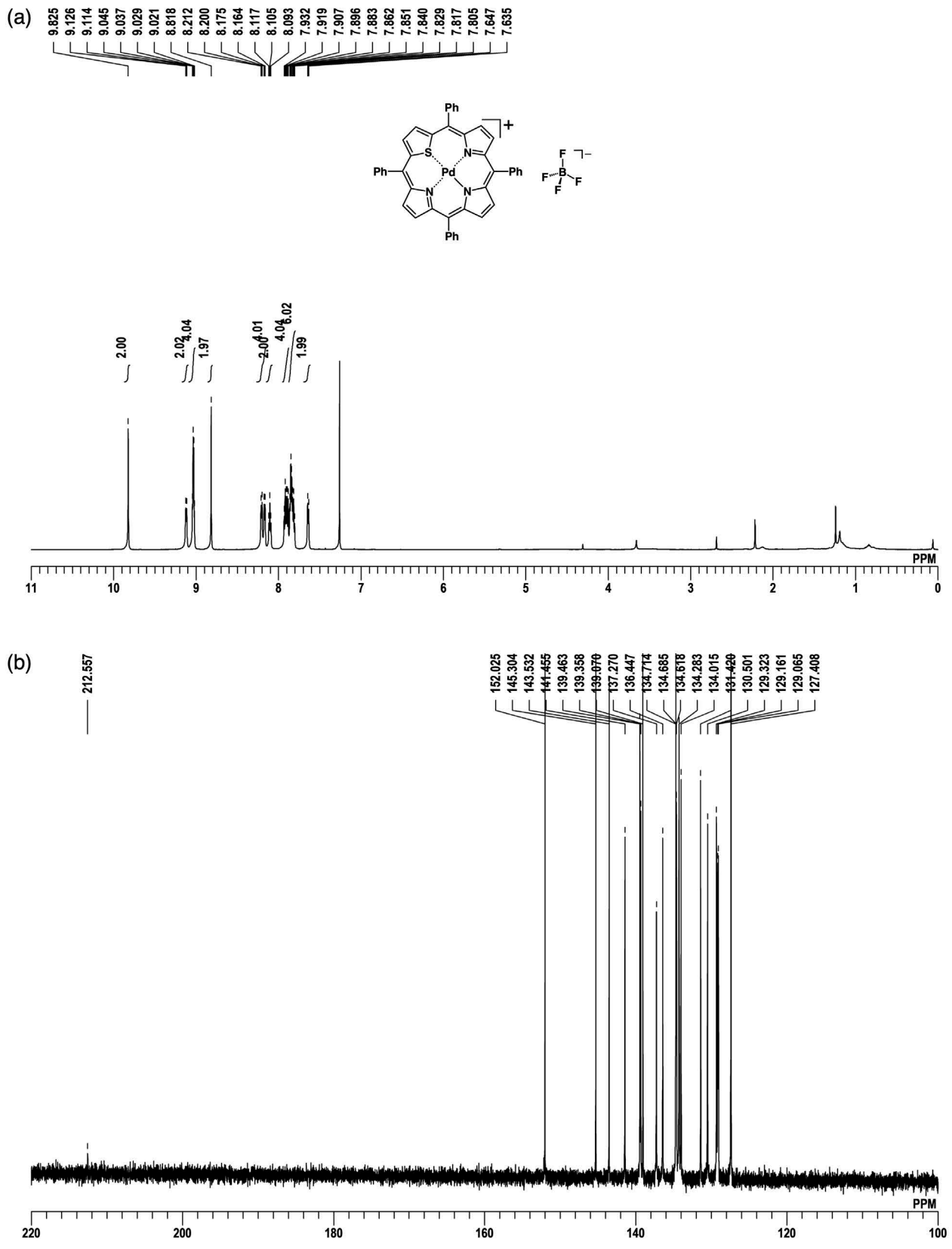

Fig. S1 (a) ^{1}H NMR, (b) ^{13}C NMR, and (c) ^{19}F NMR spectra of **1pd**$^{+}$-BF_4^- in $CDCl_3$ at –60, –60, and 20 °C, respectively.

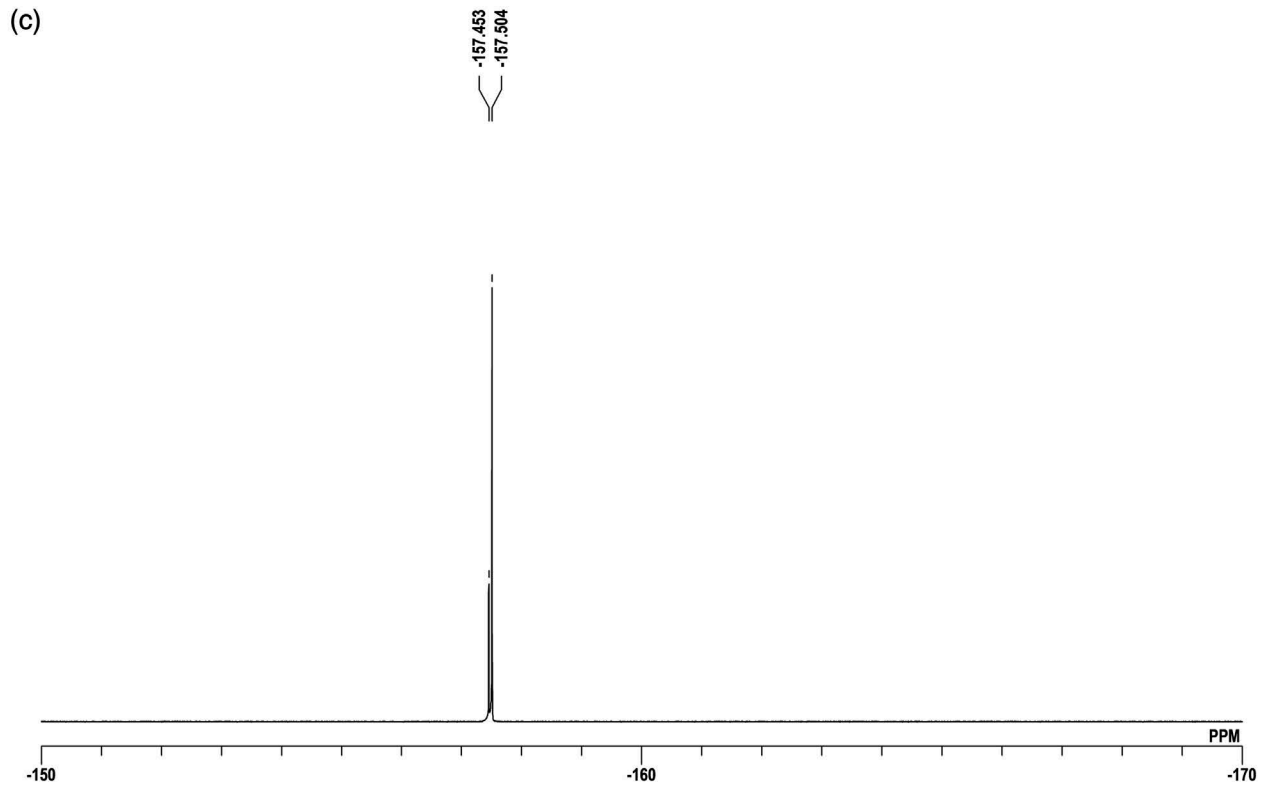

Fig. S1 (Continued)

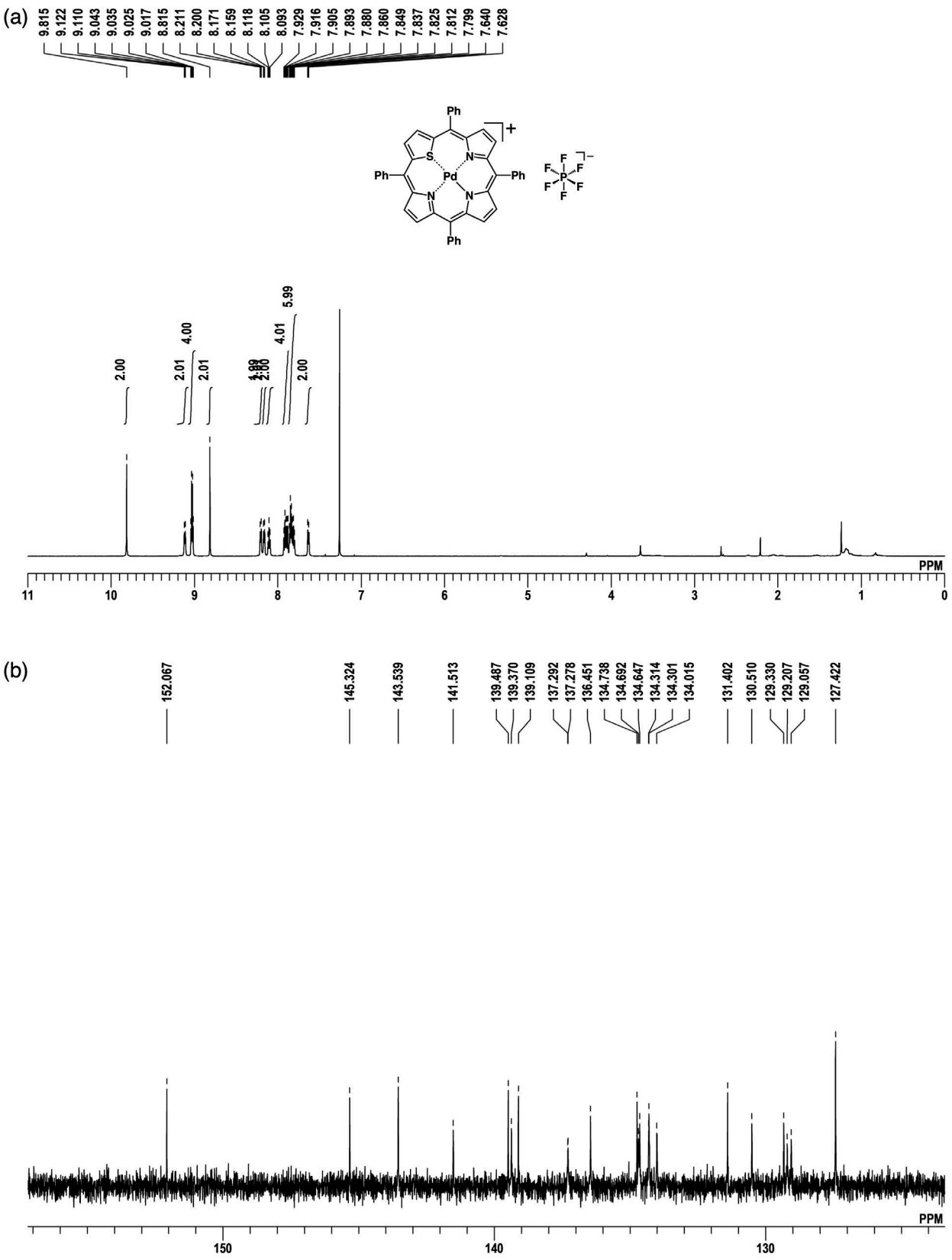

Fig. S2 (a) ^{1}H NMR, (b) ^{13}C NMR, and (c) ^{19}F NMR spectra of **1pd**$^{+}$-PF_6^- in $CDCl_3$ at –60, –60, and 20 °C, respectively.

(c)

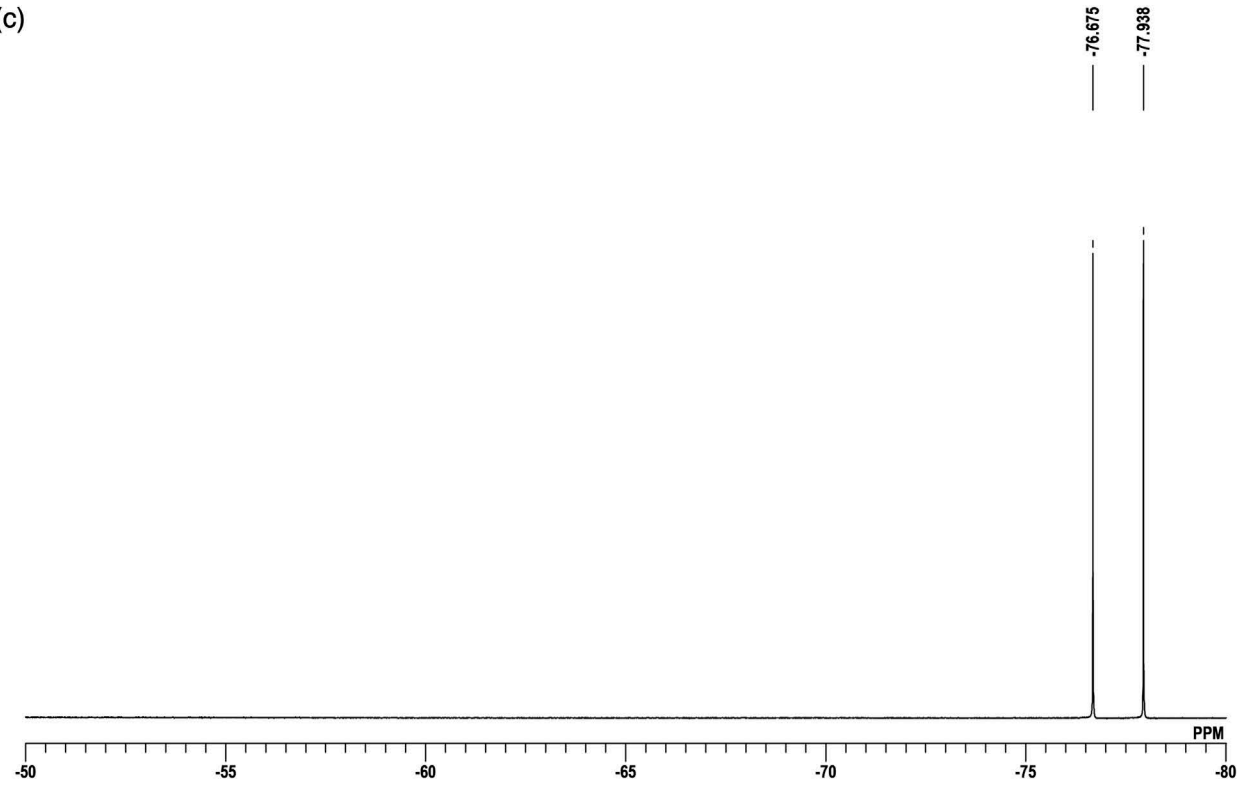

Fig. S2 (Continued)

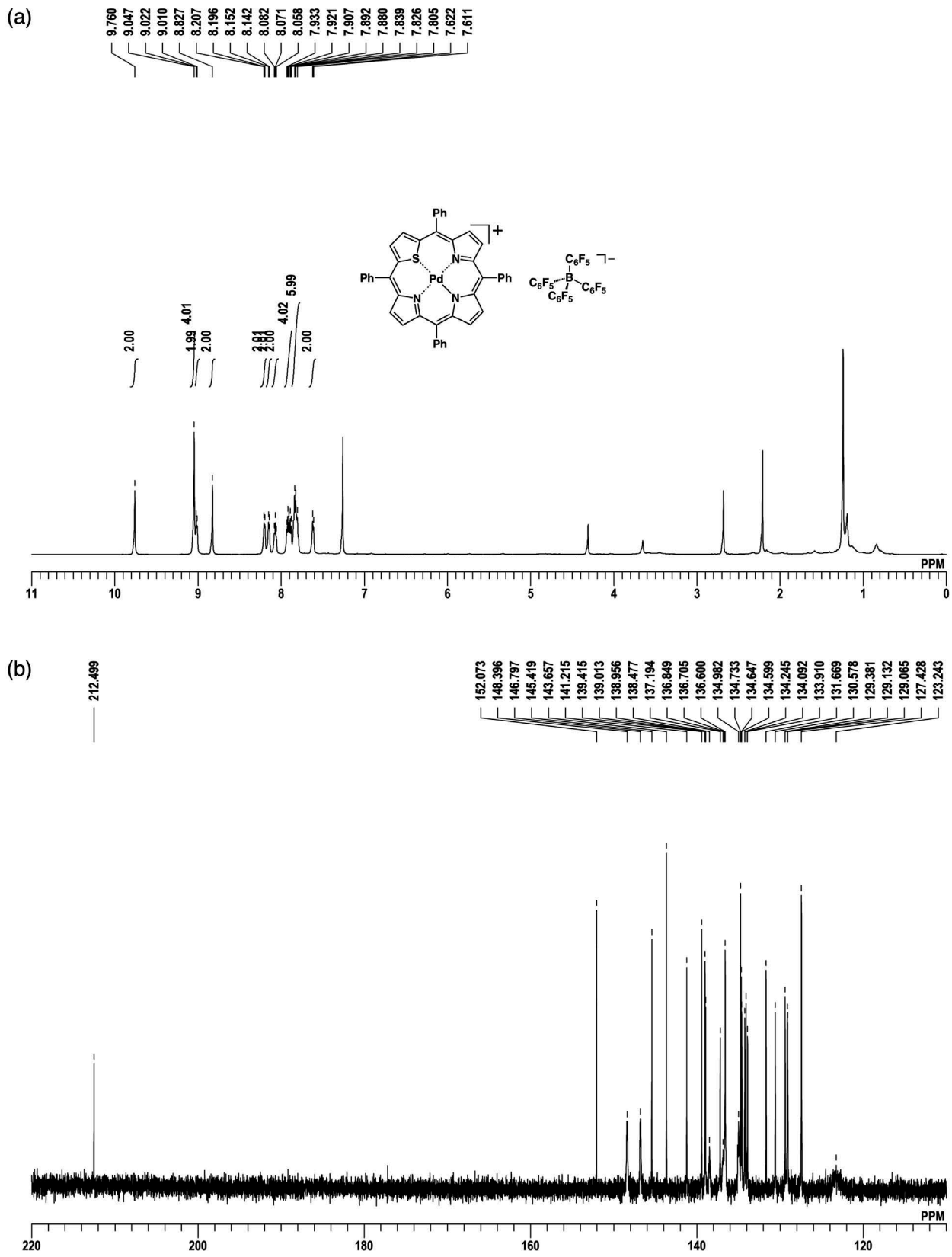

Fig. S3 (a) ^{1}H NMR, (b) ^{13}C NMR, and (c) ^{19}F NMR spectra of **1pd**$^{+}$-B(C_6F_5)$_4^{-}$ in $CDCl_3$ at –60, –60, and 20 °C, respectively.

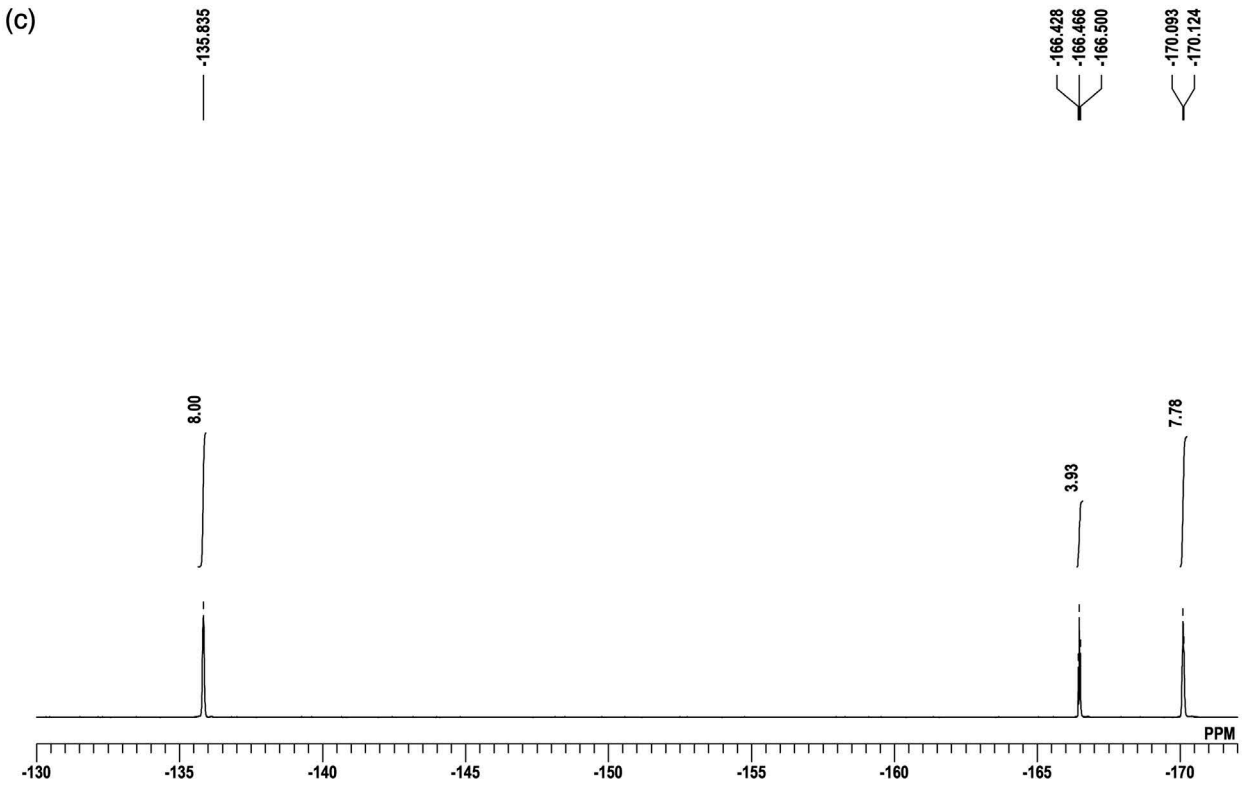

Fig. S3 (Continued)

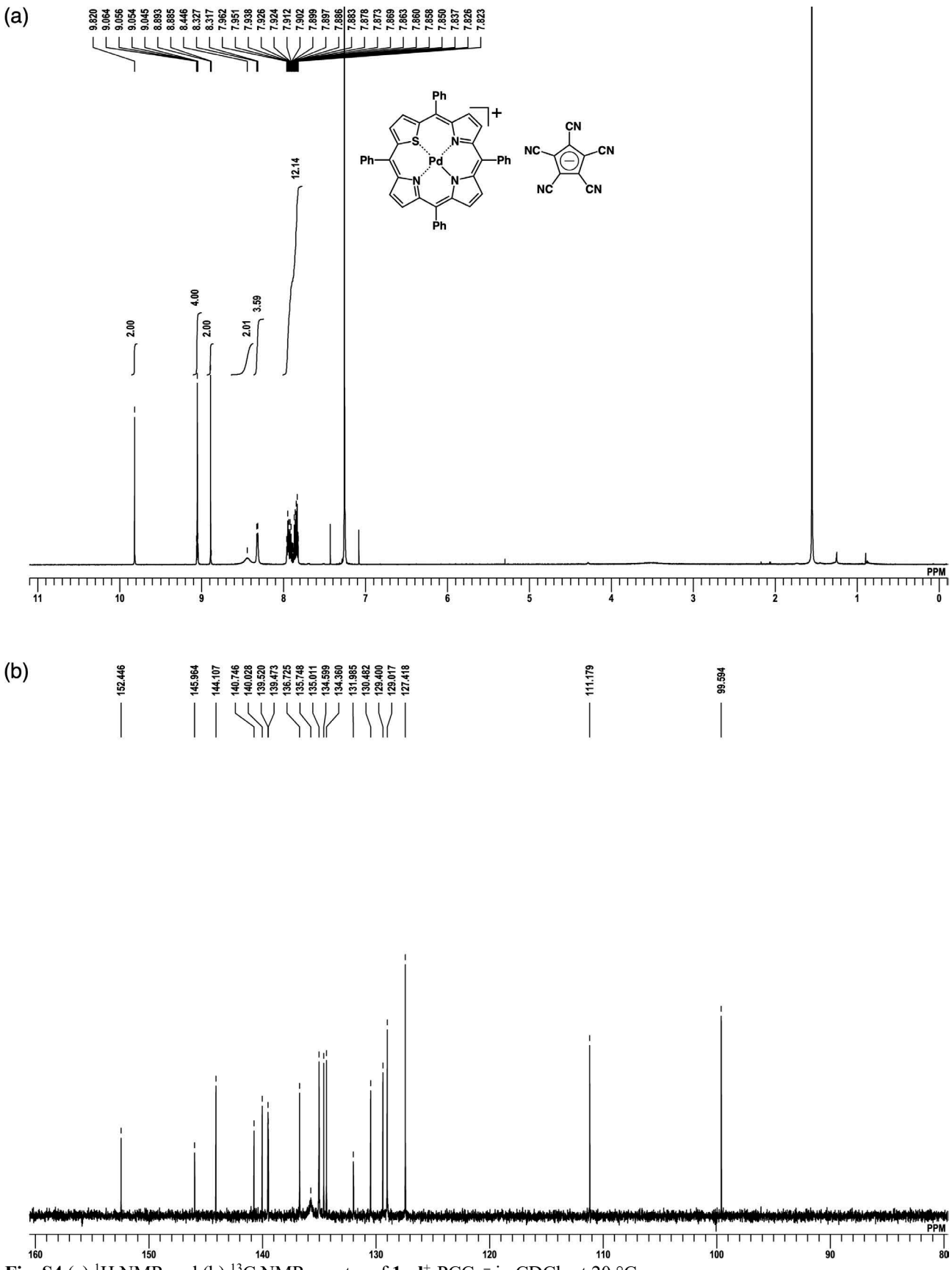

Fig. S4 (a) ^{1}H NMR and (b) ^{13}C NMR spectra of **1pd**$^{+}$-PCCp^{-} in $CDCl_3$ at 20 °C.

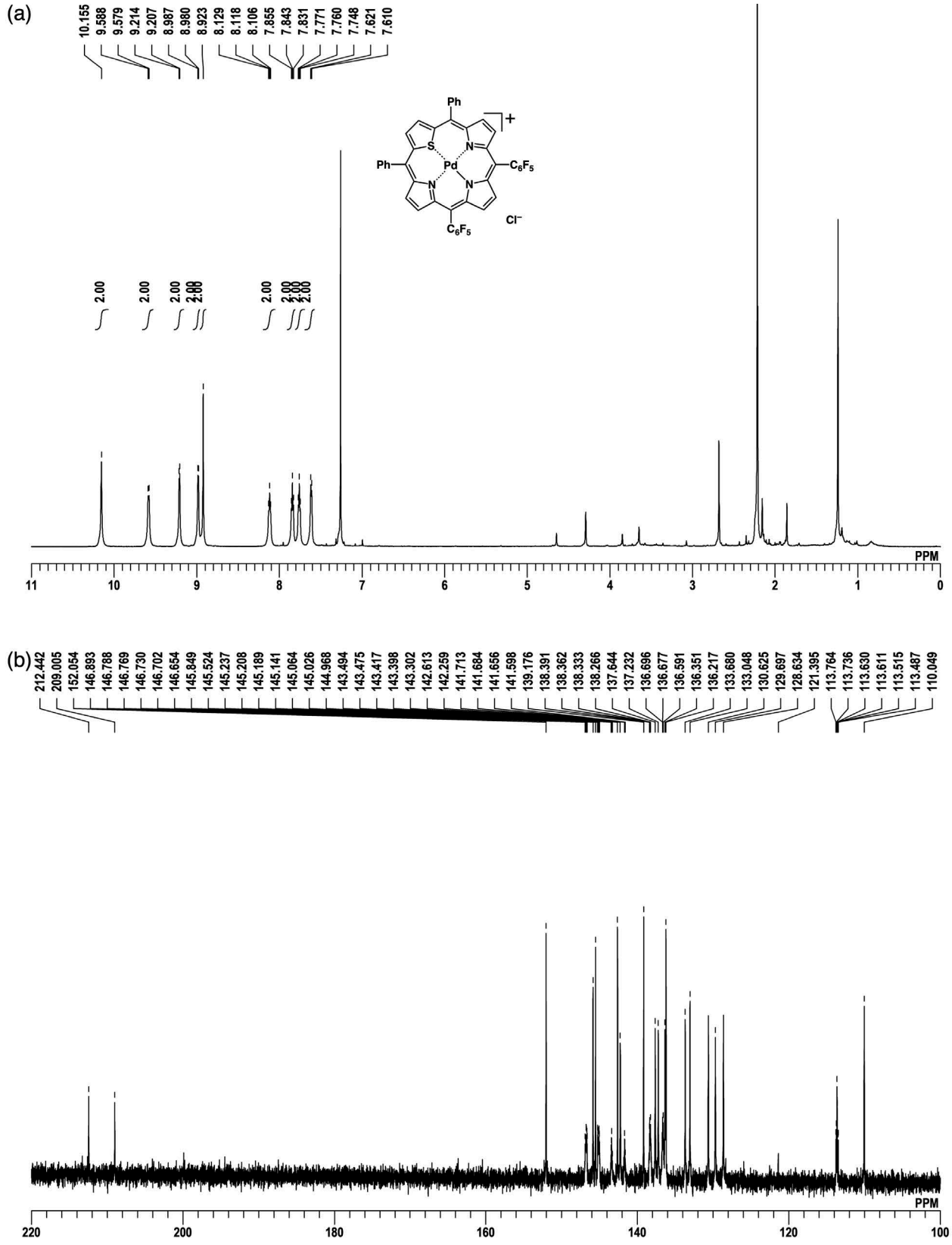

Fig. S5 (a) ^{1}H NMR, (b) ^{13}C NMR, and (c) ^{19}F NMR spectra of **2pd**$^{+}$-Cl^{-} in $CDCl_3$ at –60, –60, and 20 °C, respectively.

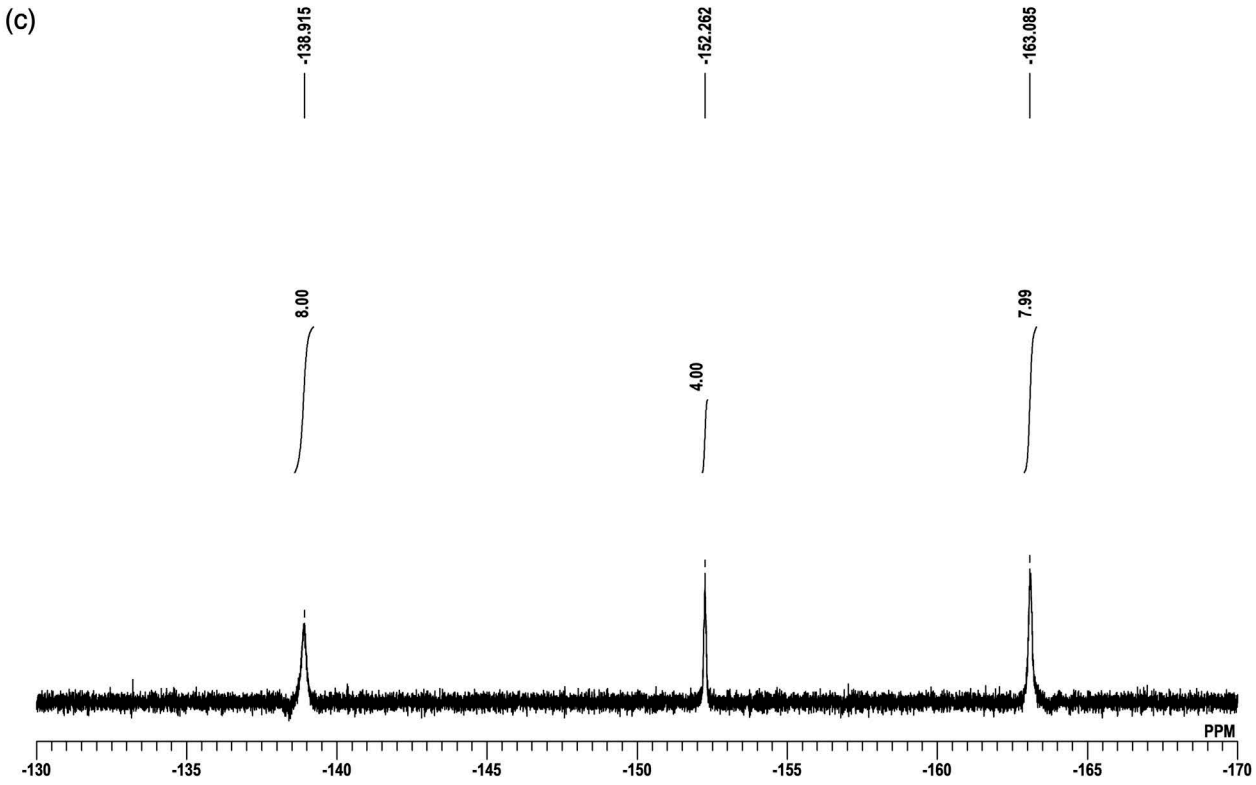

Fig. S5 (Continued)

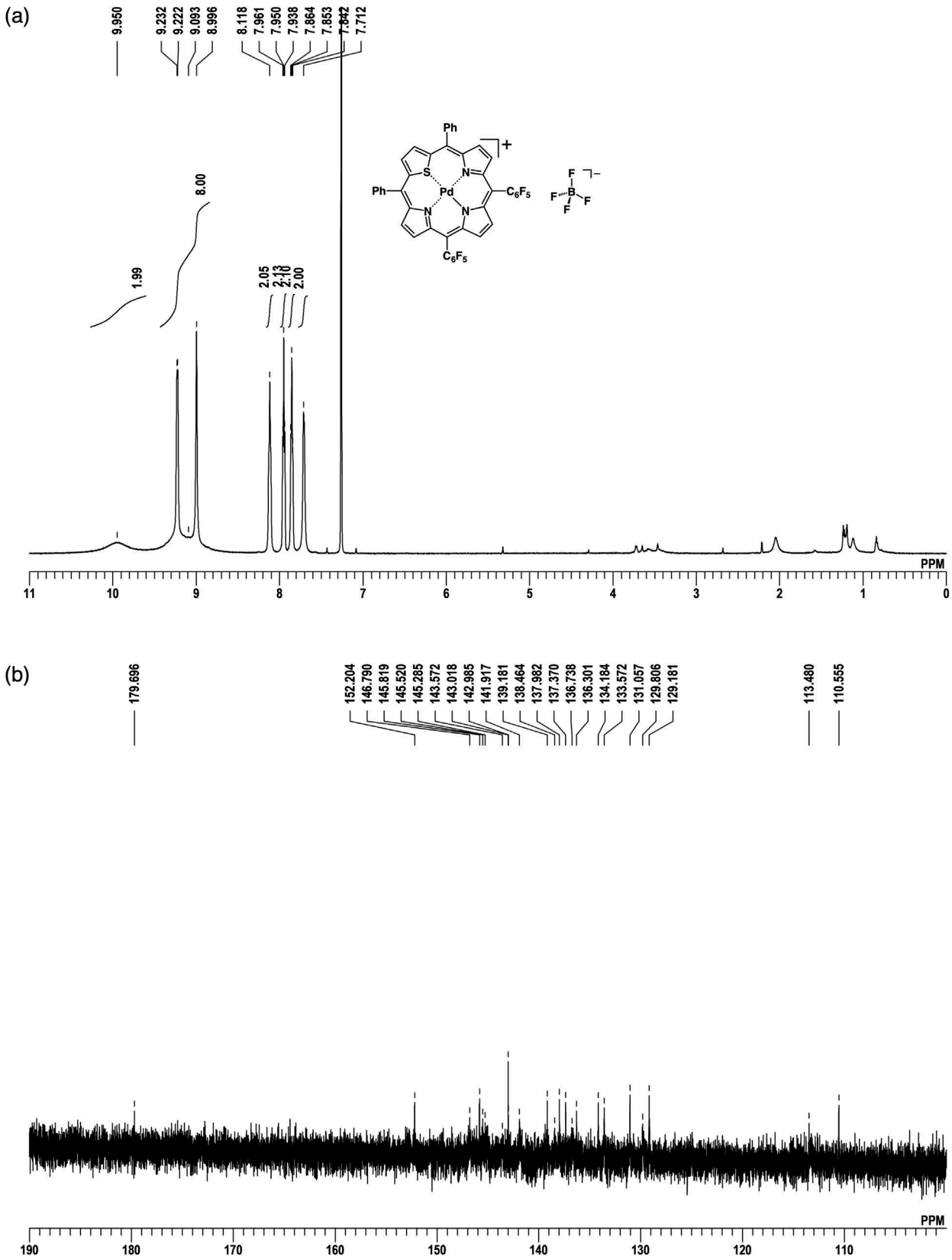

Fig. S6 (a) ^{1}H NMR, (b) ^{13}C NMR, and (c) ^{19}F NMR spectra of **2pd**$^{+}$-BF_4^- in $CDCl_3$ at –60, –60, and 20 °C, respectively.

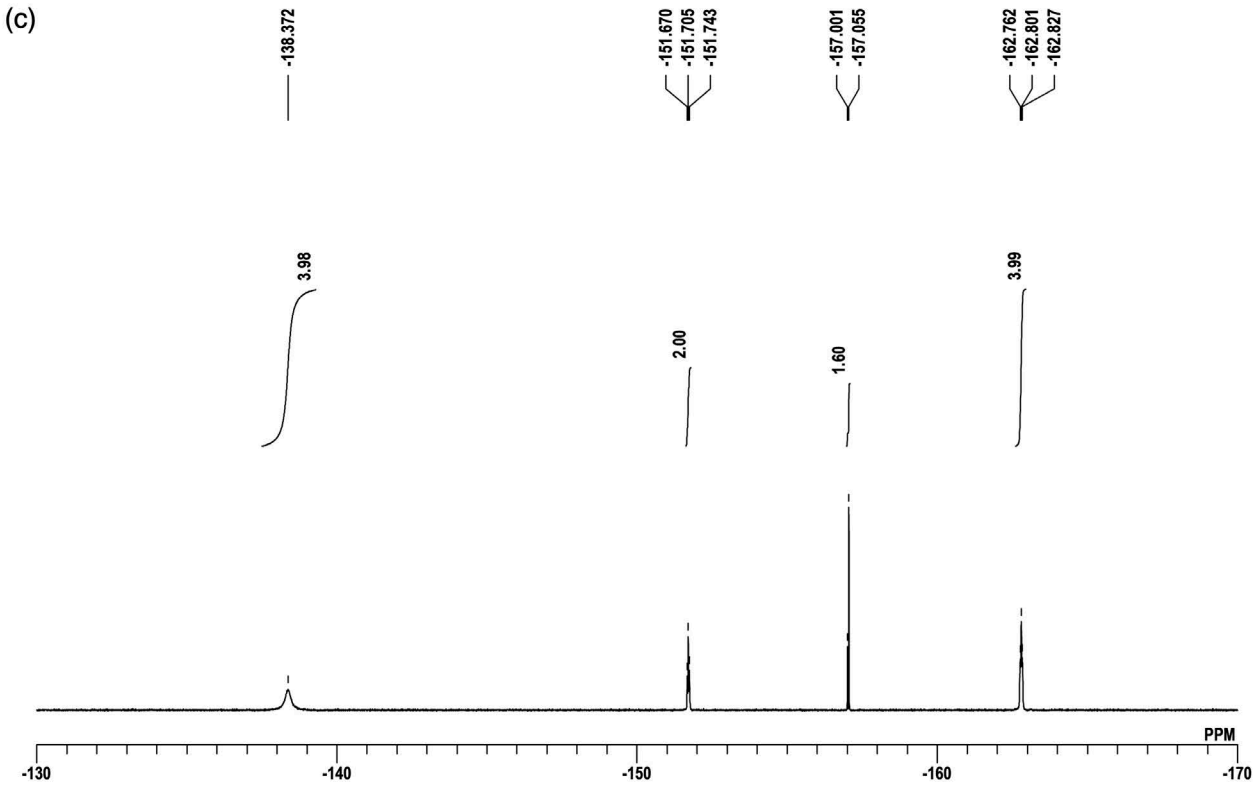

Fig. S6 (Continued)

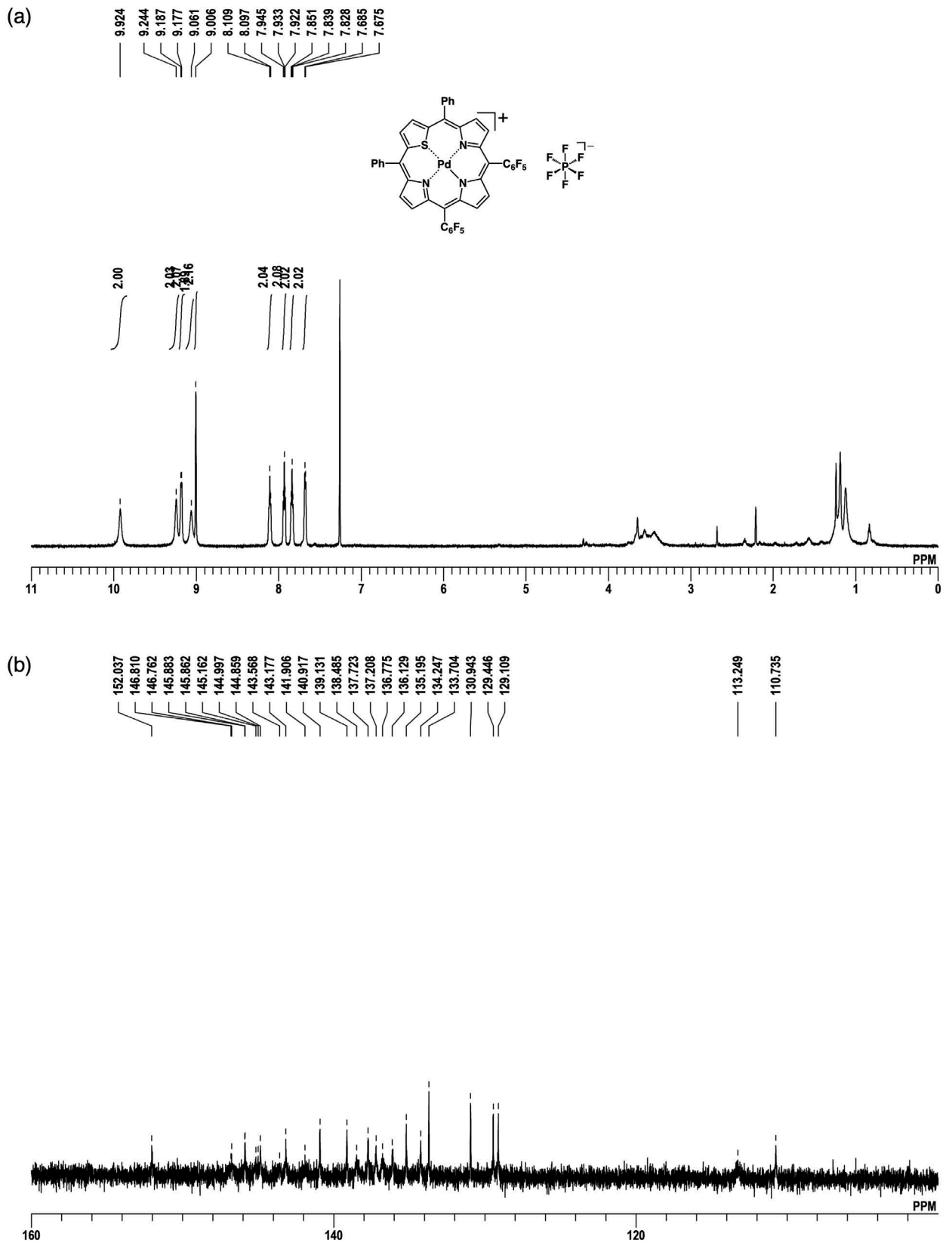

Fig. S7 (a) ^{1}H NMR, (b) ^{13}C NMR, and (c) ^{19}F NMR spectra of **2pd**$^{+}$-PF_6^- in $CDCl_3$ at –60, –60, and 20 °C, respectively.

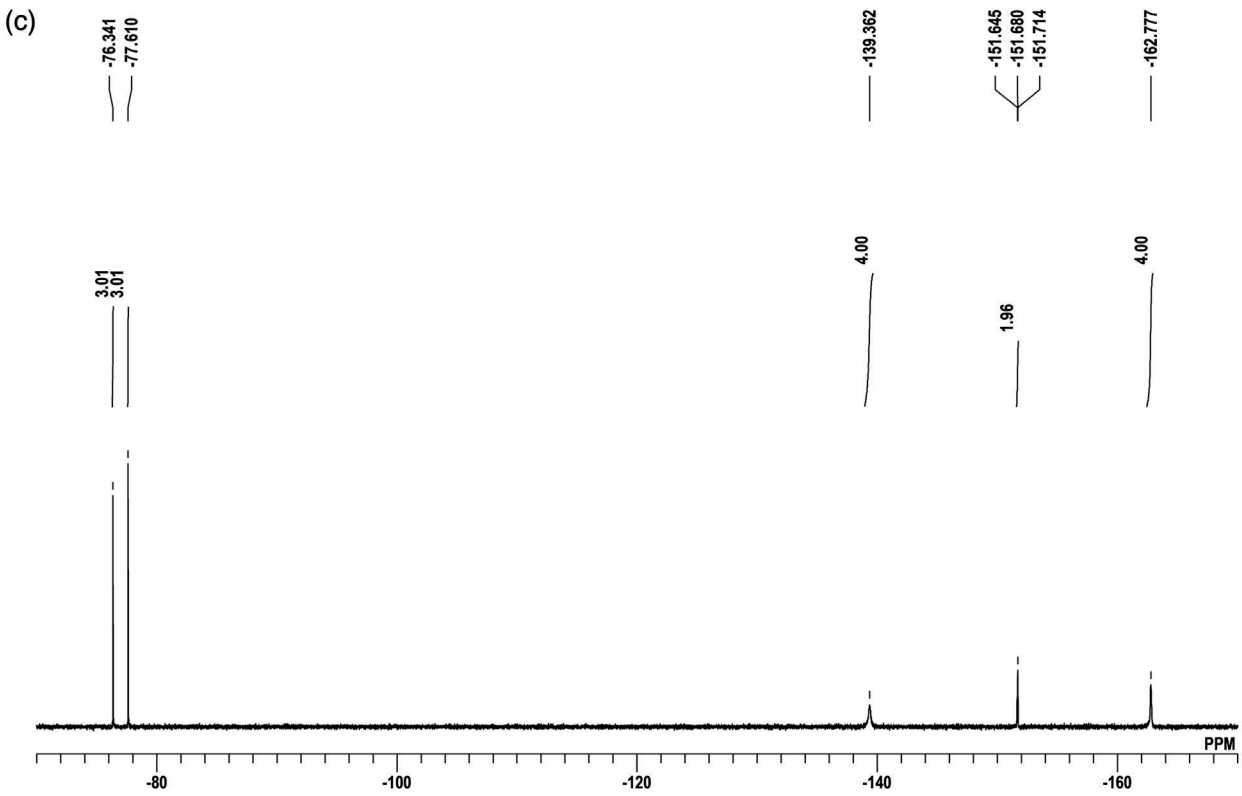

Fig. S7 (Continued)

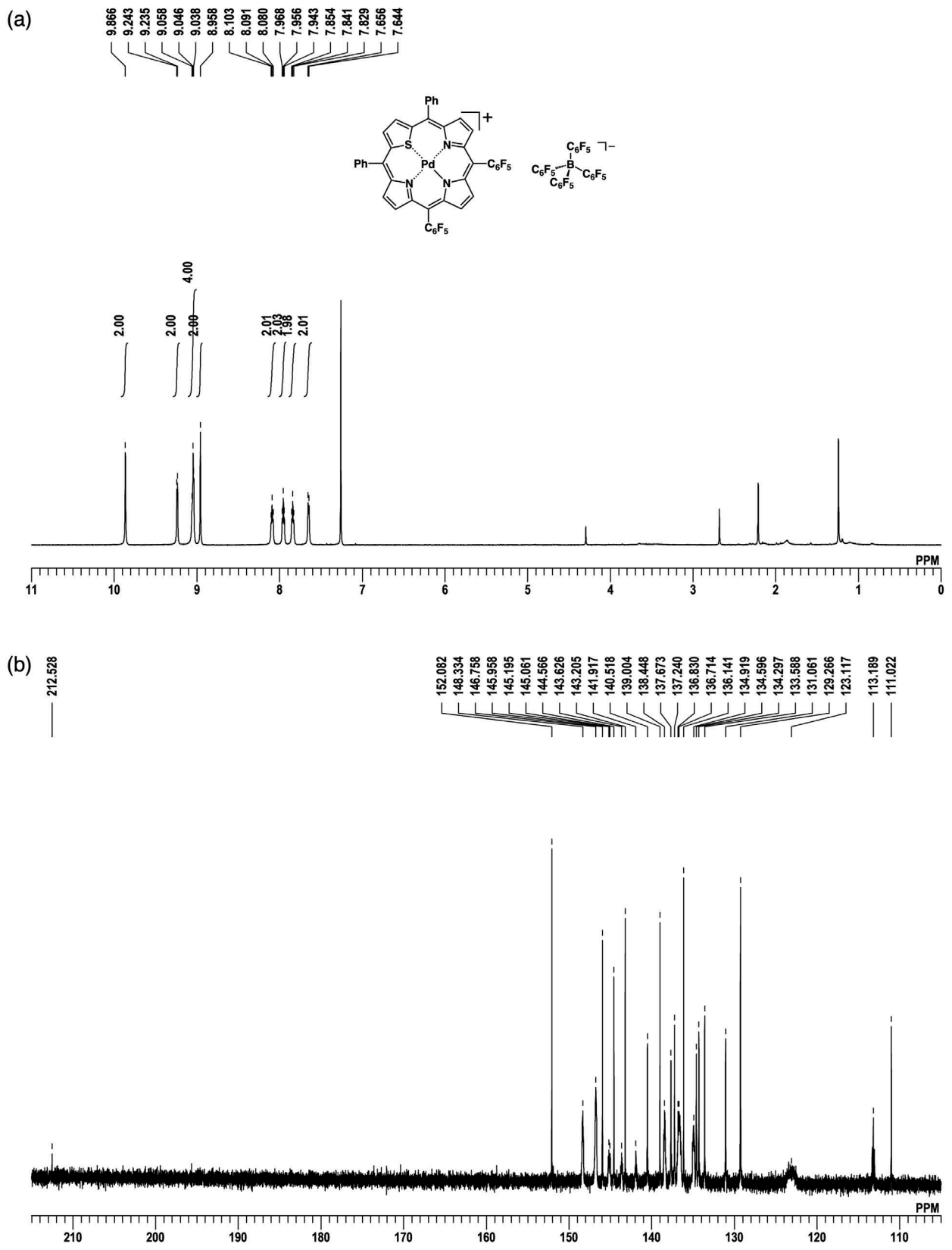

Fig. S8 (a) ^{1}H NMR, (b) ^{13}C NMR, and (c) ^{19}F NMR spectra of **2pd**$^{+}$-B(C_6F_5)$_4^{-}$ in $CDCl_3$ at –60, –60, and 20 °C, respectively.

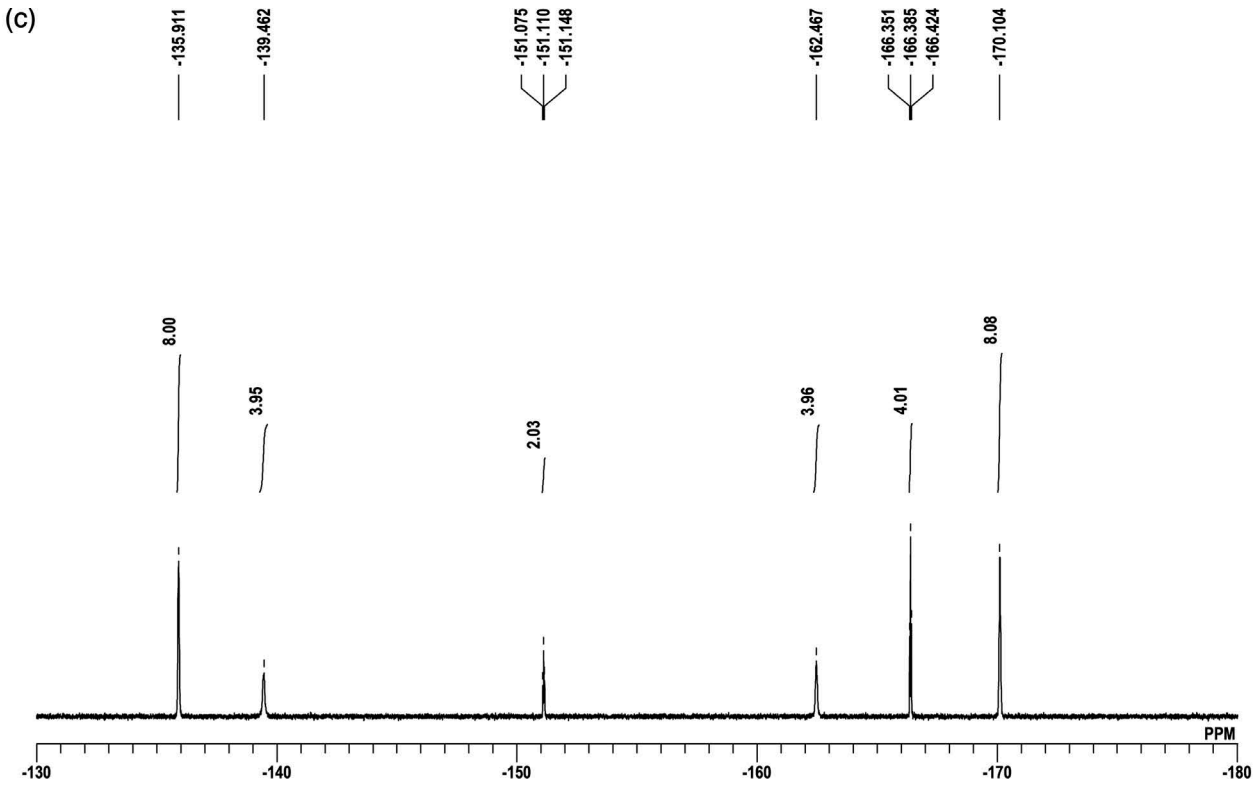

Fig. S8 (Continued)

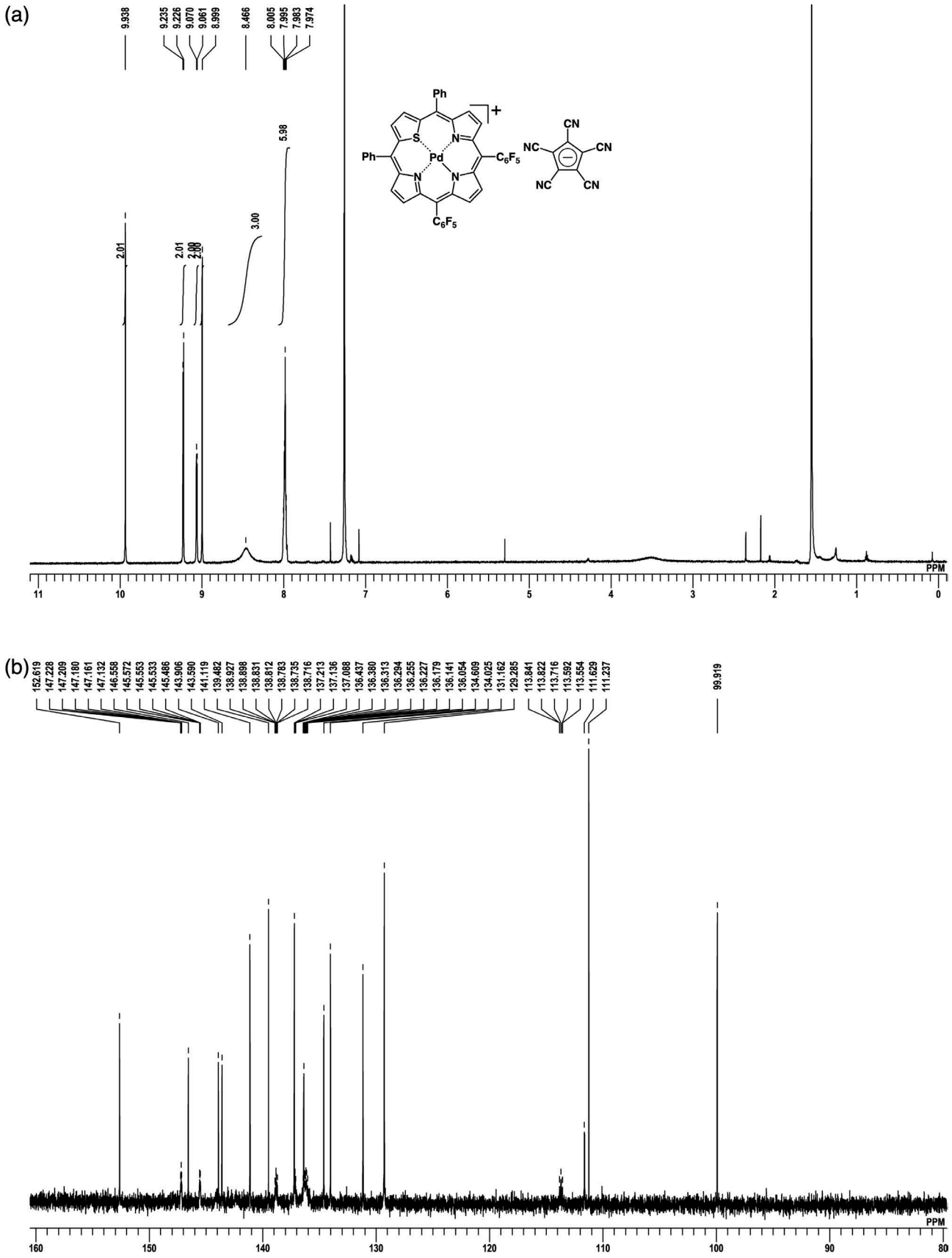

Fig. S9 (a) ^{1}H NMR, (b) ^{13}C NMR, and (c) ^{19}F NMR spectra of **2pd**$^{+}$-PCCp^{-} in $CDCl_3$ at 20 °C.

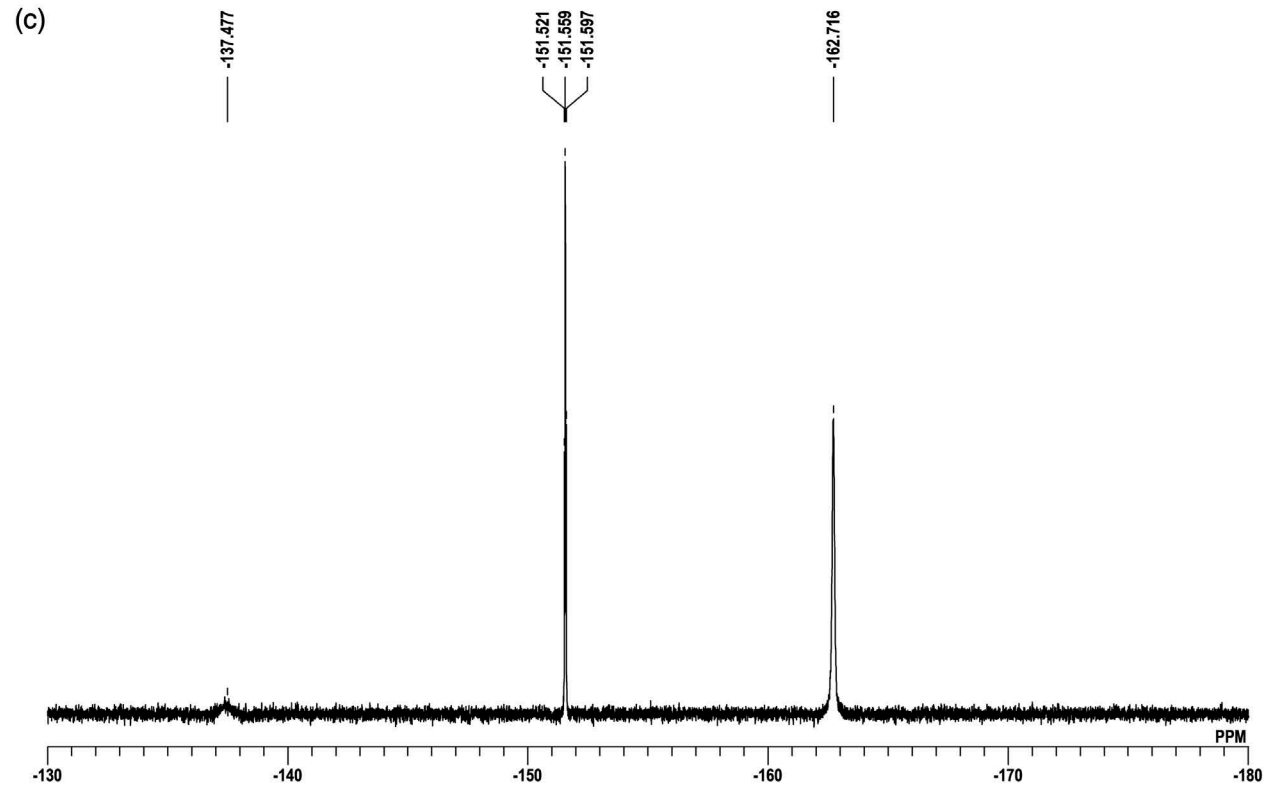

Fig. S9 (Continued)

2. X-ray crystallographic data

Method for single-crystal X-ray analysis. Crystallographic data are summarized in Table S1. A single crystal of **1pd**$^+$-BF_4^- was obtained by vapor diffusion of *n*-hexane into a $CHCl_3$ solution with a small amount of chlorobenzene. The data crystal was a brown block of approximate dimensions 0.06 mm × 0.03 mm × 0.02 mm. A single crystal of **1pd**$^+$-PF_6^- was obtained by vapor diffusion of *n*-hexane into a CH_2Cl_2 solution with a small amount of 1-octanol. The data crystal was a green prism of approximate dimensions 0.30 mm × 0.05 mm × 0.05 mm. A single crystal of **1pd**$^+$-$B(C_6F_5)_4^-$ was obtained by vapor diffusion of *n*-hexane into a CH_2Cl_2 solution with a small amount of 1-pentanol. The data crystal was a green prism of approximate dimensions 0.03 mm × 0.03 mm × 0.01 mm. A single crystal of **1pd**$^+$-$PCCp^-$ was obtained by vapor diffusion of *n*-hexane into a $CHCl_3$ solution. The data crystal was a green plate of approximate dimensions 0.20 mm × 0.10 mm × 0.02 mm. A single crystal of **2pd**$^+$-BF_4^- was obtained by vapor diffusion of *n*-hexane into a CH_2Cl_2 solution with a small amount of 1-butanol. The data crystal was a green prism of approximate dimensions 0.02 mm × 0.02 mm × 0.01 mm. A single crystal of **2pd**$^+$-PF_6^- was obtained by vapor diffusion of *n*-hexane into a $CHCl_3$ solution with a small amount of chlorobenzene. The data crystal was a green prism of approximate dimensions 0.09 mm × 0.07 mm × 0.03 mm. A single crystal of **2pd**$^+$-$PCCp^-$ was obtained by vapor diffusion of *n*-hexane into a $CHCl_3$ solution with a small amount of chlorobenzene. The data crystal was a green prism of approximate dimensions 0.08 mm × 0.05 mm × 0.03 mm. The data of **1pd**$^+$-BF_4^- and **2pd**$^+$-PF_6^- were collected at 90 K on a DECTRIS PILATUS3 CdTe 1M diffractometer with Si (311) monochromated synchrotron radiation (λ = 0.41440 and 0.41360 Å, respectively) at BL02B1 (SPring-8),[S5] whereas those of **1pd**$^+$-PF_6^-, **1pd**$^+$-$B(C_6F_5)_4^-$, **1pd**$^+$-$PCCp^-$, **2pd**$^+$-BF_4^-, and **2pd**$^+$-$PCCp^-$ were collected at 90, 100, 90, 100, and 100 K, respectively, on a Dectris EIGER X 1M diffractometer with Si (111) monochromated synchrotron radiation (λ = 0.80977, 0.81250, 0.81070, 0.81250, and 0.81200 Å, respectively) at BL40XU (SPring-8).[S6] All the structures were solved by dual-space method. The structures were refined by a full-matrix least-squares method by using a SHELXL 2014[S7] (Yadokari-XG).[S8] In each structure, the non-hydrogen atoms were refined anisotropically. CIF files (CCDC-2280002–2280005, 2333278–2333280 (these values correspond to **1pd**$^+$-BF_4^-, **1pd**$^+$-PF_6^-, **1pd**$^+$-$PCCp^-$, **2pd**$^+$-PF_6^-, **1pd**$^+$-$B(C_6F_5)_4^-$, **2pd**$^+$-BF_4^-, and **2pd**$^+$-$PCCp^-$, respectively)) can be obtained free of charge from the Cambridge Crystallographic Data Centre via www.ccdc.cam.ac.uk/data_request/cif.

Table S1 Crystallographic details.

	1pd$^+$-BF_4^-	**1pd**$^+$-PF_6^-	**1pd**$^+$-$B(C_6F_5)_4^-$	**1pd**$^+$-$PCCp^-$	**2pd**$^+$-BF_4^-
formula	$C_{44}H_{28}N_3PdS\cdot BF_4\cdot CHCl_3$	$C_{44}H_{28}N_3PdS\cdot F_6P\cdot 2CH_2Cl_2$	$C_{44}H_{28}N_3PdS\cdot C_{24}BF_{20}\cdot C_6H_{14}$	$C_{44}H_{28}N_3PdS\cdot C_{10}N_5\cdot CHCl_3$	$C_{44}H_{18}F_{10}N_3PdS\cdot BF_4\cdot 2C_4H_{10}O$
fw	943.33	1051.97	1502.37	1046.67	1744.36
crystal size, mm	0.06 × 0.03 × 0.02	0.30 × 0.05 × 0.05	0.03 × 0.03 × 0.01	0.20 × 0.10 × 0.02	0.02 × 0.02 × 0.01
crystal system	triclinic	monoclinic	monoclinic	triclinic	monoclinic
space group	$P\bar{1}$ (no. 2)	$P2_1/c$ (no. 14)	$P2_1/n$ (no. 14)	$P\bar{1}$ (no. 2)	$C2/c$ (no. 15)
a, Å	9.276(8)	13.7700(11)	13.54600(10)	14.7468(4)	21.7683(5)
b, Å	14.42(2)	16.0819(18)	27.1678(3)	17.6065(4)	21.6032(4)
c, Å	15.664(13)	19.035(2)	16.8019(2)	20.5210(4)	22.7133(9)
α, °	112.75(4)	90	90	69.671(2)	90
β, °	91.73(3)	90.479(6)	99.6330(10)	82.618(2)	100.780(3)
γ, °	91.28(3)	90	90	65.328(2)	90
V, Å^3	1930(4)	4215.1(8)	6096.16(11)	4539.3(2)	10492.8(5)
ρ_{calcd}, gcm^{-3}	1.623	1.658	1.637	1.532	1.656
Z	2	4	4	4	6
T, K	90(2)	90(2)	100(2)	90(2)	100(2)
μ, mm^{-1}	0.730 [a]	0.932 [a]	0.634 [a]	0.962 [a]	0.613 [a]
no. of reflns	52135	43483	74655	49257	62952
no. of unique reflns	8737	7692	14014	16604	12183
variables	593	571	935	1258	559
λ, Å	0.41440 [a]	0.80977 [a]	0.81250 [a]	0.81070 [a]	0.81250 [a]
R_1 ($I > 2\sigma(I)$)	0.0494	0.0592	0.0467	0.0822	0.1069
wR_2 ($I > 2\sigma(I)$)	0.1132	0.1456	0.1175	0.1797	0.3517
GOF	1.038	1.141	1.024	1.039	1.418

[a] Synchrotron radiation.

Table S1 (Continued)

	2pd^{+}-PF_6^-	**2pd**$^{+}$-$PCCp^-$
formula	$C_{44}H_{18}F_{10}N_3PdS \cdot F_6P \cdot 0.5C_6H_5Cl$	$C_{44}H_{18}F_{10}N_3PdS \cdot C_{10}N_5 \cdot 3.3CH_2Cl_2$
fw	1118.32	1247.59
crystal size, mm	0.09× 0.07× 0.03	0.08× 0.05× 0.03
crystal system	orthorhombic	monoclinic
space group	$Pna2_1$ (no. 33)	$P2_1$ (no. 4)
a, Å	28.140(11)	13.3831(3)
b, Å	14.513(9)	7.1785(2)
c, Å	20.554(10)	26.0801(5)
α, °	90	90
β, °	90	93.166(2)
γ, °	90	90
V, Å^3	8394(7)	2501.71(10)
ρ_{calcd}, gcm^{-3}	1.770	1.656
Z	8	2
T, K	90(2)	100(2)
μ, mm^{-1}	0.659 [a]	0.959 [a]
no. of reflns	240860	29396
no. of unique reflns	19243	10962
variables	1252	734
λ, Å	0.41360 [a]	0.81200 [a]
R_1 ($I > 2\sigma(I)$)	0.0364	0.0537
wR_2 ($I > 2\sigma(I)$)	0.0914	0.1382
GOF	1.017	1.029

[a] Synchrotron radiation.

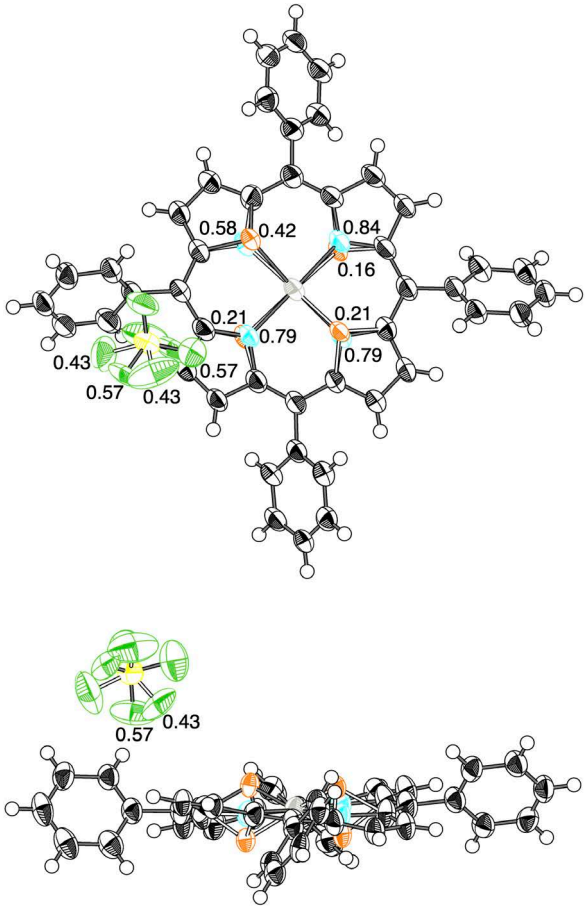

Fig. S10 Ortep drawing of single-crystal X-ray structure (top and side views) of **1pd**$^{+}$-BF_4^{-}. Disordered structures are represented by gray and white bonds for major and minor structures, respectively, in the ratios of 42 : 21 : 21 : 16 and 57 : 43 for the porphyrin inner atoms (according to the existence of sulfur) and a BF_4^{-} unit, respectively. Thermal ellipsoids are scaled to the 50% probability level. Solvent molecules are omitted for clarity. Atom color code: black, white (sphere), yellow, blue, yellow green, orange, and light gray refer to carbon, hydrogen, boron, nitrogen, fluorine, sulfur, and palladium, respectively.

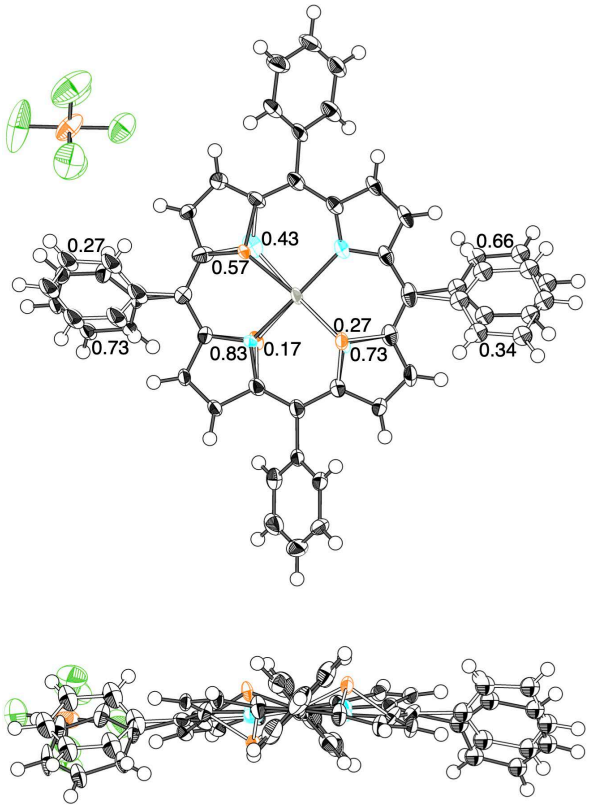

Fig. S11 Ortep drawing of single-crystal X-ray structure (top and side views) of **1pd**$^{+}$-PF_6^{-}. Disordered structures are represented by gray and white bonds for major and minor structures, respectively, in the ratios of 57 : 27 : 17, 73 : 27, and 66 : 34 for the porphyrin inner atoms (according to the existence of sulfur) and two phenyl groups, respectively. Thermal ellipsoids are scaled to the 50% probability level. Solvent molecules are omitted for clarity. Atom color code: black, white (sphere), blue, yellow green, light orange, orange, and light gray refer to carbon, hydrogen, nitrogen, fluorine, phosphorus, sulfur, and palladium, respectively.

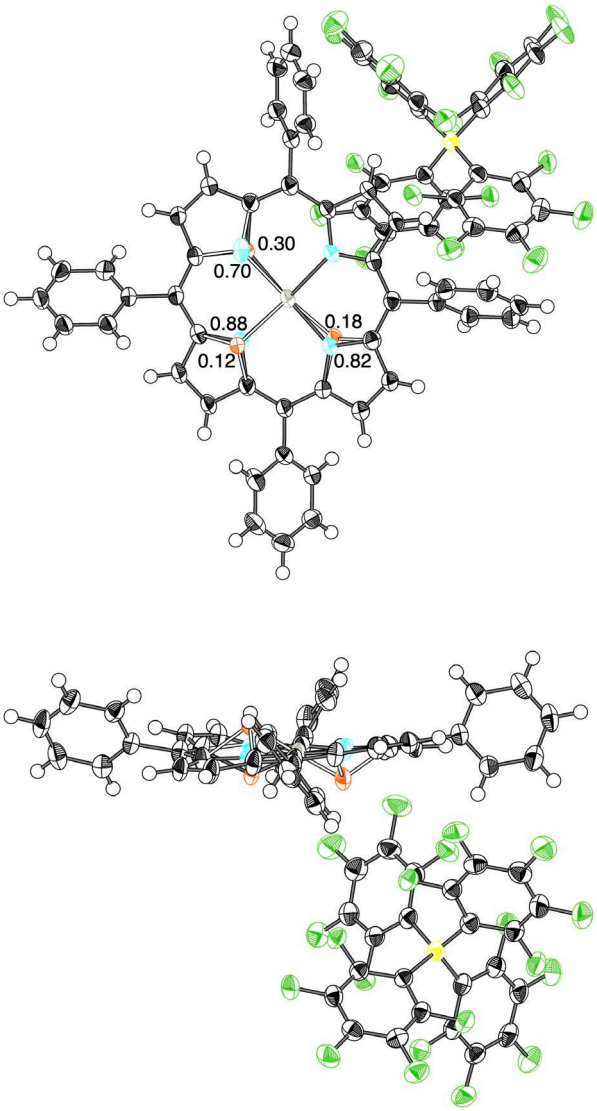

Fig. S12 Ortep drawing of single-crystal X-ray structure (top and side views) of **1pd**$^{+}$-FABA^{-}. Disordered structures are represented by gray and white bonds for major and minor structures, respectively, in the ratio of 30 : 18 : 12 for the porphyrin inner atoms (according to the existence of sulfur). Thermal ellipsoids are scaled to the 50% probability level. Solvent molecules are omitted for clarity. Atom color code: black, white (sphere), yellow, blue, yellow green, orange, and light gray refer to carbon, hydrogen, boron, nitrogen, fluorine, sulfur, and palladium, respectively.

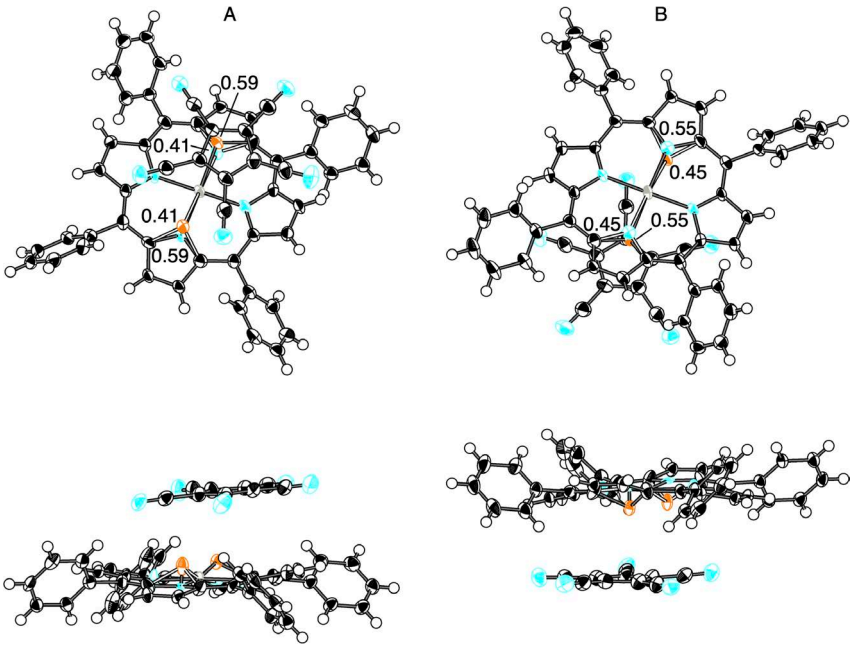

Fig. S13 Ortep drawing of single-crystal X-ray structure (top and side views) of **1pd**$^{+}$-PCCp^{-} with two independent structures (A and B). Disordered structures are represented by gray and white bonds for major and minor structures, respectively, in the ratios of 55 : 45 and 59 : 41 for the porphyrin inner atoms (according to the existence of sulfur). Thermal ellipsoids are scaled to the 50% probability level. Solvent molecules are omitted for clarity. Atom color code: black, white (sphere), blue, orange, and light gray refer to carbon, hydrogen, nitrogen, sulfur, and palladium, respectively.

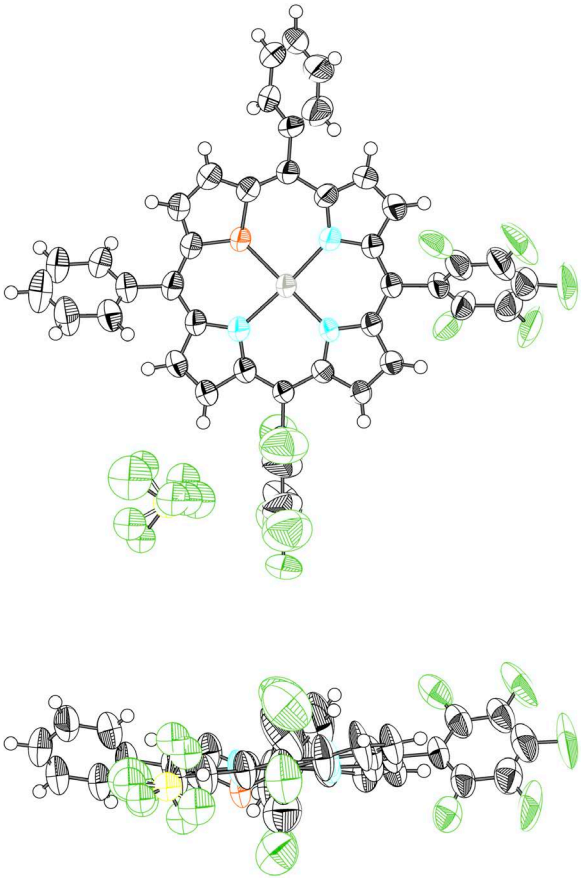

Fig. S14 Ortep drawing of single-crystal X-ray structure (top and side views) of **2pd**$^{+}$-BF_4^{-}. Disordered structures are represented by gray and white bonds for major and minor structures, respectively, in the ratio of 58 : 42 for a BF_4^{-} unit. Thermal ellipsoids are scaled to the 50% probability level. Solvent molecules are omitted for clarity. Atom color code: black, white (sphere), yellow, blue, yellow green, orange, and light gray refer to carbon, hydrogen, boron, nitrogen, fluorine, sulfur, and palladium, respectively.

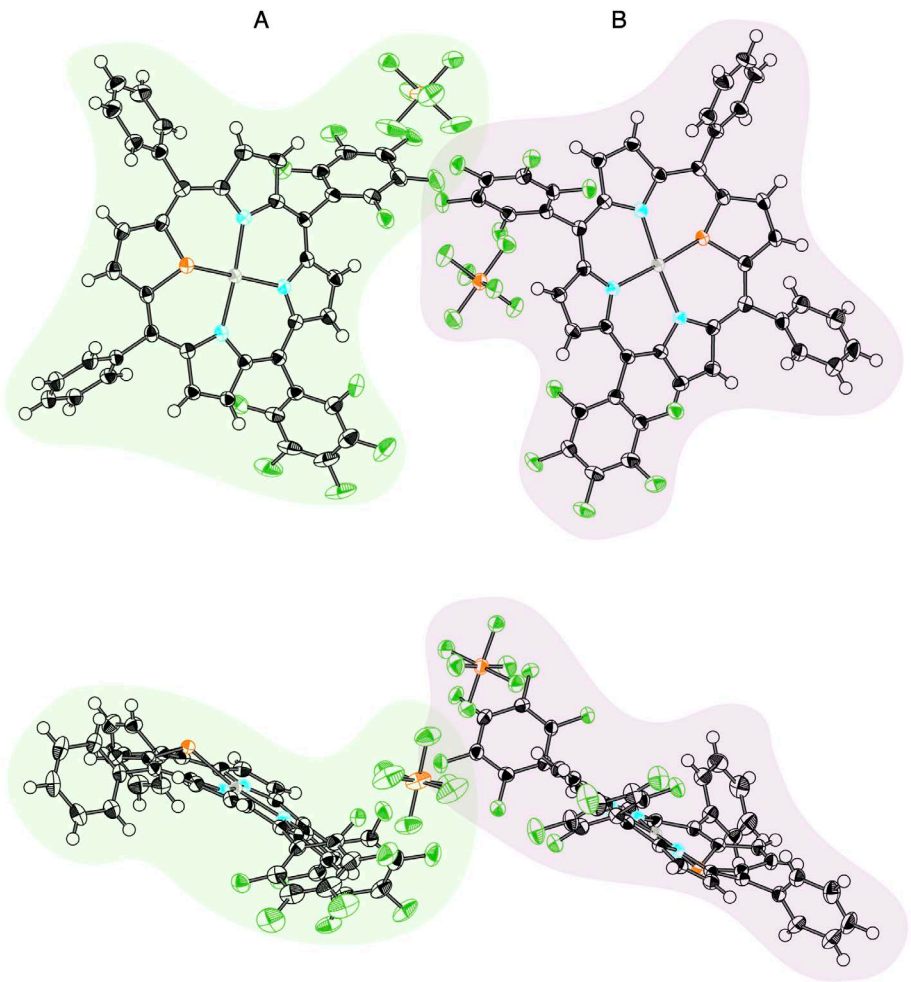

Fig. S15 Ortep drawing of single-crystal X-ray structure (top and side views) of **2pd**$^{+}$-PF_6^{-} with two independent structures (A and B). Thermal ellipsoids are scaled to the 50% probability level. Solvent molecules are omitted for clarity. Atom color code: black, white (sphere), blue, yellow green, light orange, orange, and light gray refer to carbon, hydrogen, nitrogen, fluorine, phosphorus, sulfur, and palladium, respectively.

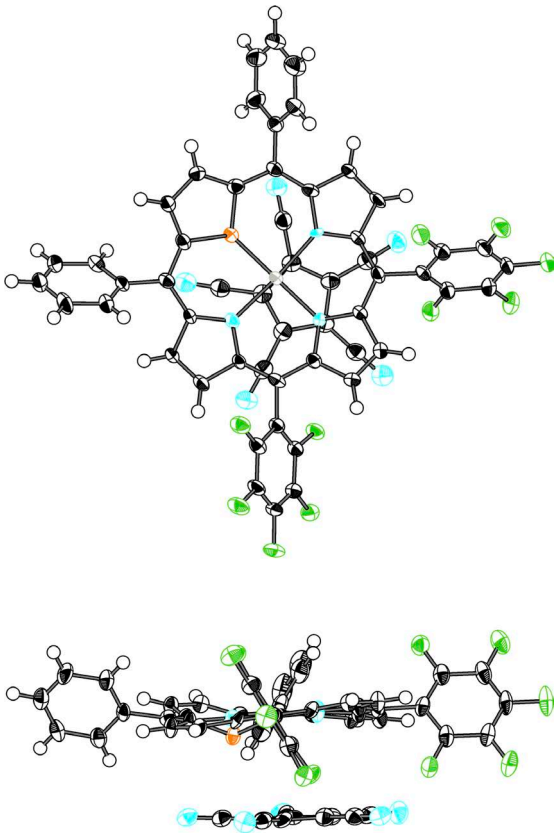

Fig. S16 Ortep drawing of single-crystal X-ray structure (top and side views) of **2pd**$^{+}$-PCCp^{-}. Thermal ellipsoids are scaled to the 50% probability level. Solvent molecules are omitted for clarity. Atom color code: black, white (sphere), blue, yellow green, orange, and light gray refer to carbon, hydrogen, nitrogen, fluorine, sulfur, and palladium, respectively.

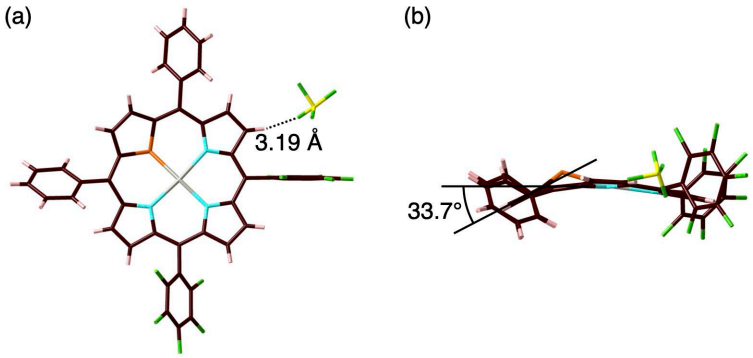

Fig. S17 Crystal structures of **1pd**$^{+}$-BF_4^{-} as (a) top and (b) side views. The dihedral angle between the thiophene plane and the core porphyrin plane (25 atoms) is 28.8°. Mean-plane deviation of the **1pd**$^{+}$ core part (25 atoms) and τ_4 value[S9] are 0.31 Å and 0.13, respectively. The C(–H)···F distance between **1pd**$^{+}$ and BF_4^{-} is 3.26 Å. Solvent molecules are omitted for clarity. Atom color code: brown, pink, yellow, blue, yellow green, orange, and light gray refer to carbon, hydrogen, boron, nitrogen, fluorine, sulfur, and palladium, respectively.

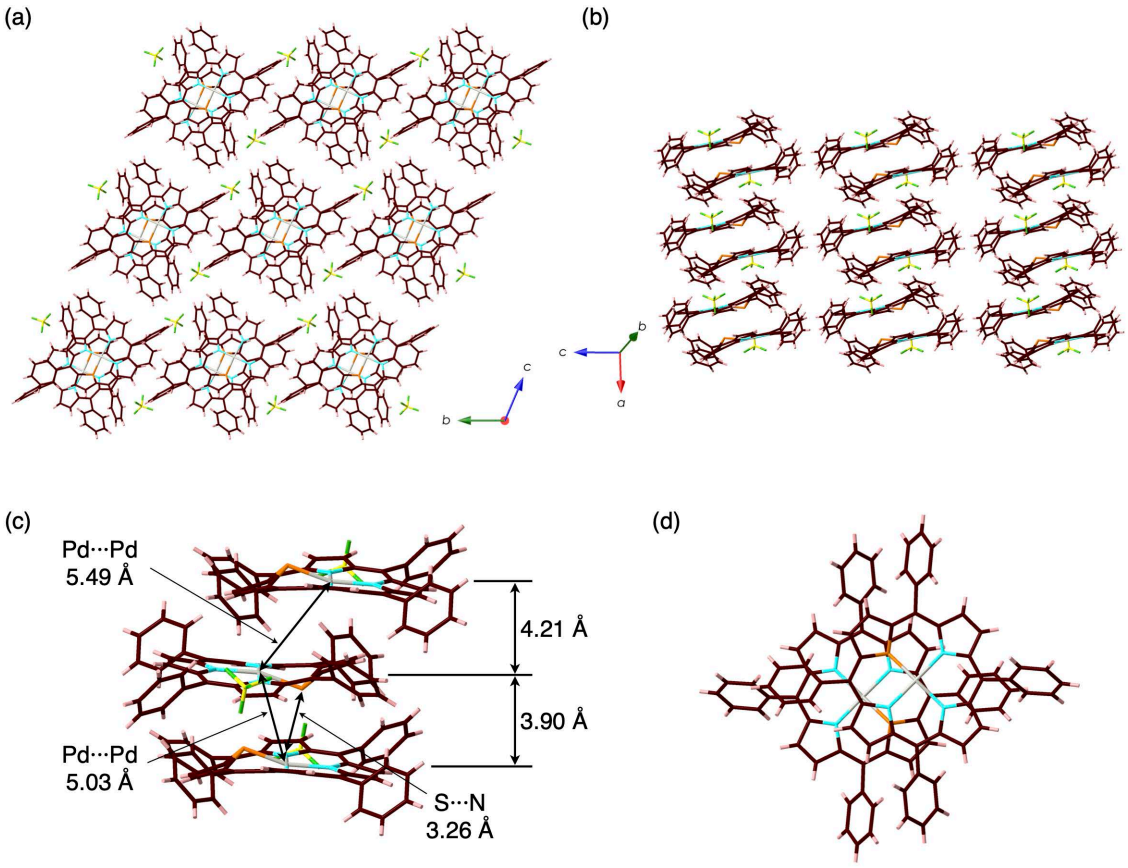

Fig. S18 Packing diagram (stacking assembly) of **1pd**$^{+}$-BF_4^{-} as (a) top and (b) side views and (c) enlarged side and (d) stacked dimer views. The stacking distances between two **1pd**$^{+}$ (core 25 atoms) and the Pd···Pd distances in the column are 3.90/4.21 and 5.03/5.49 Å, respectively. The S···N distance in two stacked **1pd**$^{+}$ units is 3.26 Å. Solvent molecules are omitted for clarity. Atom color code: brown, pink, yellow, blue, yellow green, orange, and light gray refer to carbon, hydrogen, boron, nitrogen, fluorine, sulfur, and palladium, respectively.

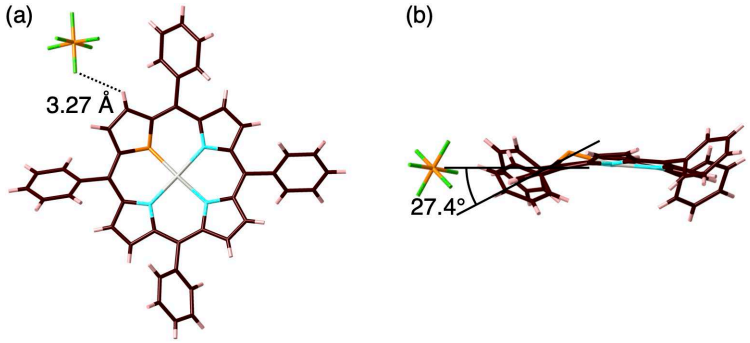

Fig. S19 Crystal structures of **1pd**$^{+}$-PF_6^{-} as (a) top and (b) side views. The dihedral angle between the thiophene plane and the core porphyrin plane (25 atoms) is 27.4°. Mean-plane deviation of the **1pd**$^{+}$ core part (25 atoms) and τ_4 value[S9] are 0.31 Å and 0.093, respectively. The C(–H)···F distance between **1pd**$^{+}$ and PF_6^{-} is 3.27 Å. Solvent molecules are omitted for clarity. Atom color code: brown, pink, blue, yellow green, light orange, orange, and light gray refer to carbon, hydrogen, nitrogen, fluorine, phosphorus, sulfur, and palladium, respectively.

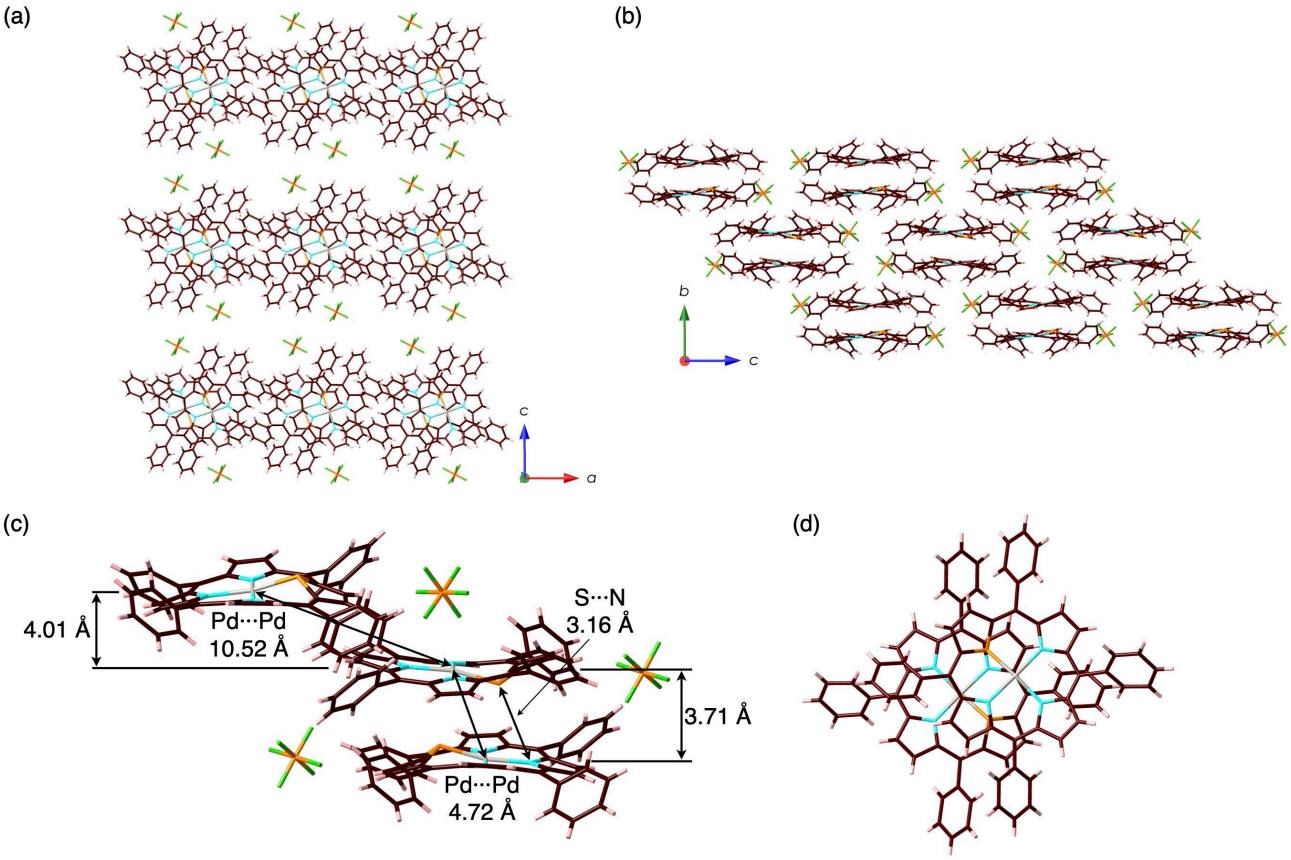

Fig. S20 Packing diagram (stacking assembly) of **1pd**$^{+}$-PF_6^{-} as (a) top and (b) side views and (c) enlarged side and (d) stacked dimer views. The stacking distances between two **1pd**$^{+}$ (core 25 atoms) and the Pd···Pd distances in the column are 3.71/4.01 and 4.72/10.52 Å, respectively. The S···N distance in two stacked **1pd**$^{+}$ units is 3.16 Å. Solvent molecules are omitted for clarity. Atom color code: brown, pink, blue, yellow green, light orange, orange, and light gray refer to carbon, hydrogen, nitrogen, fluorine, phosphorus, sulfur, and palladium, respectively.

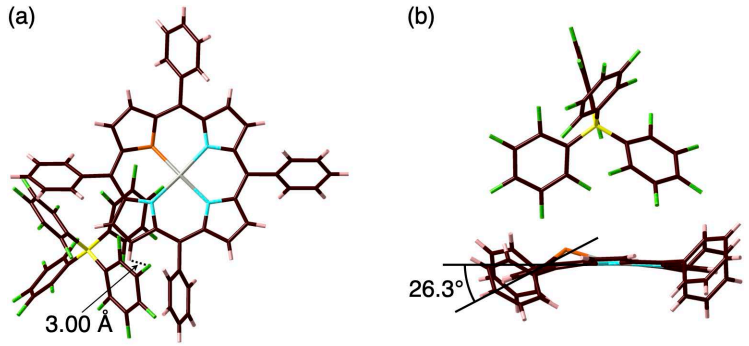

Fig. S21 Crystal structures of **1pd**$^{+}$-$B(C_6F_5)_4^{-}$ as (a) top and (b) side views. The dihedral angle between the thiophene plane and the core porphyrin plane (25 atoms) is 26.3°. Mean-plane deviation of the **1pd**$^{+}$ core part (25 atoms) and τ_4 value[S9] are 0.23 Å and 0.12, respectively. The C(–H)···F distance between **1pd**$^{+}$ and $B(C_6F_5)_4^{-}$ is 3.00 Å. Solvent molecules are omitted for clarity. Atom color code: brown, pink, yellow, blue, yellow green, orange, and light gray refer to carbon, hydrogen, boron, nitrogen, fluorine, sulfur, and palladium, respectively.

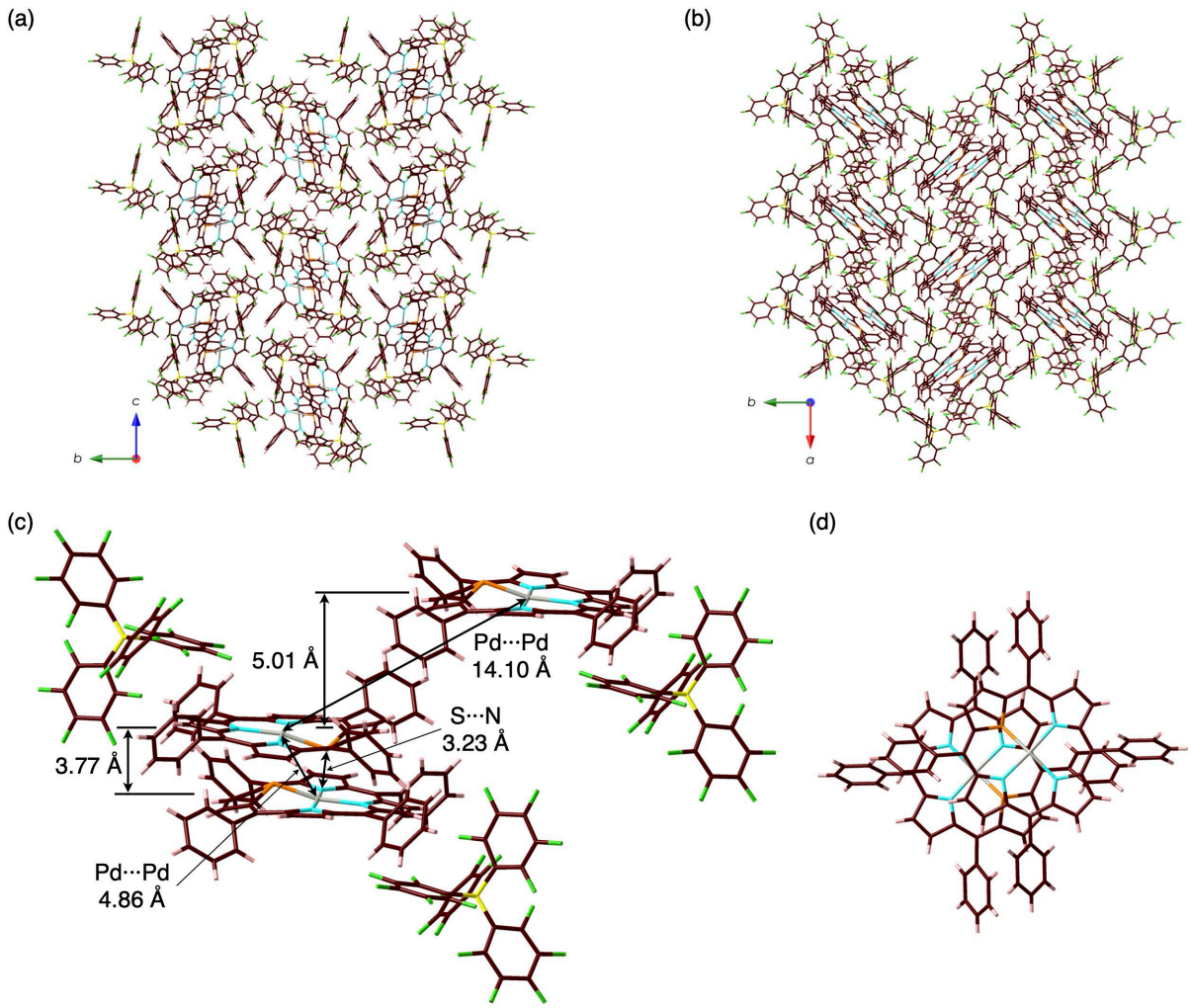

Fig. S22 Packing diagram (stacking assembly) of **1pd**$^{+}$-B(C_6F_5)$_4^{-}$ as (a) top and (b) side views and (c) enlarged side and (d) stacked dimer views. The stacking distances between two **1pd**$^{+}$ (core 25 atoms) and the Pd···Pd distances in the column are 3.77/5.01 and 4.86/14.10 Å, respectively. The S···N distance in two stacked **1pd**$^{+}$ units is 3.23 Å. Solvent molecules are omitted for clarity. Atom color code: brown, pink, yellow, blue, yellow green, orange, and light gray refer to carbon, hydrogen, boron, nitrogen, fluorine, sulfur, and palladium, respectively.

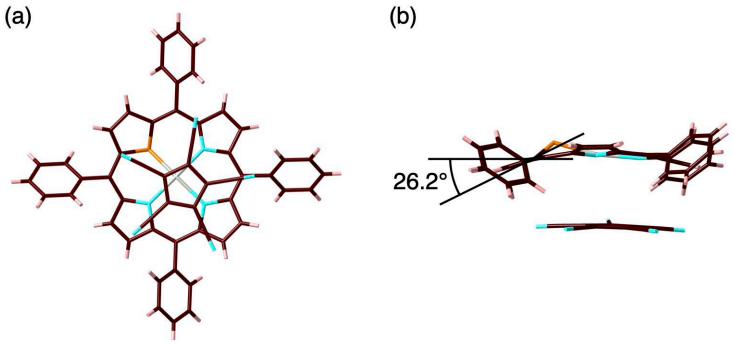

Fig. S23 Crystal structures of **1pd**$^{+}$-PCCp^{-} as (a) top and (b) side views. The dihedral angle between the thiophene plane and the core porphyrin plane (25 atoms) is 26.2°. Mean-plane deviation of the **1pd**$^{+}$ core part (25 atoms) and τ_4 value[S9] are 0.29 Å and 0.090, respectively. Solvent molecules are omitted for clarity. Atom color code: brown, pink, blue, orange, and light gray refer to carbon, hydrogen, nitrogen, sulfur, and palladium, respectively.

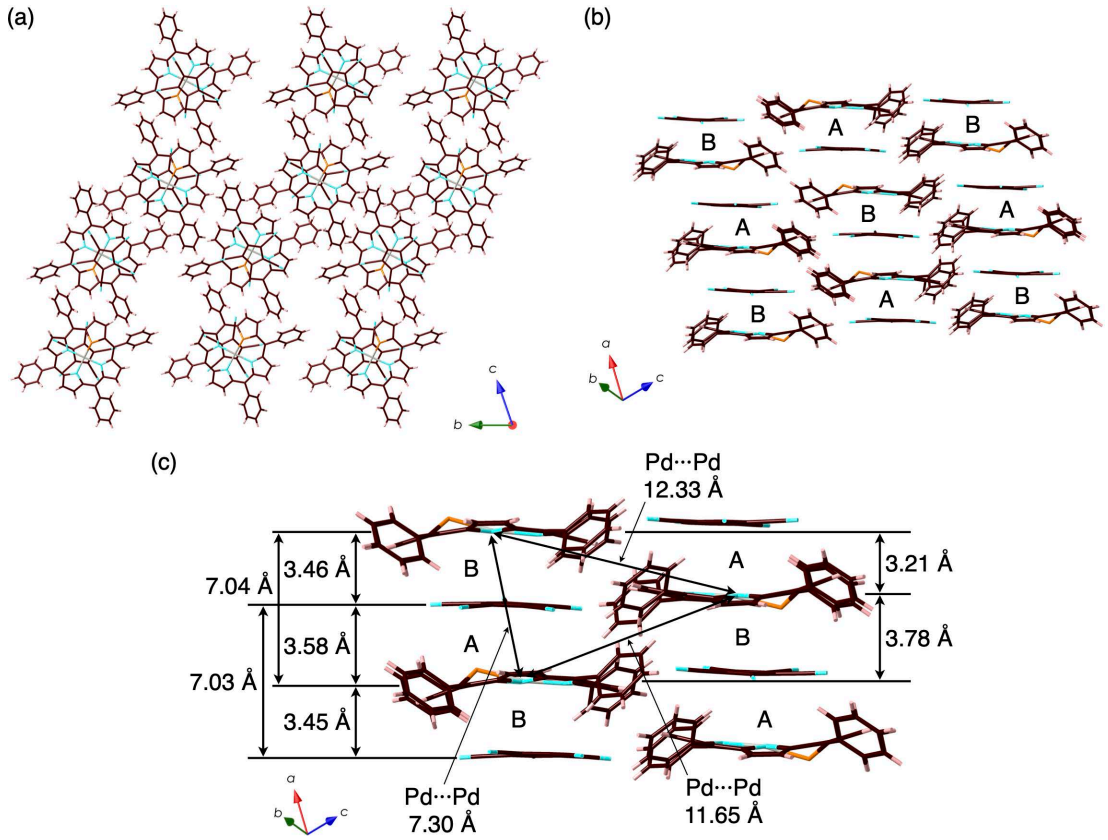

Fig. S24 Packing diagram (stacking assembly) of **1pd**$^{+}$-PCCp^{-} as (a) top and (b) side views and (c) an enlarged side view. Two independent structures are labelled as A and B in (b). The stacking distances between **1pd**$^{+}$ (core 25 atoms) and PCCp^{-} are 3.45, 3.46, and 3.58 Å. The distances between two **1pd**$^{+}$, that between two PCCp^{-}, and the Pd···Pd distances in the column are 3.21/3.78/7.04, 7.03, and 7.30/11.65/12.33 Å, respectively. Solvent molecules are omitted for clarity. Atom color code: brown, pink, blue, orange, and light gray refer to carbon, hydrogen, nitrogen, sulfur, and palladium, respectively.

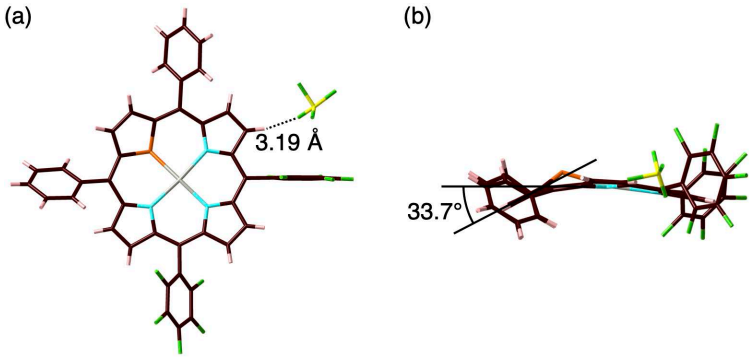

Fig. S25 Crystal structures of **2pd**$^{+}$-BF_4^{-} as (a) top and (b) side views. The dihedral angle between the thiophene plane and the core porphyrin plane (25 atoms) is 33.7°. Mean-plane deviation of the **2pd**$^{+}$ core part (25 atoms) and τ_4 value[S9] are 0.30 Å and 0.097, respectively. The C(–H)···F distance between **2pd**$^{+}$ and BF_4^{-} is 3.19 Å. Solvent molecules are omitted for clarity. Atom color code: brown, pink, yellow, blue, yellow green, orange, and light gray refer to carbon, hydrogen, boron, nitrogen, fluorine, sulfur, and palladium, respectively.

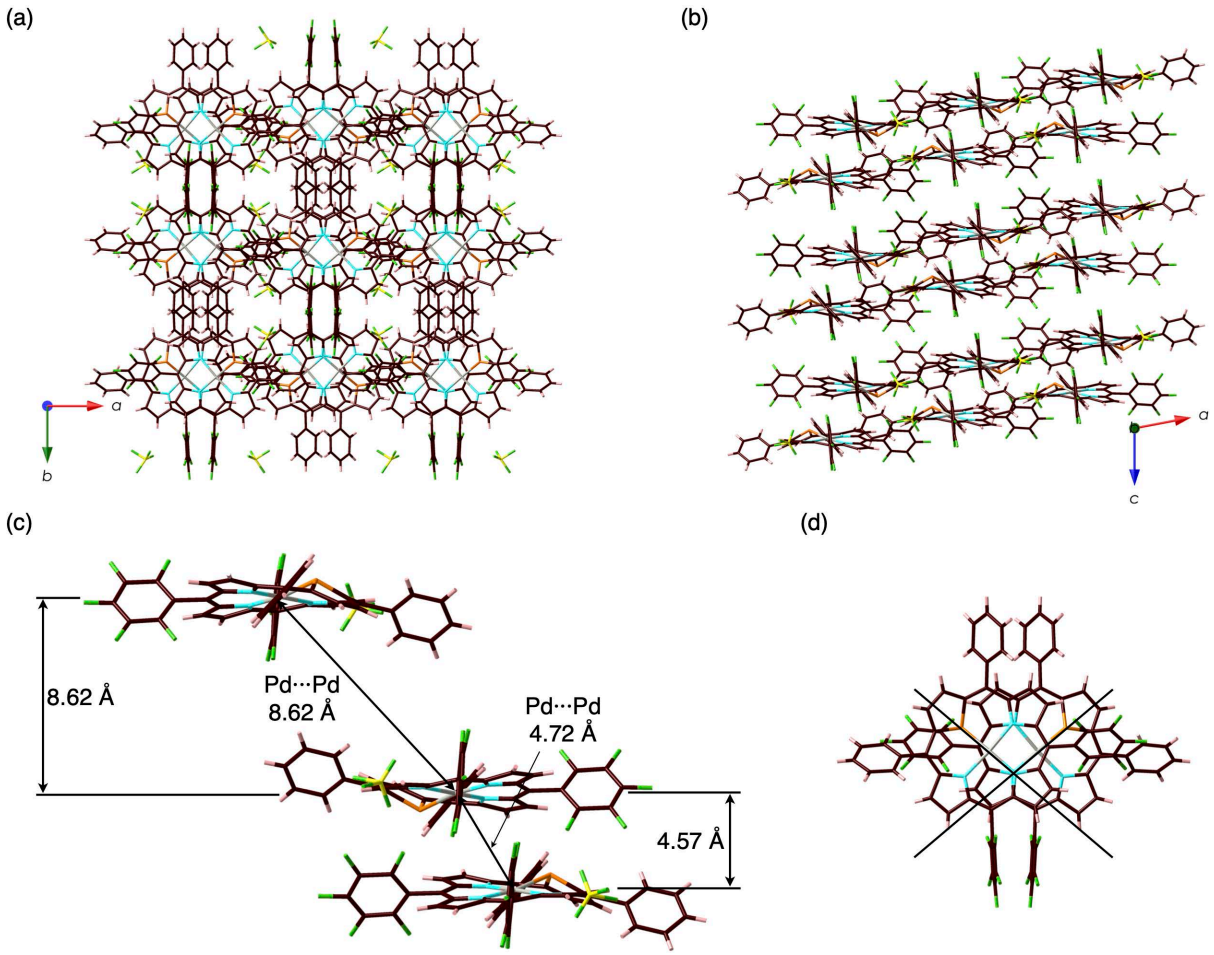

Fig. S26 Packing diagram (stacking assembly) of **2pd**$^{+}$-BF_4^- as (a) top and (b) side views and (c) enlarged side and (d) stacked dimer views. The stacking distances between two **2pd**$^{+}$ (core 25 atoms) and the Pd···Pd distances in the column are 4.57/8.62 and 4.72/8.62 Å, respectively. **2pd**$^{+}$ formed the stacked dimer with nearly perpendicular orientation as seen in the lines through S and counter N in (d). Solvent molecules are omitted for clarity. Atom color code: brown, pink, yellow, blue, yellow green, orange, and light gray refer to carbon, hydrogen, boron, nitrogen, fluorine, sulfur, and palladium, respectively.

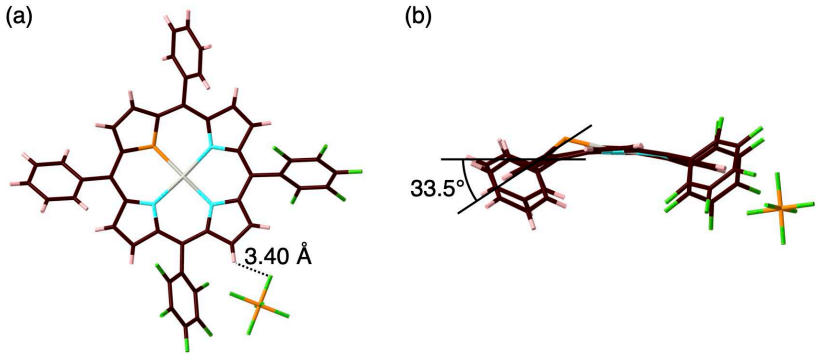

Fig. S27 Crystal structures of **2pd**$^{+}$-PF_6^- as (a) top and (b) side views. The dihedral angle between the thiophene plane and the core porphyrin plane (25 atoms) is 33.5°. Mean-plane deviation of the **2pd**$^{+}$ core part (25 atoms) and τ_4 value[S9] are 0.32 Å and 0.097, respectively. Solvent molecules are omitted for clarity. Atom color code: brown, pink, blue, yellow green, light orange, orange, and light gray refer to carbon, hydrogen, nitrogen, fluorine, phosphorus, sulfur, and palladium, respectively.

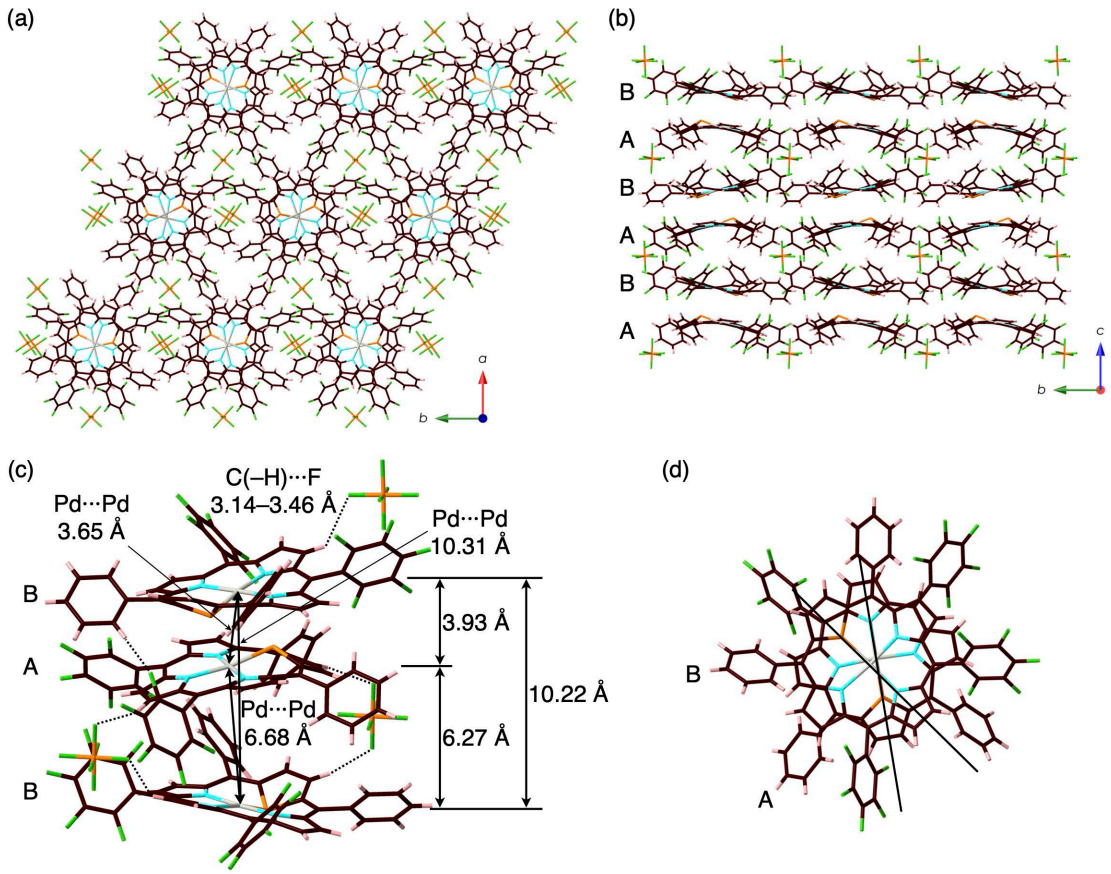

Fig. S28 Packing diagram (stacking assembly) of **2pd**$^{+}$-PF_6^{-} as (a) top and (b) side views and (c) enlarged side and (d) stacked dimer views. Two independent structures are labelled as A and B in (b)–(d). The distances between two **2pd**$^{+}$ and the Pd···Pd distances in the column are 3.93/6.27/10.22 and 3.65/6.68/10.29 Å, respectively. **2pd**$^{+}$ formed the stacked dimer with modestly antiparallel orientation as seen in the lines through S and counter N in (d). Solvent molecules are omitted for clarity. Atom color code: brown, pink, blue, yellow green, light orange, orange, and light gray refer to carbon, hydrogen, nitrogen, fluorine, phosphorus, sulfur, and palladium, respectively.

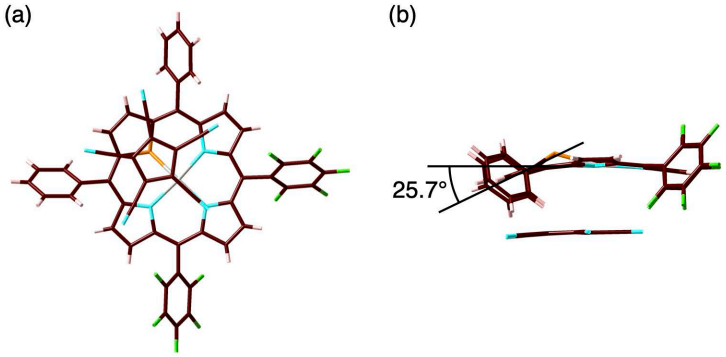

Fig. S29 Crystal structures of **2pd**$^{+}$-$PCCp^{-}$ as (a) top and (b) side views. The dihedral angle between the thiophene plane and the core porphyrin plane (25 atoms) is 25.7°. Mean-plane deviation of the **2pd**$^{+}$ core part (25 atoms) and τ_4 value[S9] are 0.24 Å and 0.13, respectively. Solvent molecules are omitted for clarity. Atom color code: brown, pink, blue, yellow green, orange, and light gray refer to carbon, hydrogen, nitrogen, fluorine, sulfur, and palladium, respectively.

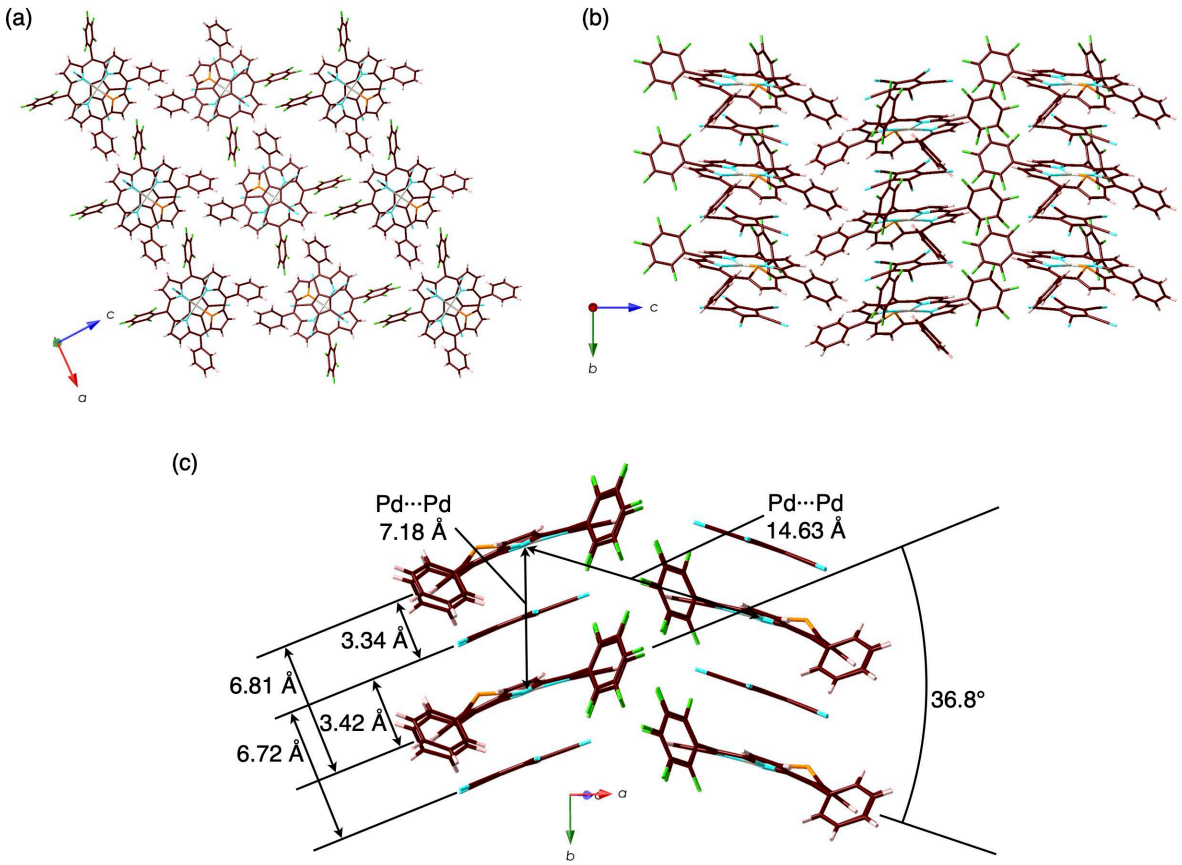

Fig. S30 Packing diagram (stacking assembly) of **2pd**$^{+}$-PCCp^{-} as (a) top and (b) side views and (c) enlarged side view. The stacking distances between **2pd**$^{+}$ (core 25 atoms) and PCCp^{-} are 3.34 and 3.42 Å. The distances between two **2pd**$^{+}$, two PCCp^{-} and the Pd···Pd distances in the column are 6.81, 6.72, and 7.18/14.63 Å, respectively. The dihedral angle between the two core porphyrin planes (25 atoms) is 36.8°. Solvent molecules are omitted for clarity. Atom color code: brown, pink, blue, yellow green, orange, and light gray refer to carbon, hydrogen, nitrogen, fluorine, sulfur, and palladium, respectively.

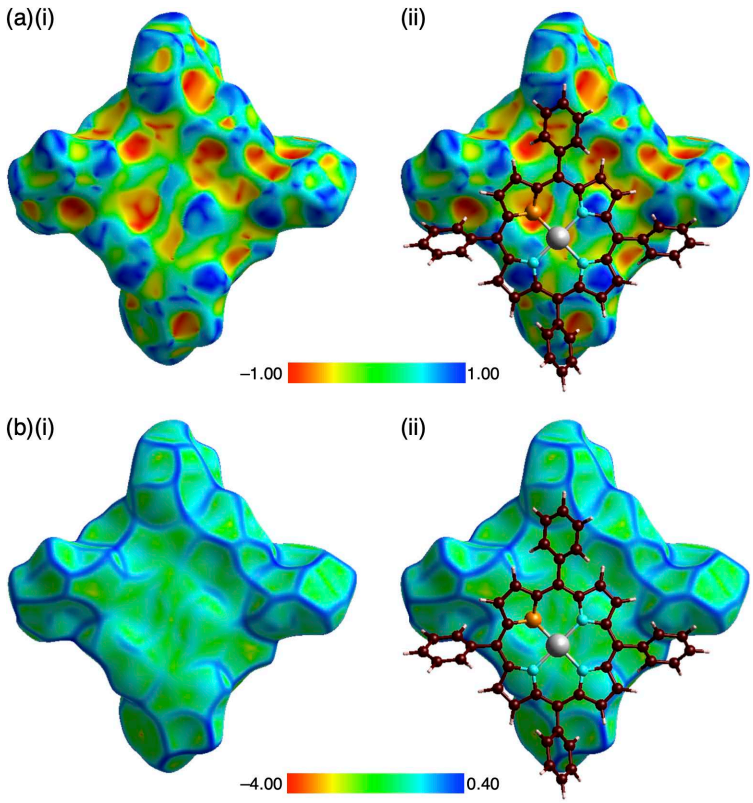

Fig. S31 Hirshfeld surface[S10,11] of **1pd**$^+$ whose sulfur atom is close to the neighboring **1pd**$^+$ in the crystal structure of **1pd**$^+$-BF_4^- (a major disordered structure) mapped over (a) shape-index property and (b) curvedness property: (i) only surface and (ii) surface with a ball-and-stick model of the neighboring **1pd**$^+$. Shape index is a qualitative measure of shape and is sensitive to subtle changes in surface shape, particularly in a flat region by differing by sign represent complementary bumps (blue) and hollows (red), whereas curvedness is a function of the root-mean-square curvature of the surface, and maps of curvedness typically show large regions of green (relatively flat) separated by dark blue edges (large positive curvature). The flat region on the curvedness surface suggested the characteristic mapping pattern for stacking in dimeric **1pd**$^+$. Atom color code: brown, pink, blue, orange, and light gray refer to carbon, hydrogen, nitrogen, sulfur, and palladium, respectively.

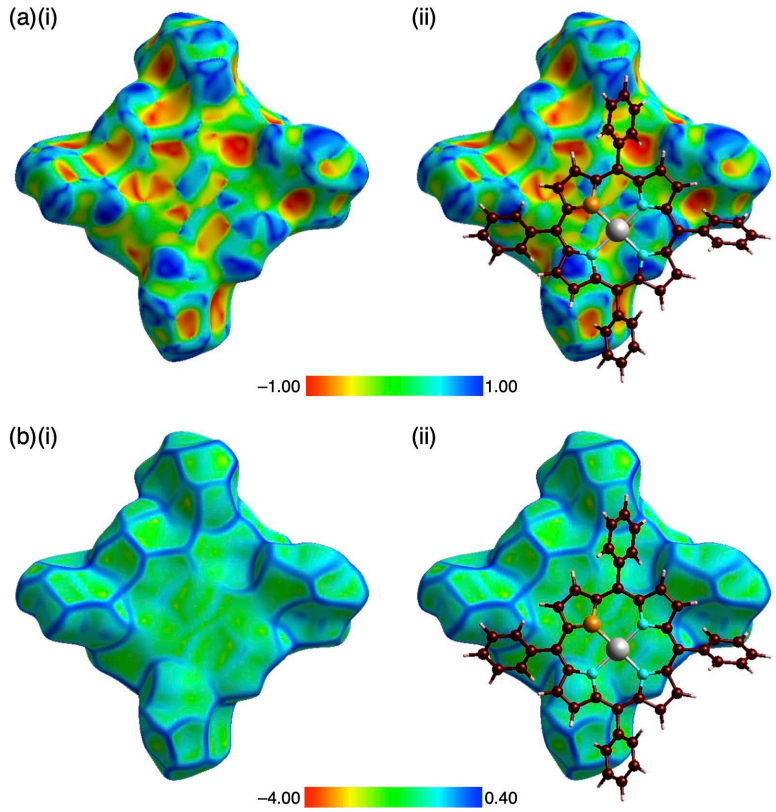

Fig. S32 Hirshfeld surface[S10,11] of **1pd**$^+$ whose sulfur atom is far from the neighboring **1pd**$^+$ in the crystal structure of **1pd**$^+$-BF_4^- (a major disordered structure) mapped over (a) shape-index property and (b) curvedness property: (i) only surface and (ii) surface with a ball-and-stick model of the neighboring **1pd**$^+$. Shape index is a qualitative measure of shape and is sensitive to subtle changes in surface shape, particularly in a flat region by differing by sign represent complementary bumps (blue) and hollows (red), whereas curvedness is a function of the root-mean-square curvature of the surface, and maps of curvedness typically show large regions of green (relatively flat) separated by dark blue edges (large positive curvature). The flat region on the curvedness surface suggested the characteristic mapping pattern for stacking in dimeric **1pd**$^+$. Atom color code: brown, pink, blue, orange, and light gray refer to carbon, hydrogen, nitrogen, sulfur, and palladium, respectively.

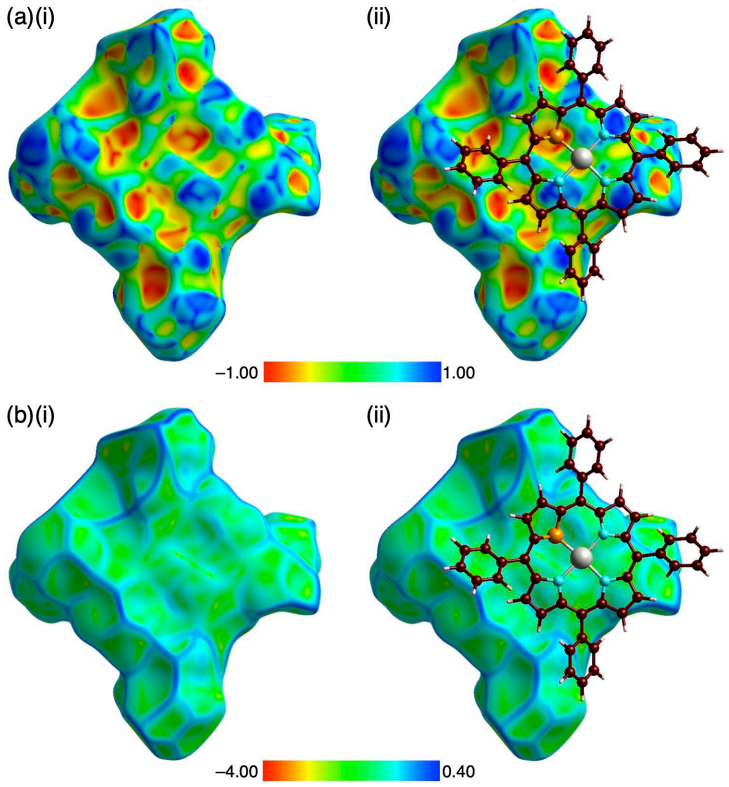

Fig. S33 Hirshfeld surface[S10,11] of **1pd**$^{+}$ in the crystal structure of **1pd**$^{+}$-PF_6^{-} (a major disordered structure) mapped over (a) shape-index property and (b) curvedness property: (i) only surface and (ii) surface with a ball-and-stick model of the neighboring **1pd**$^{+}$. Shape index is a qualitative measure of shape and is sensitive to subtle changes in surface shape, particularly in a flat region by differing by sign represent complementary bumps (blue) and hollows (red), whereas curvedness is a function of the root-mean-square curvature of the surface, and maps of curvedness typically show large regions of green (relatively flat) separated by dark blue edges (large positive curvature). The flat region on the curvedness surface suggested the characteristic mapping pattern for stacking in dimeric **1pd**$^{+}$. Atom color code: brown, pink, blue, orange, and light gray refer to carbon, hydrogen, nitrogen, sulfur, and palladium, respectively.

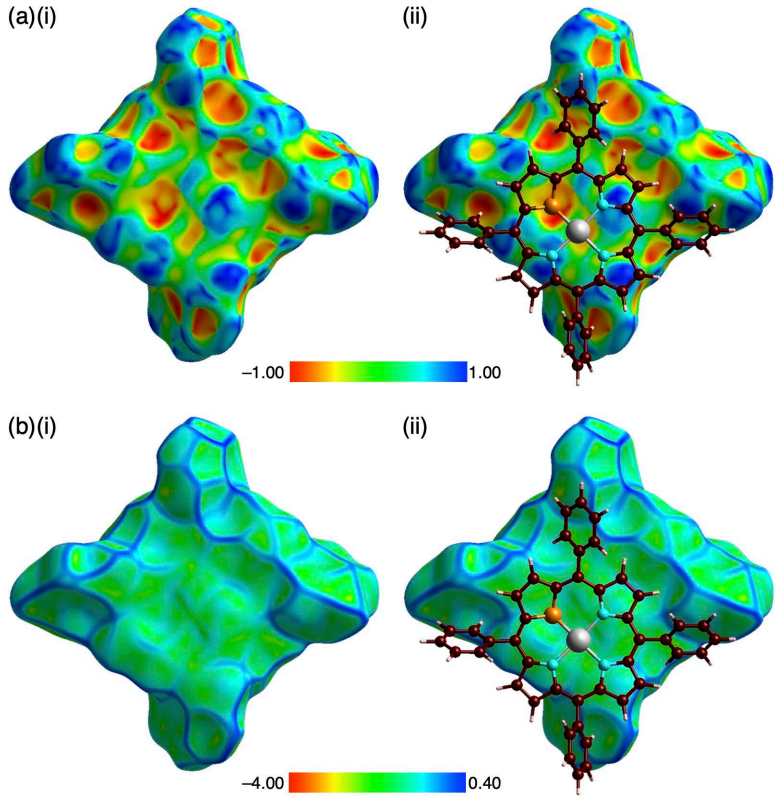

Fig. S34 Hirshfeld surface[S10,11] of **1pd**$^{+}$ in the crystal structure of **1pd**$^{+}$-B(C_6F_5)$_4^{-}$ (a major disordered structure) mapped over (a) shape-index property and (b) curvedness property: (i) only surface and (ii) surface with a ball-and-stick model of the neighboring **1pd**$^{+}$. Shape index is a qualitative measure of shape and is sensitive to subtle changes in surface shape, particularly in a flat region by differing by sign represent complementary bumps (blue) and hollows (red), whereas curvedness is a function of the root-mean-square curvature of the surface, and maps of curvedness typically show large regions of green (relatively flat) separated by dark blue edges (large positive curvature). The flat region on the curvedness surface suggested the characteristic mapping pattern for stacking in dimeric **1pd**$^{+}$. Atom color code: brown, pink, blue, orange, and light gray refer to carbon, hydrogen, nitrogen, sulfur, and palladium, respectively.

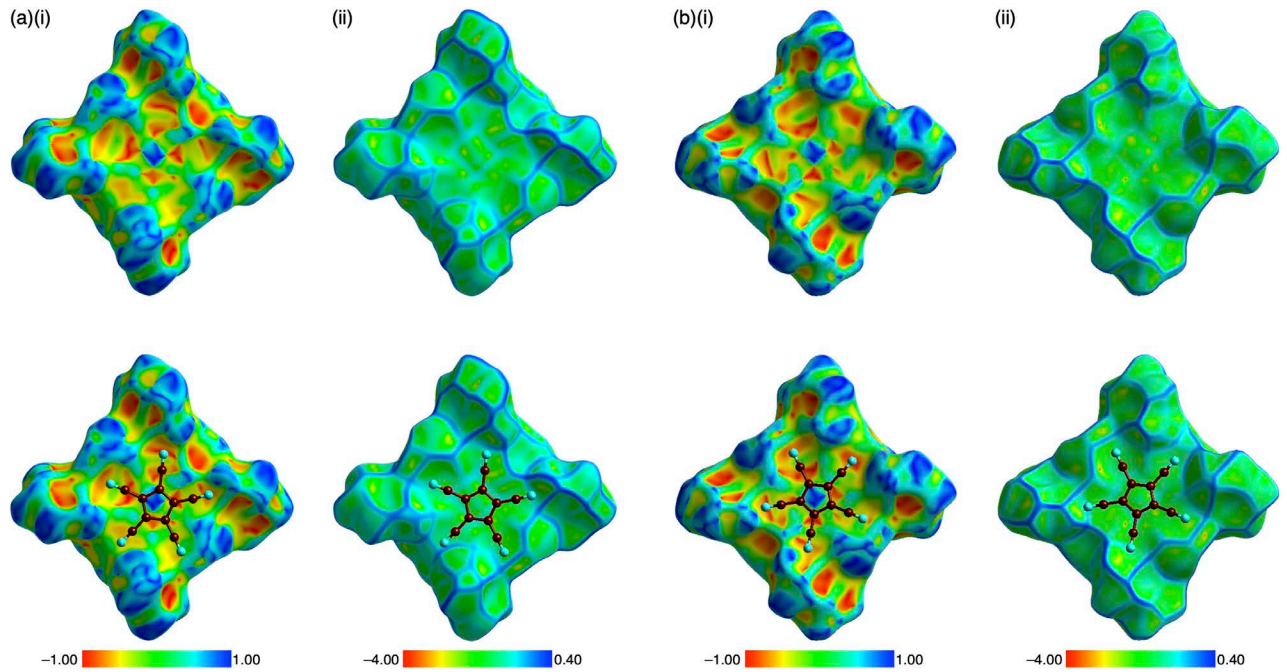

Fig. S35 Hirshfeld surface[S10,11] of **1pd**$^{+}$ whose sulfur atom is far from the PCCp^{-} in the crystal structure of **1pd**$^{+}$-PCCp^{-} (a major disordered structure) as (a) independent structure A and (b) structure B mapped over (i) shape-index and (ii) curvedness properties: only surface (top) and surface with a ball-and-stick model of the neighboring PCCp^{-} (bottom). Shape index is a qualitative measure of shape and is sensitive to subtle changes in surface shape, particularly in a flat region by differing by sign represent complementary bumps (blue) and hollows (red), whereas curvedness is a function of the root-mean-square curvature of the surface, and maps of curvedness typically show large regions of green (relatively flat) separated by dark blue edges (large positive curvature). The surfaces of **1pd**$^{+}$ showed the red and blue triangles arranged in bow-tie shapes on the shape-index surface and flat region on the curvedness surface, indicating the characteristic mapping pattern for $^{i}\pi$–$^{i}\pi$ stacking.[S12] Atom color code: brown and blue refer to carbon and nitrogen, respectively.

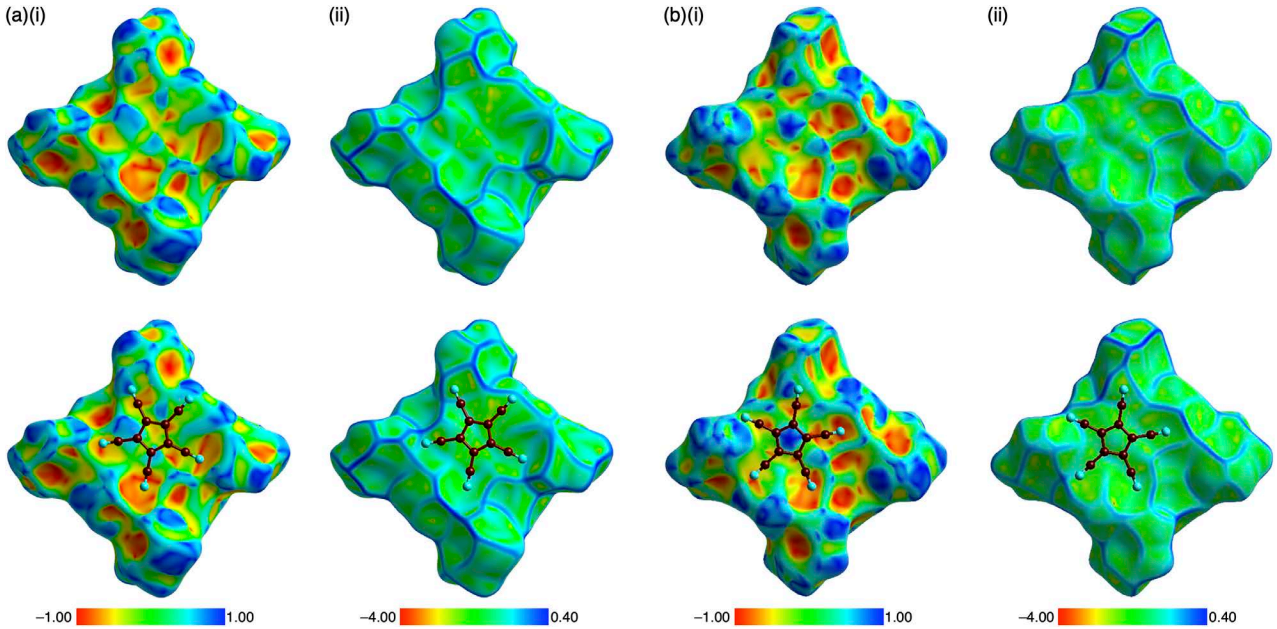

Fig. S36 Hirshfeld surface[S10,11] of **1pd**$^{+}$ whose sulfur atom is close to the PCCp^{-} in the crystal structure of **1pd**$^{+}$-PCCp^{-} (a major disordered structure) as (a) independent structure A and (b) structure B mapped over (i) shape-index and (ii) curvedness properties: only surface (top) and surface with a ball-and-stick model of the neighboring PCCp^{-} (bottom). Shape index is a qualitative measure of shape and is sensitive to subtle changes in surface shape, particularly in a flat region by differing by sign represent complementary bumps (blue) and hollows (red), whereas curvedness is a function of the root-mean-square curvature of the surface, and maps of curvedness typically show large regions of green (relatively flat) separated by dark blue edges (large positive curvature). The flat region on the curvedness surface suggested the characteristic mapping pattern for stacking in **1pd**$^{+}$-PCCp^{-}, whereas bow-tie shapes were not shown in (a) due to the deviated sulfur atom. Atom color code: brown and blue refer to carbon and nitrogen, respectively.

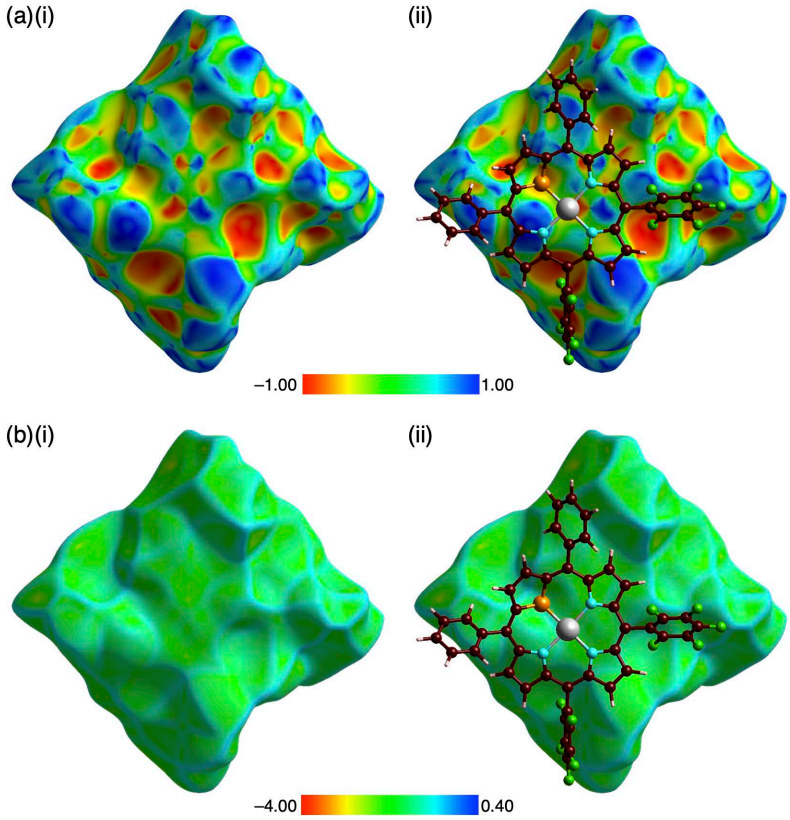

Fig. S37 Hirshfeld surface[S10,11] of **2pd**$^{+}$ whose sulfur atom is far from the neighboring **2pd**$^{+}$ in the crystal structure of **2pd**$^{+}$-BF_4^- (a major disordered structure) mapped over (a) shape-index property and (b) curvedness property: (i) only surface and (ii) surface with a ball-and-stick model of the neighboring **2pd**$^{+}$. Shape index is a qualitative measure of shape and is sensitive to subtle changes in surface shape, particularly in a flat region by differing by sign represent complementary bumps (blue) and hollows (red), whereas curvedness is a function of the root-mean-square curvature of the surface, and maps of curvedness typically show large regions of green (relatively flat) separated by dark blue edges (large positive curvature). The flat region on the curvedness surface suggested the characteristic mapping pattern for stacking in dimeric **1pd**$^{+}$. Atom color code: brown, pink, blue, yellow green, orange, and light gray refer to carbon, hydrogen, nitrogen, fluorine, sulfur, and palladium, respectively.

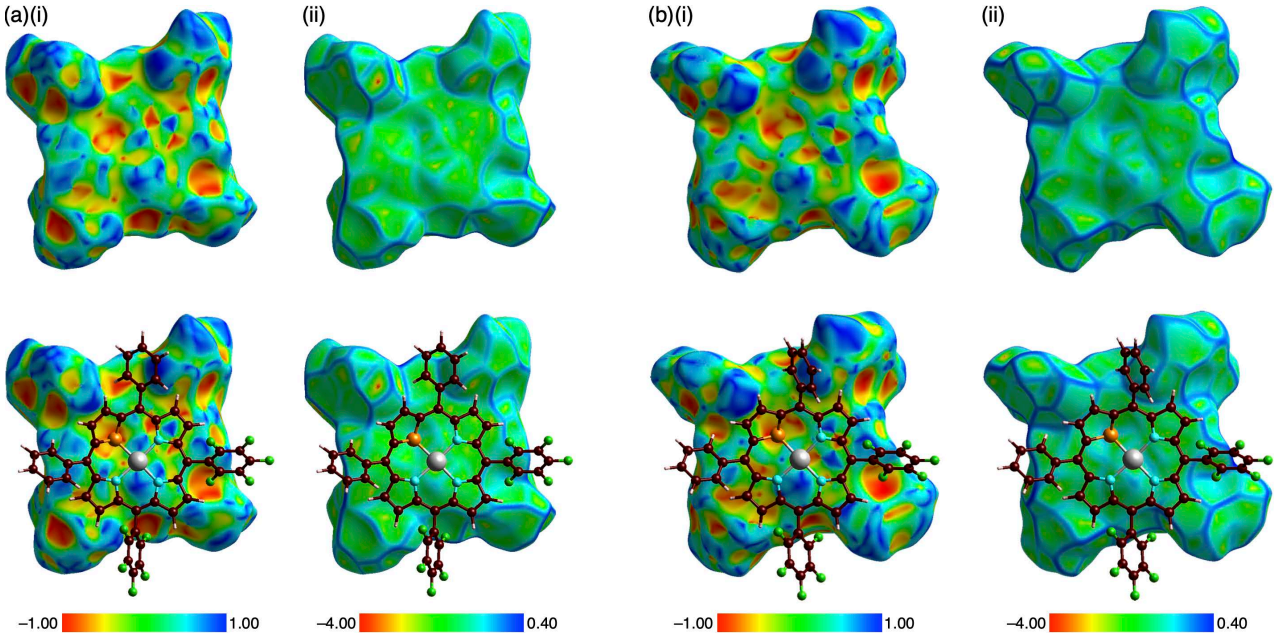

Fig. S38 Hirshfeld surface[S10,11] of **2pd**$^{+}$ in the crystal structure of **2pd**$^{+}$-PF_6^{-} (a major disordered structure) as (a) independent structure A and (b) structure B mapped over (i) shape-index and (ii) curvedness properties: only surface (top) and surface with a ball-and-stick model of the neighboring **2pd**$^{+}$ (bottom). Shape index is a qualitative measure of shape and is sensitive to subtle changes in surface shape, particularly in a flat region by differing by sign represent complementary bumps (blue) and hollows (red), whereas curvedness is a function of the root-mean-square curvature of the surface, and maps of curvedness typically show large regions of green (relatively flat) separated by dark blue edges (large positive curvature). The surfaces of **2pd**$^{+}$ showed the red and blue triangles arranged in bow-tie shapes on the shape-index surface and flat region on the curvedness surface, indicating the characteristic mapping pattern for $^{i}\pi$–$^{i}\pi$ stacking.[S12] Atom color code: brown, pink, blue, yellow green, orange, and light gray refer to carbon, hydrogen, nitrogen, fluorine, sulfur, and palladium, respectively.

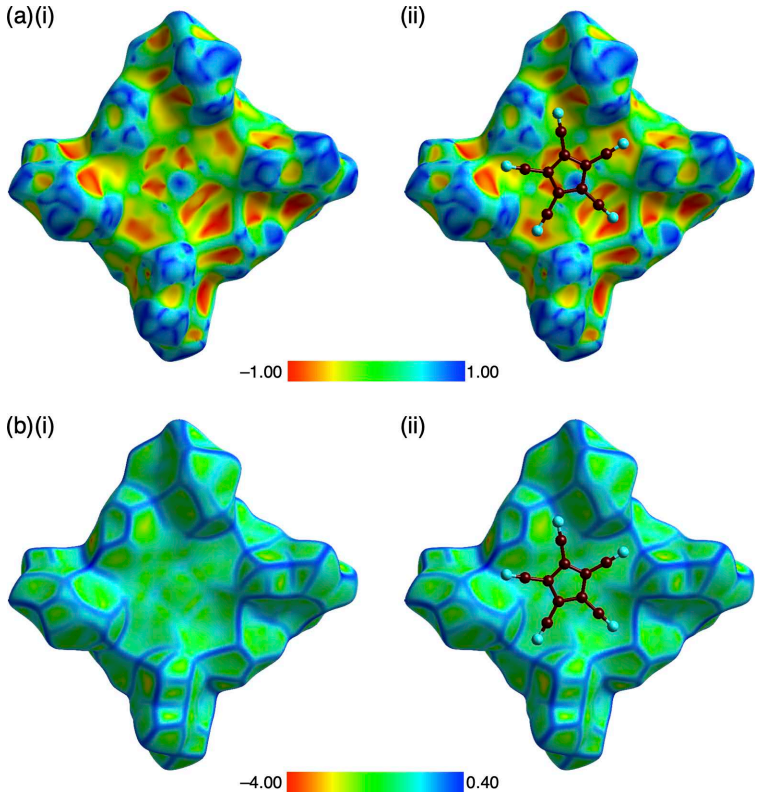

Fig. S39 Hirshfeld surface[S10,11] of **2pd**$^{+}$ whose sulfur atom is far from the PCCp^{-} in the crystal structure of **2pd**$^{+}$-PCCp^{-} (a major disordered structure) mapped over (a) shape-index property and (b) curvedness property: (i) only surface and (ii) surface with a ball-and-stick model of the neighboring PCCp^{-}. Shape index is a qualitative measure of shape and is sensitive to subtle changes in surface shape, particularly in a flat region by differing by sign represent complementary bumps (blue) and hollows (red), whereas curvedness is a function of the root-mean-square curvature of the surface, and maps of curvedness typically show large regions of green (relatively flat) separated by dark blue edges (large positive curvature). The surfaces of **2pd**$^{+}$ showed the red and blue triangles arranged in bow-tie shapes on the shape-index surface and flat region on the curvedness surface, indicating the characteristic mapping pattern for $^{i}\pi$–$^{i}\pi$ stacking.[S12] Atom color code: brown and blue refer to carbon and nitrogen, respectively.

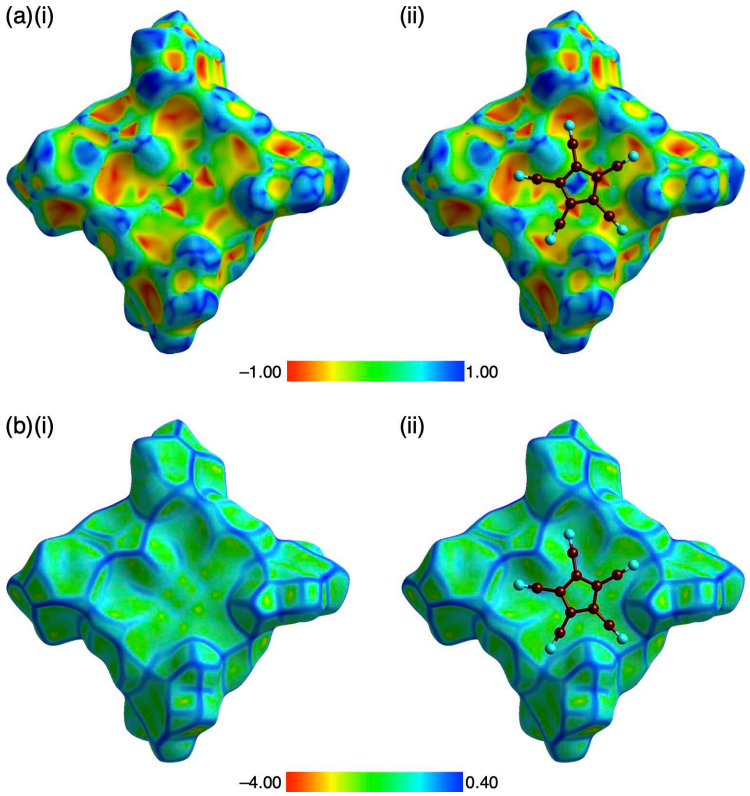

Fig. S40 Hirshfeld surface[S10,11] of **2pd**$^{+}$ whose sulfur atom is close to the PCCp^{-} in the crystal structure of **2pd**$^{+}$-PCCp^{-} (a major disordered structure) mapped over (a) shape-index property and (b) curvedness property: (i) only surface and (ii) surface with a ball-and-stick model of the neighboring PCCp^{-}. Shape index is a qualitative measure of shape and is sensitive to subtle changes in surface shape, particularly in a flat region by differing by sign represent complementary bumps (blue) and hollows (red), whereas curvedness is a function of the root-mean-square curvature of the surface, and maps of curvedness typically show large regions of green (relatively flat) separated by dark blue edges (large positive curvature). The flat region on the curvedness surface suggested the characteristic mapping pattern for stacking in **2pd**$^{+}$-PCCp^{-}, whereas bow-tie shapes were not shown in (a) due to the deviated sulfur atom. Atom color code: brown and blue refer to carbon and nitrogen, respectively.

[S5] K. Sugimoto, H. Ohsumi, S. Aoyagi, E. Nishibori, C. Moriyoshi, Y. Kuroiwa, H. Sawa and M. Takata, *AIP Conf. Proc.*, 2010, **1234**, 887–890.
[S6] (a) N. Yasuda, H. Murayama, Y. Fukuyama, J. E. Kim, S. Kimura, K. Toriumi, Y. Tanaka, Y. Moritomo, Y. Kuroiwa, K. Kato, H. Tanaka and M. Takata, *J. Synchrotron Rad.*, 2009, **16**, 352–357; (b) N. Yasuda, Y. Fukuyama, K. Toriumi, S. Kimura and M. Takata, *AIP Conf. Proc.*, 2010, **1234**, 147–150.
[S7] G. M. Sheldrick, *Acta Crystallogr. Sect. A*, 2008, **64**, 112–122.
[S8] (a) *Yadokari-XG*, *Software for Crystal Structure Analyses*, K. Wakita, 2001; (b) C. Kabuto, S. Akine, T. Nemoto and E. Kwon, *J. Cryst. Soc. Jpn.*, 2009, **51**, 218–224.
[S9] L. Yang, D. R. Powell and R. P. Houser, *Dalton Trans.*, 2007, 955–964.
[S10] P. R. Spackman, M. J. Turner, J. J. McKinnon, S. K. Wolff, D. J. Grimwood, D. Jayatilaka and M. A. Spackman, *J. Appl. Cryst.*, 2021, **54**, 1006–1011.
[S11] (a) M. A. Spackman and D. Jayatilaka, *CrystEngComm*, 2009, **11**, 19–32; (b) J. J. McKinnon, M. A. Spackman and A. S. Mitchell, *Acta Crystallogr. Sect. B*, 2004, **60**, 627–668.
[S12] Y. Sasano, H. Tanaka, Y. Haketa, Y. Kobayashi, Y. Ishibashi, T. Morimoto, R. Sato, Y. Shigeta, N. Yasuda, T. Asahi and H. Maeda, *Chem. Sci.*, 2021, **12**, 9645–9657.

3. Theoretical studies

DFT calculations. DFT calculations were carried out using *Gaussian 16* program.[S13]

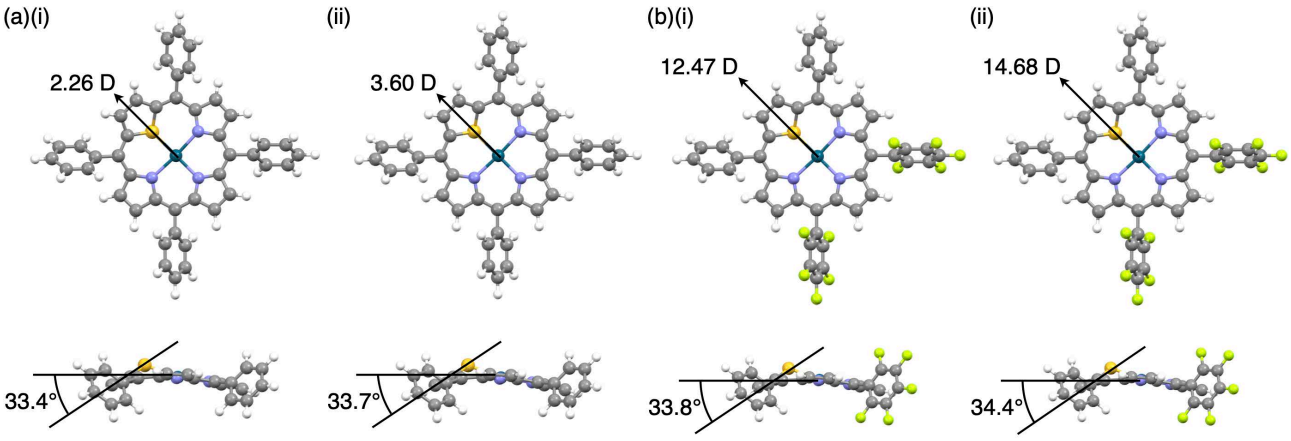

Fig. S41 Optimized structures of (a) **1pd**$^+$ and (b) **2pd**$^+$ at (i) B3LYP/6-31+G(d,p) with LanL2DZ for Pd and (ii) PCM-B3LYP/6-31+G(d,p) with LanL2DZ for Pd (CH_2Cl_2) as top (top) and side (bottom) views. The dipole moments and the dihedral angles between the thiophene plane and the core porphyrin plane (25 atoms) are 2.26/3.60/12.47/14.68 D and 33.4°/33.7°/33.8°/34.4°, respectively. Mean-plane deviation of the core part (25 atoms) and τ_4 value[S9] are 0.30/0.30/0.29/0.29 Å and 0.13/0.13/0.12/0.12, respectively.

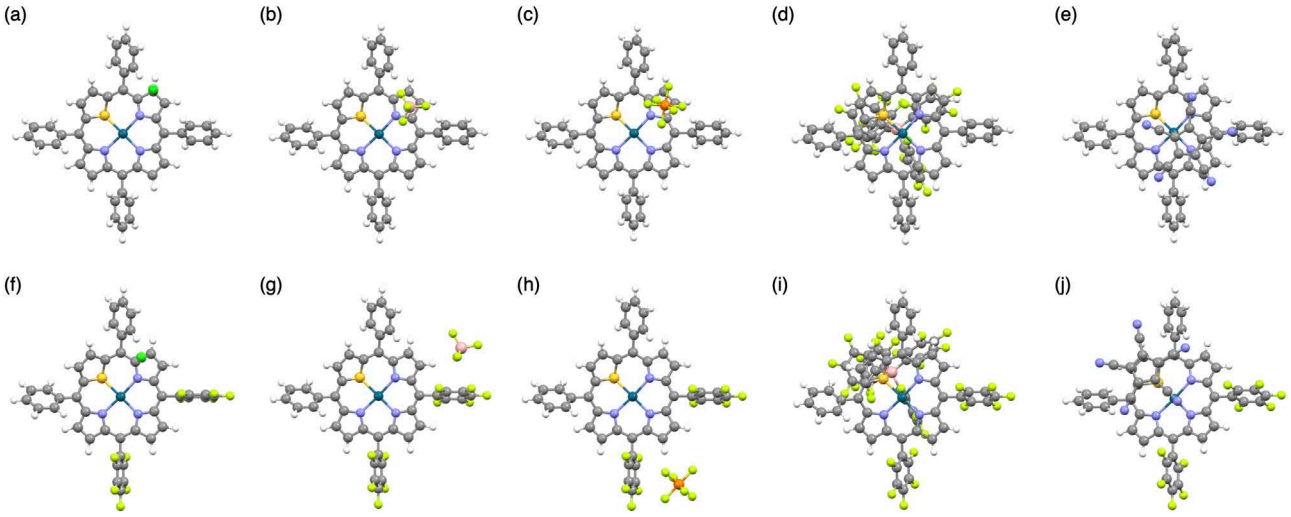

Fig. S42 Optimized structures of (a) **1pd**$^+$-Cl^-, (b) **1pd**$^+$-BF_4^-, (c) **1pd**$^+$-PF_6^-, (d) **1pd**$^+$-$B(C_6F_5)_4^-$, (e) **1pd**$^+$-$PCCp^-$, (f) **2pd**$^+$-Cl^-, (g) **2pd**$^+$-BF_4^-, (h) **2pd**$^+$-PF_6^-, (i) **2pd**$^+$-$B(C_6F_5)_4^-$, and (j) **2pd**$^+$-$PCCp^-$. **1pd**$^+$-X^- (X^- = Cl^-, BF_4^-, PF_6^-, $B(C_6F_5)_4^-$, $PCCp^-$) and **2pd**$^+$-X (X^- = Cl^-, BF_4^-, PF_6^-, $PCCp^-$) were calculated at PCM-B3LYP/6-31+G(d,p) (CH_2Cl_2) with LanL2DZ for Pd (CH_2Cl_2), whereas **2pd**$^+$-$B(C_6F_5)_4^-$ were calculated at PCM-B3LYP/6-31G(d,p) with LanL2DZ for Pd (CH_2Cl_2). Crystal structures (Fig. S10–16) were used for the initial structures for the optimization of **1pd**$^+$-BF_4^-, **1pd**$^+$-PF_6^-, **1pd**$^+$-$PCCp^-$, **1pd**$^+$-$B(C_6F_5)_4^-$, **2pd**$^+$-BF_4^-, **2pd**$^+$-PF_6^-, and **2pd**$^+$-$PCCp^-$, whereas the structure of **1pd**$^+$-$B(C_6F_5)_4^-$ was used for the initial structure for the optimization of **2pd**$^+$-$B(C_6F_5)_4^-$. The initial structures of **1pd**$^+$-Cl^- and **2pd**$^+$-Cl^- were arranged based on the geometry of the optimized structure of **1pd**$^+$-PF_6^-.

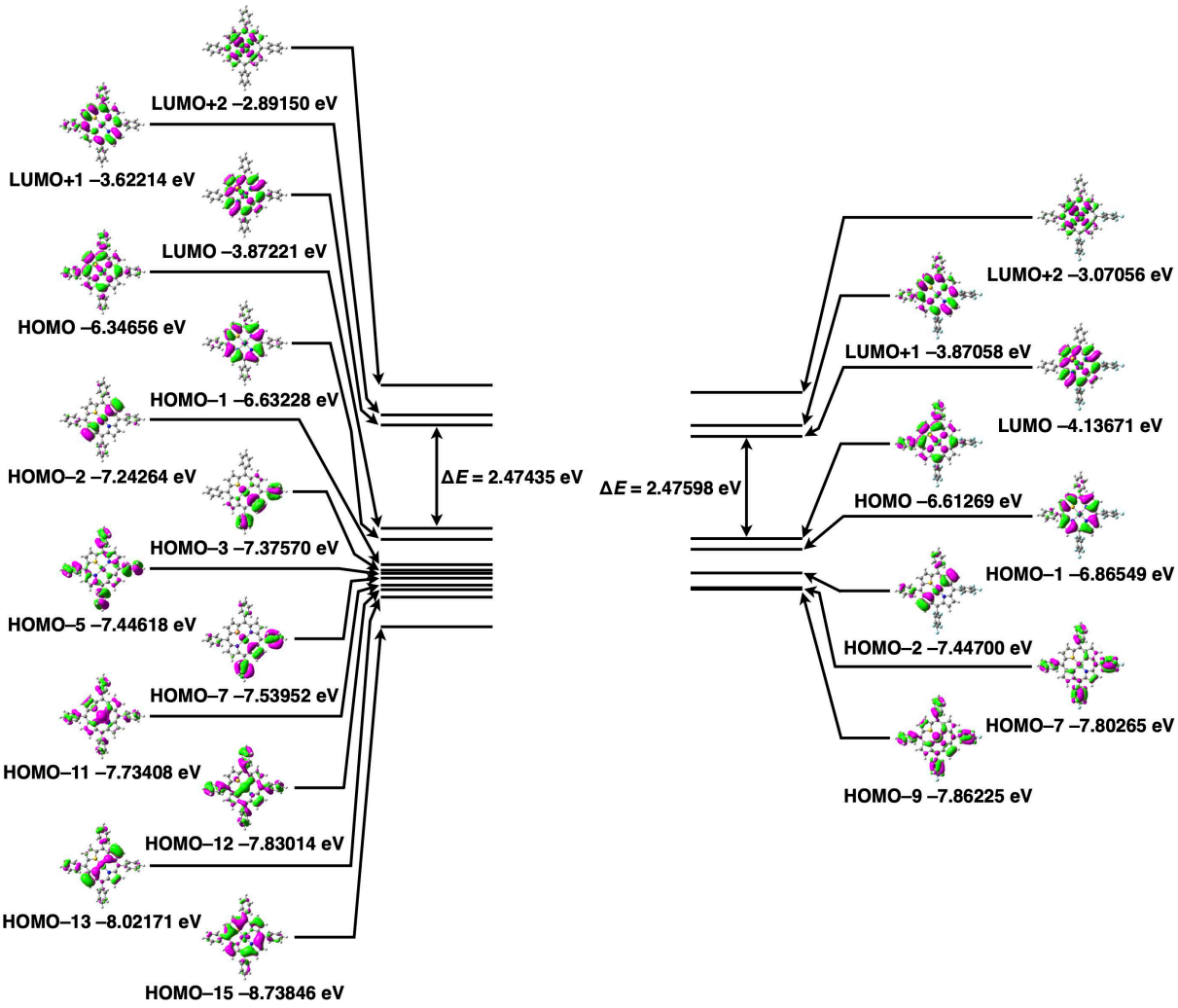

Fig. S43 Molecular orbitals (HOMO/LUMO) of **1pd**$^{+}$ (left) and **2pd**$^{+}$ (right) estimated at PCM-B3LYP/6-31+G(d,p) with LanL2DZ for Pd (CH_2Cl_2).

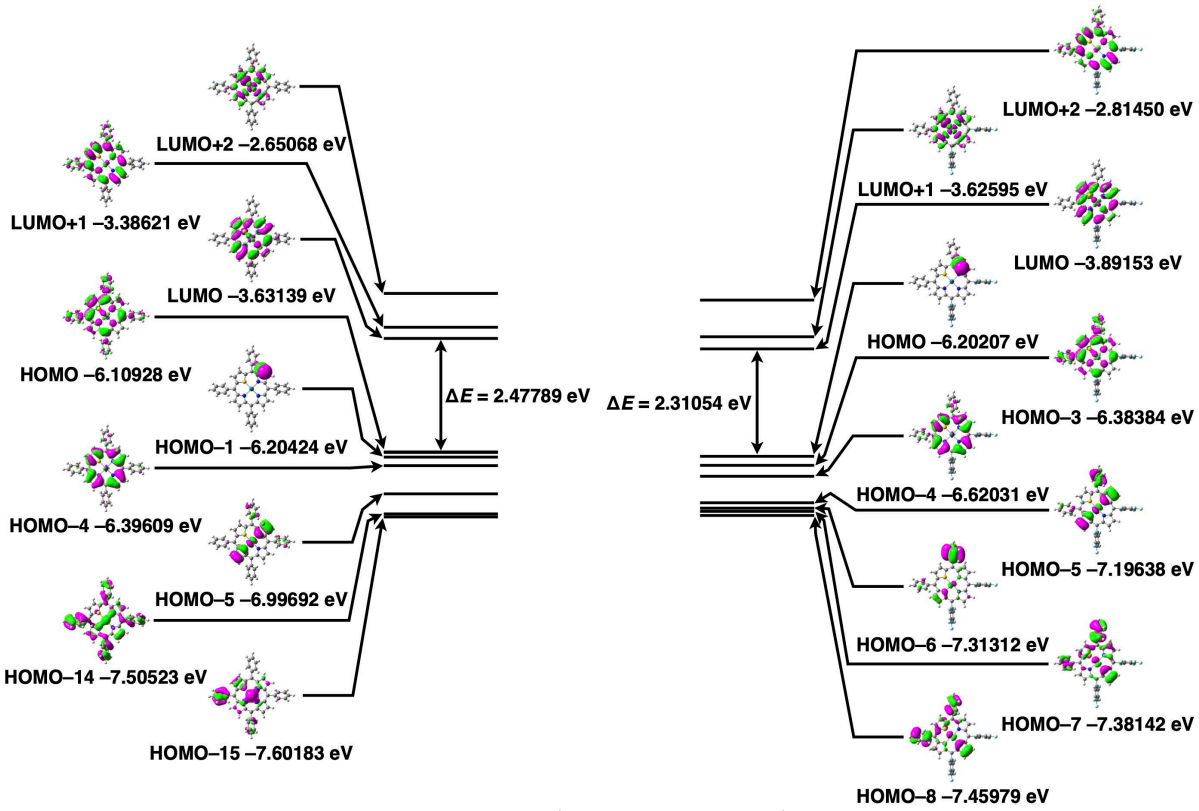

Fig. S44 Molecular orbitals (HOMO/LUMO) of **1pd**$^{+}$-Cl^{-} (left) and **2pd**$^{+}$-Cl^{-} (right) estimated at PCM-B3LYP/6-31+G(d,p) with LanL2DZ for Pd (CH_2Cl_2).

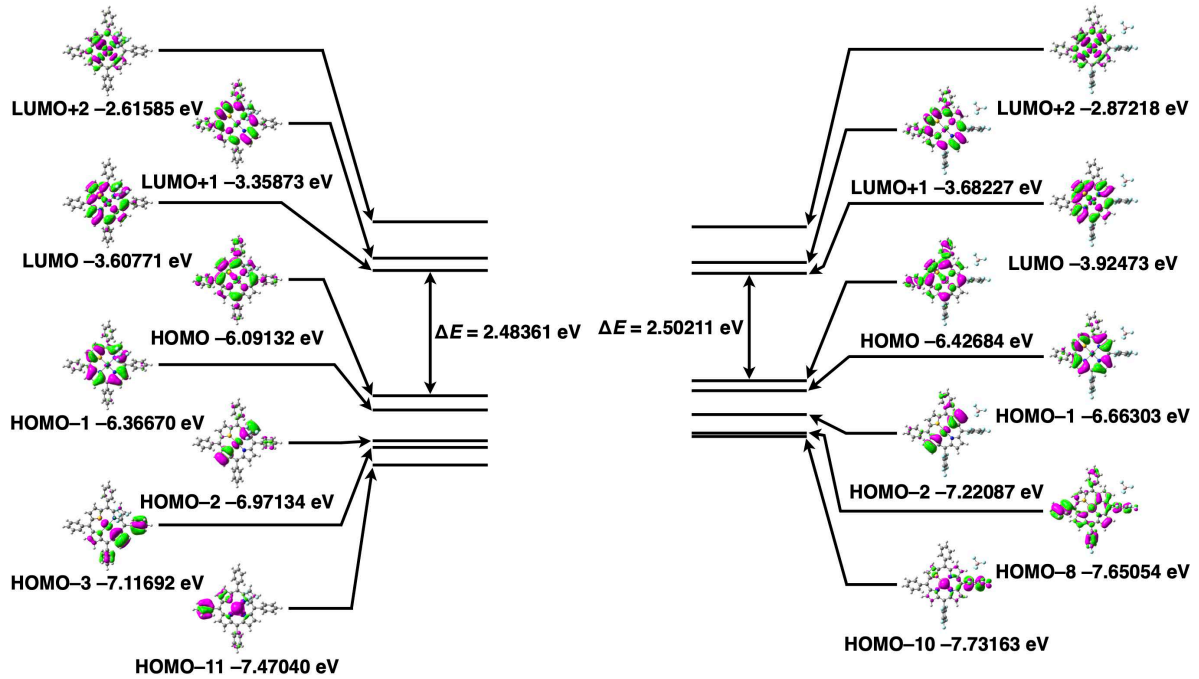

Fig. S45 Molecular orbitals (HOMO/LUMO) of **1pd**$^{+}$-BF_4^{-} (left) and **2pd**$^{+}$-BF_4^{-} (right) estimated at PCM-B3LYP/6-31+G(d,p) with LanL2DZ for Pd (CH_2Cl_2).

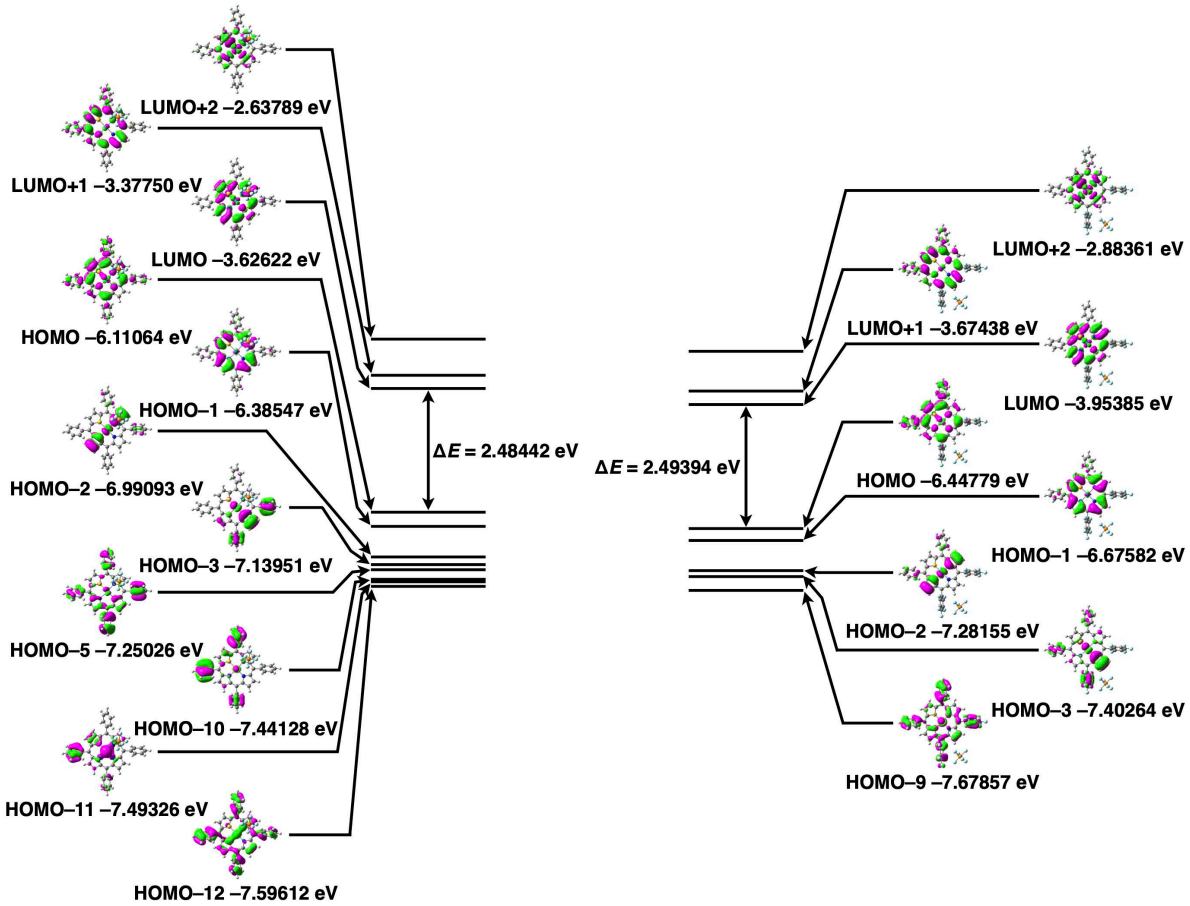

Fig. S46 Molecular orbitals (HOMO/LUMO) of **1pd**$^{+}$-PF_6^- (left) and **2pd**$^{+}$-PF_6^- (right) estimated at PCM-B3LYP/6-31+G(d,p) with LanL2DZ for Pd (CH_2Cl_2).

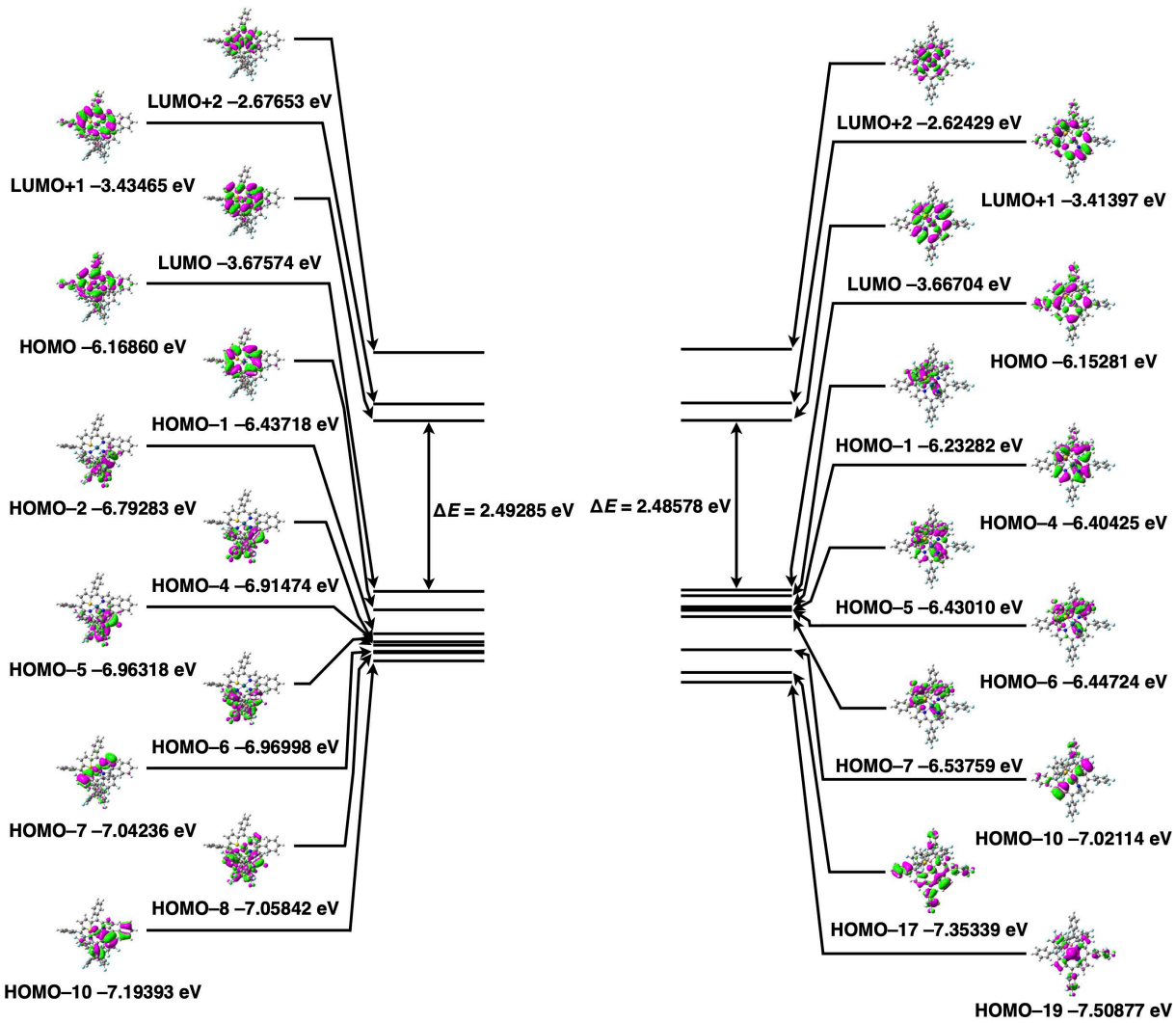

Fig. S47 Molecular orbitals (HOMO/LUMO) of **1pd**$^{+}$-B(C_6F_5)$_4^-$ (left) and **2pd**$^{+}$-B(C_6F_5)$_4^-$ (right) estimated at PCM-B3LYP/6-31+G(d,p) and B3LYP/6-31G(d,p), respectively, with LanL2DZ for Pd (CH_2Cl_2).

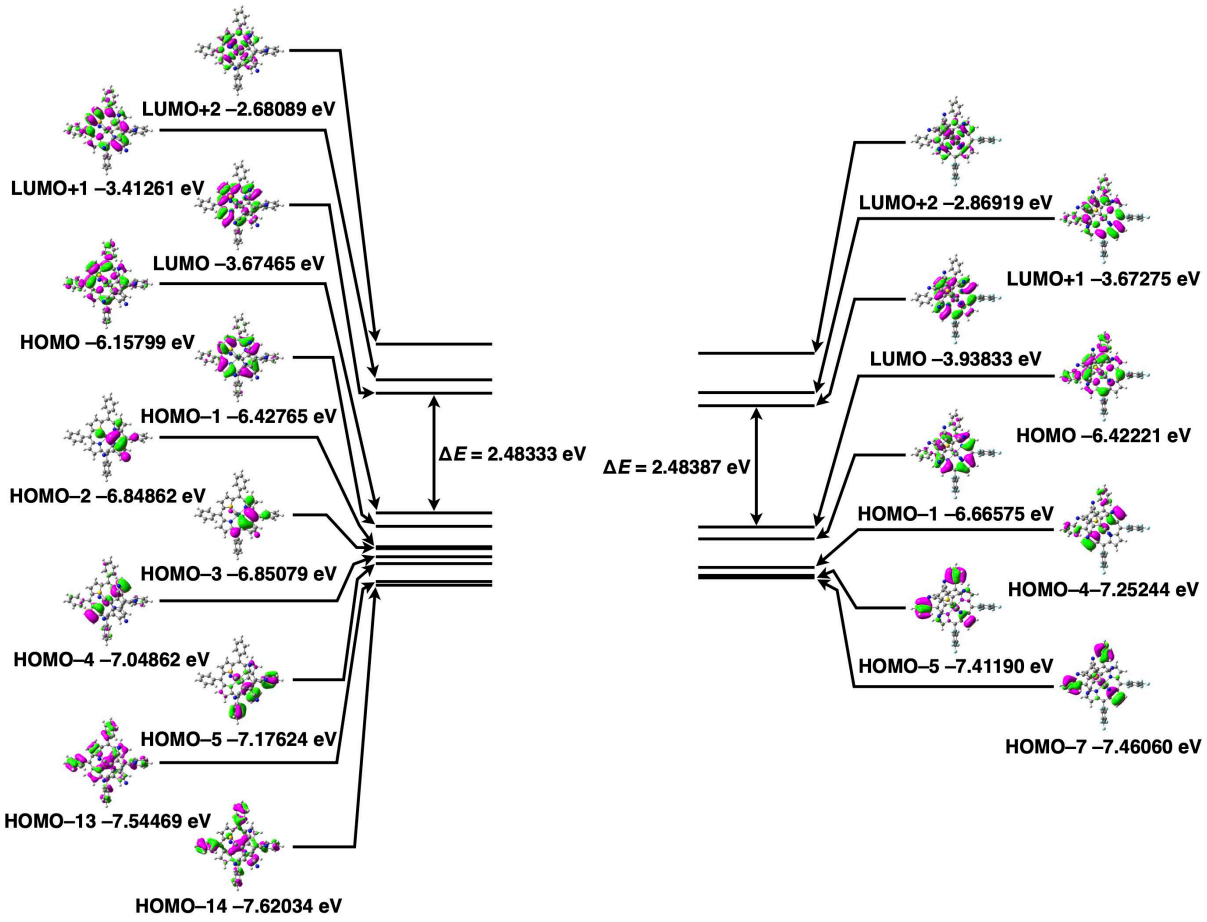

Fig. S48 Molecular orbitals (HOMO/LUMO) of **1pd**$^{+}$-PCCp^{-} (left) and **2pd**$^{+}$-PCCp^{-} (right) estimated at PCM-B3LYP/6-31+G(d,p) with LanL2DZ for Pd (CH_2Cl_2).

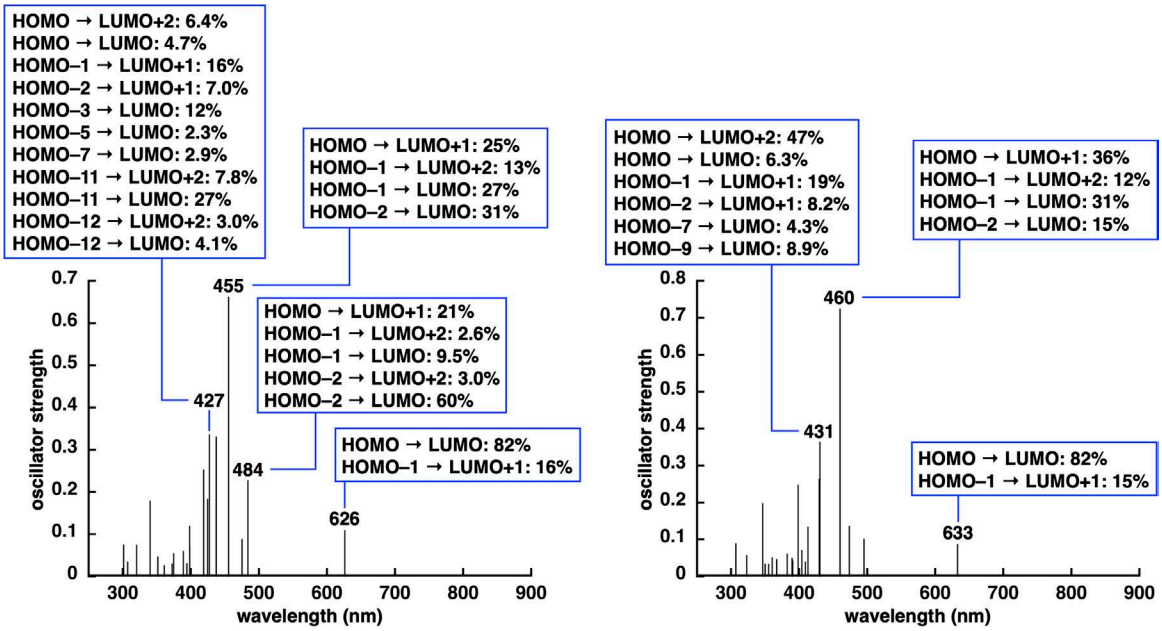

Fig. S49 TD-DFT-based UV/vis absorption stick spectra of **1pd**$^{+}$ (left) and **2pd**$^{+}$ (right) with the transitions correlated with molecular orbitals estimated at PCM-B3LYP/6-31+G(d,p) with LanL2DZ for Pd (CH_2Cl_2).

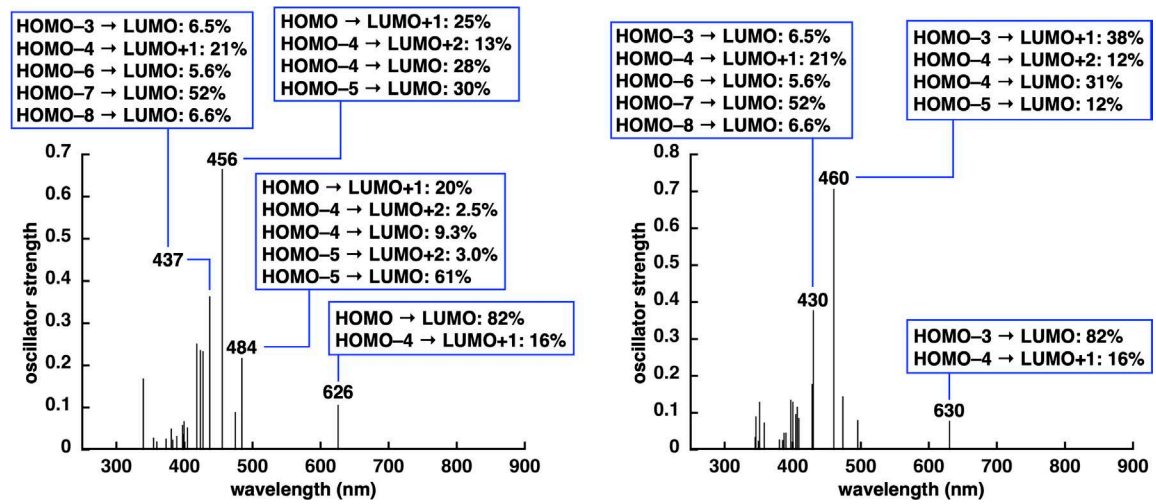

Fig. S50 TD-DFT-based UV/vis absorption stick spectra of **1pd**$^{+}$-Cl^{-} (left) and **2pd**$^{+}$-Cl^{-} (right) with the transitions correlated with molecular orbitals estimated at PCM-B3LYP/6-31+G(d,p) with LanL2DZ for Pd (CH_2Cl_2).

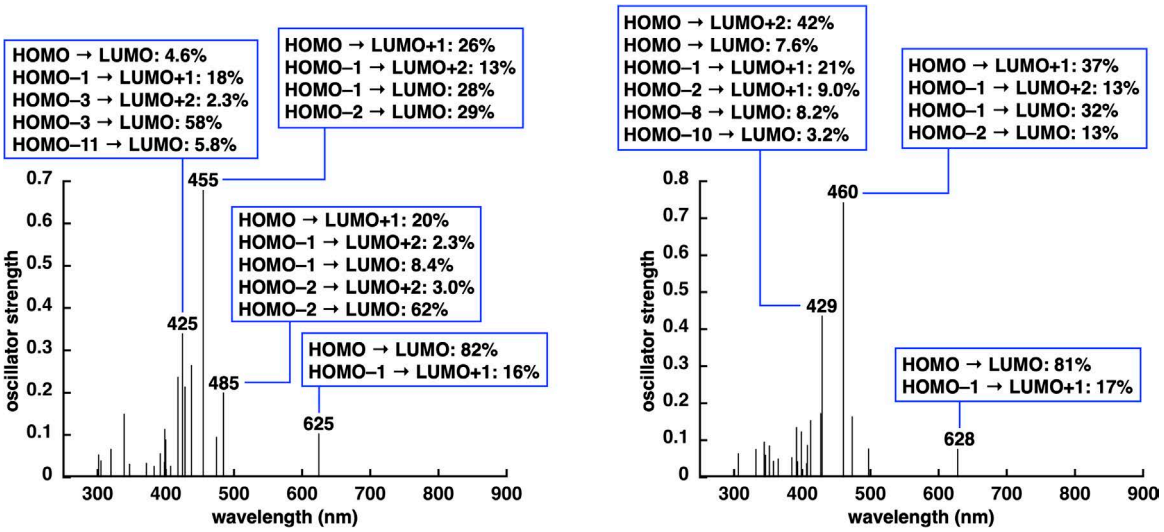

Fig. S51 TD-DFT-based UV/vis absorption stick spectra of **1pd**$^{+}$-BF_4^{-} (left) and **2pd**$^{+}$-BF_4^{-} (right) with the transitions correlated with molecular orbitals estimated at PCM-B3LYP/6-31+G(d,p) with LanL2DZ for Pd (CH_2Cl_2).

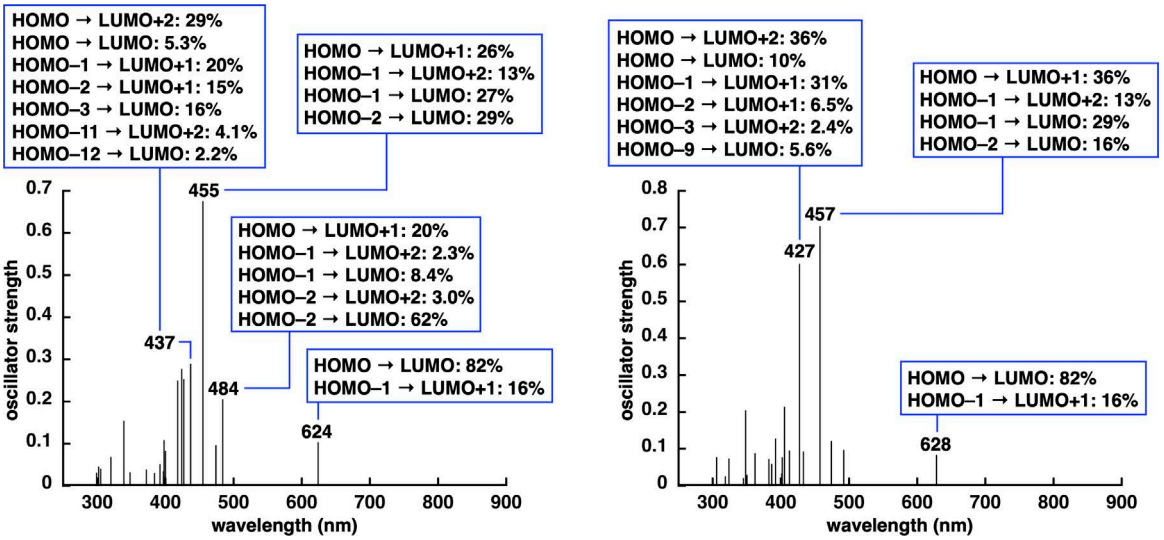

Fig. S52 TD-DFT-based UV/vis absorption stick spectra of **1pd**$^{+}$-PF_6^{-} (left) and **2pd**$^{+}$-PF_6^{-} (right) with the transitions correlated with molecular orbitals estimated at PCM-B3LYP/6-31+G(d,p) with LanL2DZ for Pd (CH_2Cl_2).

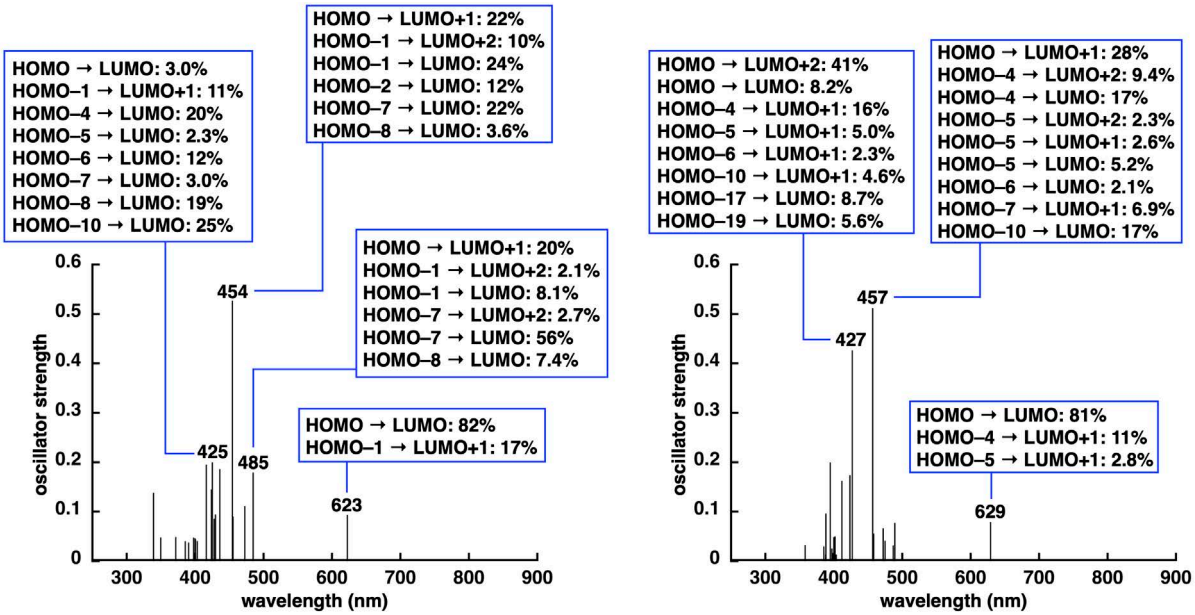

Fig. S53 TD-DFT-based UV/vis absorption stick spectra of **1pd**$^{+}$-B(C_6F_5)$_4^-$ (left) and **2pd**$^{+}$-B(C_6F_5)$_4^-$ (right) with the transitions correlated with molecular orbitals estimated at PCM-B3LYP/6-31+G(d,p) and B3LYP/6-31G(d,p), respectively, with LanL2DZ for Pd (CH_2Cl_2).

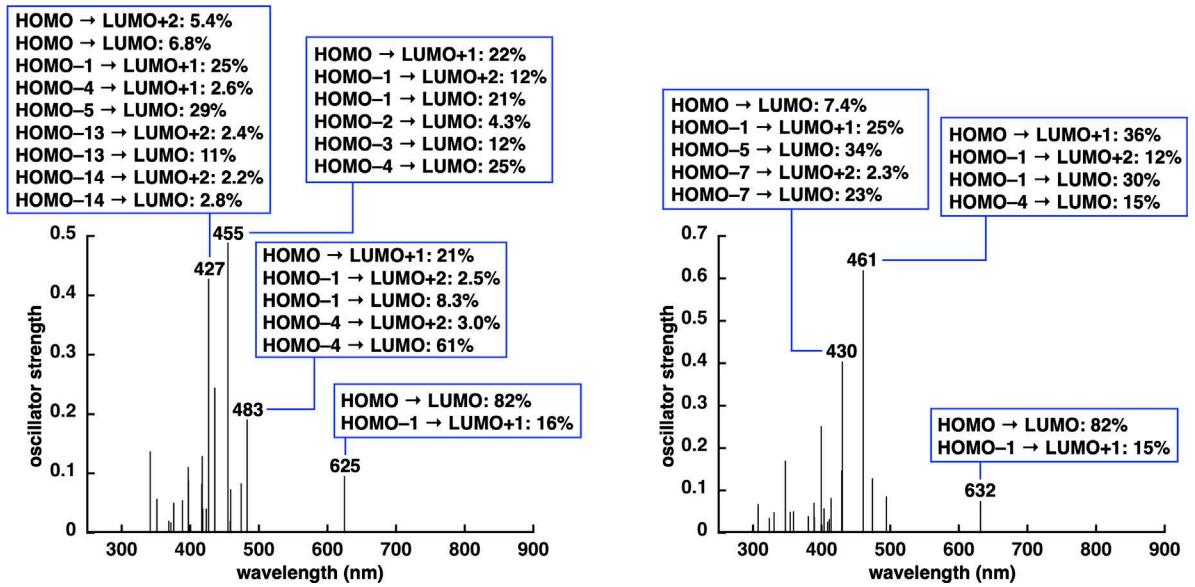

Fig. S54 TD-DFT-based UV/vis absorption stick spectra of **1pd**$^{+}$-PCCp$^-$ (left) and **2pd**$^{+}$-PCCp$^-$ (right) with the transitions correlated with molecular orbitals estimated at PCM-B3LYP/6-31+G(d,p) with LanL2DZ for Pd (CH_2Cl_2).

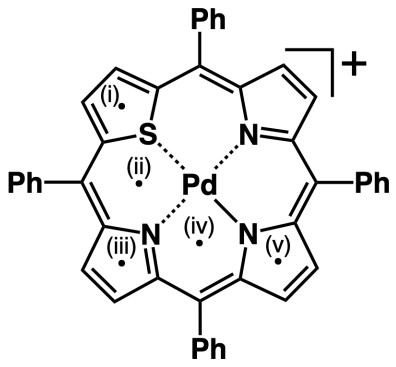

NICS(0)	NICS(1)	NICS(–1)
(i) –18.63	(i) –11.71	(i) –21.67
(ii) –17.63	(ii) –14.28	(ii) –17.13
(iii) –4.40	(iii) –8.15	(iii) –6.64
(iv) –16.23	(iv) –14.08	(iv) –14.87
(v) –4.31	(v) –6.41	(v) –8.29

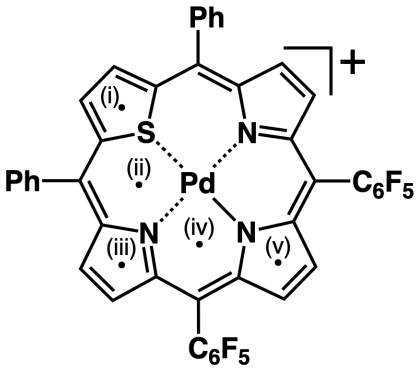

NICS(0)	NICS(1)	NICS(–1)
(i) –19.00	(i) –11.67	(i) –22.53
(ii) –18.07	(ii) –18.29	(ii) –18.29
(iii) –3.86	(iii) –7.56	(iii) –6.43
(iv) –17.36	(iv) –14.94	(iv) –15.65
(v) –3.74	(v) –6.31	(v) –7.40

Fig. S55 NICS values (ppm)[S14] of **1pd**$^+$ (top) and **2pd**$^+$ (bottom) based on the optimized structures at PCM-B3LYP/6-31+G(d,p) with LanL2DZ for Pd (CH_2Cl_2) (Fig. S41): the sides with the deviated sulfur atoms (NICS (1)) and the sides without the deviated sulfur atoms (NICS (–1)).

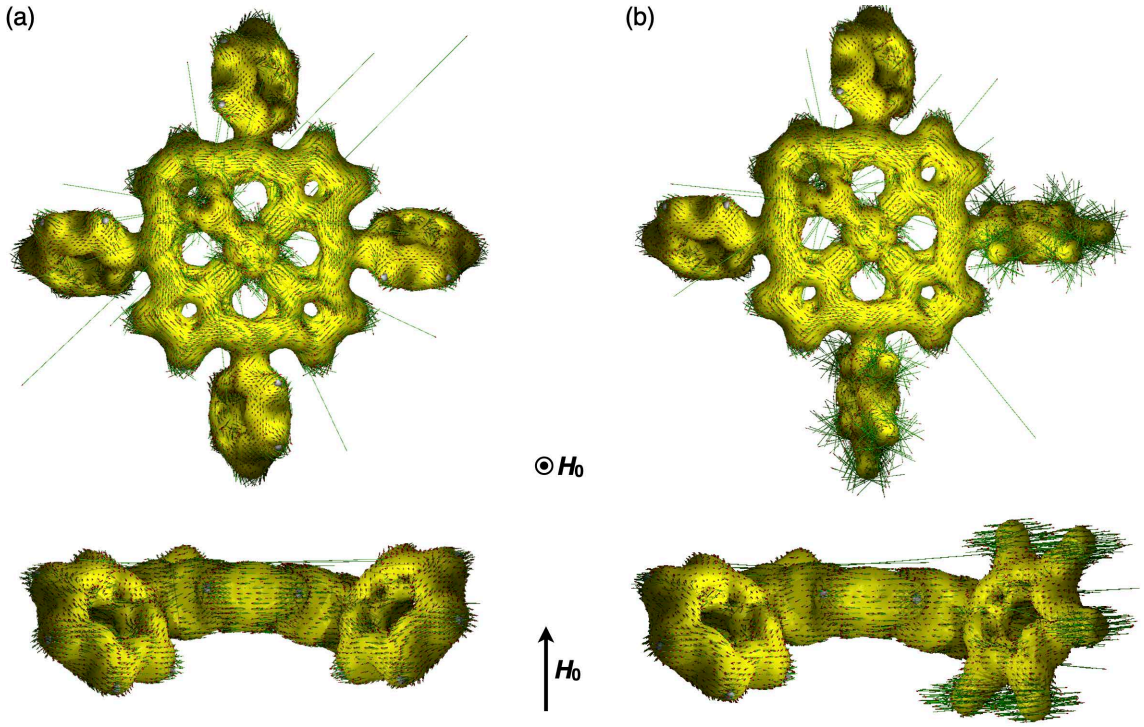

Fig. S56 Anisotropy of the induced current density (ACID)[S15] of (a) **1pd**$^+$ and (b) **2pd**$^+$ (top and side views) at isosurface value of δ = 0.015 based on the optimized structures at PCM-B3LYP/6-31+G(d,p) with LanL2DZ for Pd (CH_2Cl_2) (Fig. S41). Current density vectors are plotted on to the ACID isosurface based on the vector of the magnetic field (H_0) which is orthogonal with respect to the molecule. The theoretical results were consistent with the NICS values (Fig. S55).

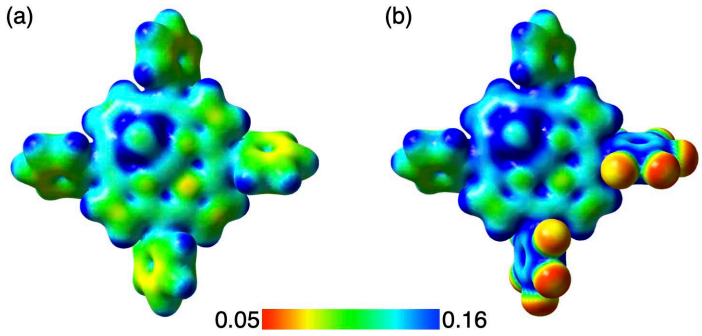

Fig. S57 Electrostatic potential (ESP) mapping (δ = 0.01) of (a) **1pd**$^{+}$ and (b) **2pd**$^{+}$ at B3LYP/6-31+G(d,p) with LanL2DZ for Pd.

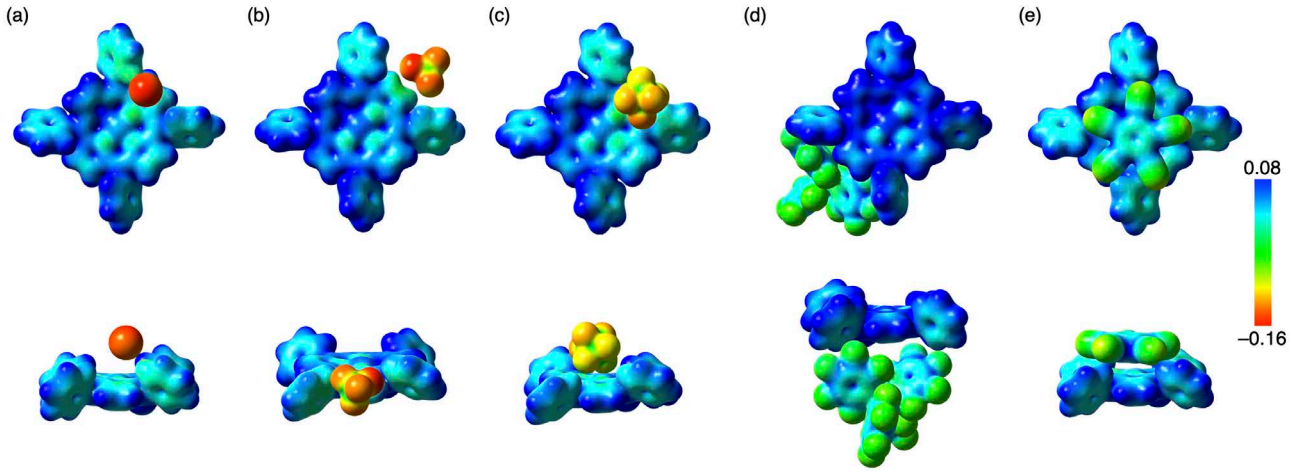

Fig. S58 Electrostatic potential (ESP) mapping (top and side views, δ = 0.01) of (a) **1pd**$^{+}$-Cl^{-}, (b) **1pd**$^{+}$-BF_4^{-}, (c) **1pd**$^{+}$-PF_6^{-}, (d) **1pd**$^{+}$-$B(C_6F_5)_4^{-}$, and (e) **1pd**$^{+}$-$PCCp^{-}$. **1pd**$^{+}$-X^{-} (X^{-} = Cl^{-}, BF_4^{-}, PF_6^{-}, $PCCp^{-}$) and **1pd**$^{+}$-$B(C_6F_5)_4^{-}$ were calculated at B3LYP/6-31+G(d,p) with LanL2DZ for Pd and B3LYP/6-31G(d,p) with LanL2DZ for Pd, respectively. Crystal structures (Fig. S10–13) were used for the calculations of **1pd**$^{+}$-X^{-} (X^{-} = BF_4^{-}, PF_6^{-}, $B(C_6F_5)_4^{-}$, $PCCp^{-}$), whereas optimized structures (Fig. S42) were used for the calculations of **1pd**$^{+}$-Cl^{-}.

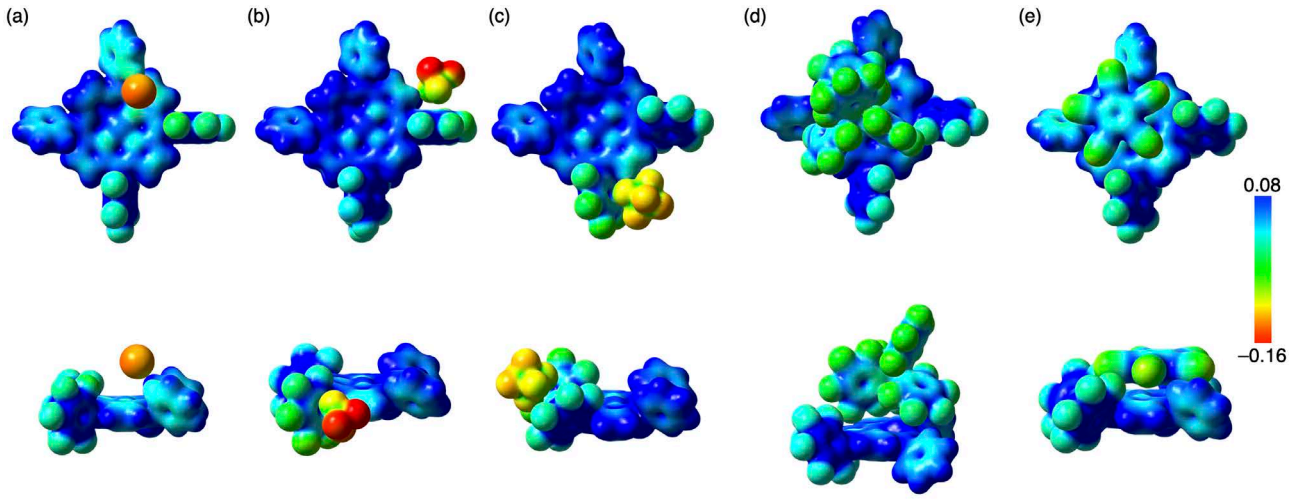

Fig. S59 ESP mapping (top and side views, δ = 0.01) of (a) **2pd**$^{+}$-Cl^{-}, (b) **2pd**$^{+}$-BF_4^{-}, (c) **2pd**$^{+}$-PF_6^{-}, (d) **2pd**$^{+}$-$B(C_6F_5)_4^{-}$, and (e) **2pd**$^{+}$-$PCCp^{-}$. **2pd**$^{+}$-X^{-} (X^{-} = Cl^{-}, BF_4^{-}, PF_6^{-}, $PCCp^{-}$) and **2pd**$^{+}$-$B(C_6F_5)_4^{-}$ were calculated at B3LYP/6-31+G(d,p) and B3LYP/6-31G(d,p), respectively, with LanL2DZ for Pd. Crystal structures (Fig. S14–16) were used for the calculations of **2pd**$^{+}$-BF_4^{-}, **2pd**$^{+}$-PF_6^{-} and **2pd**$^{+}$-$PCCp^{-}$, whereas optimized structures (Fig. S42) were used for the calculations of **2pd**$^{+}$-X^{-} (X^{-} = Cl^{-}, $B(C_6F_5)_4^{-}$).

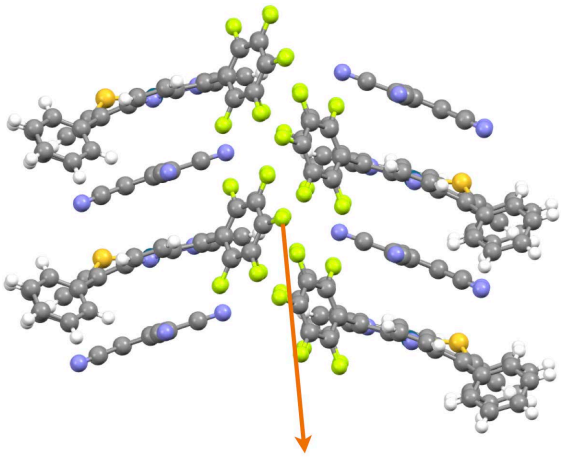

Fig. S60 Selected packing structure of **2pd**$^{+}$-PCCp^{-} (Fig. S29,30) showing the direction of dipole moment (1.97 D/*π-sip*) calculated at B3LYP/6-31+G(d,p) with LanL2DZ for Pd.

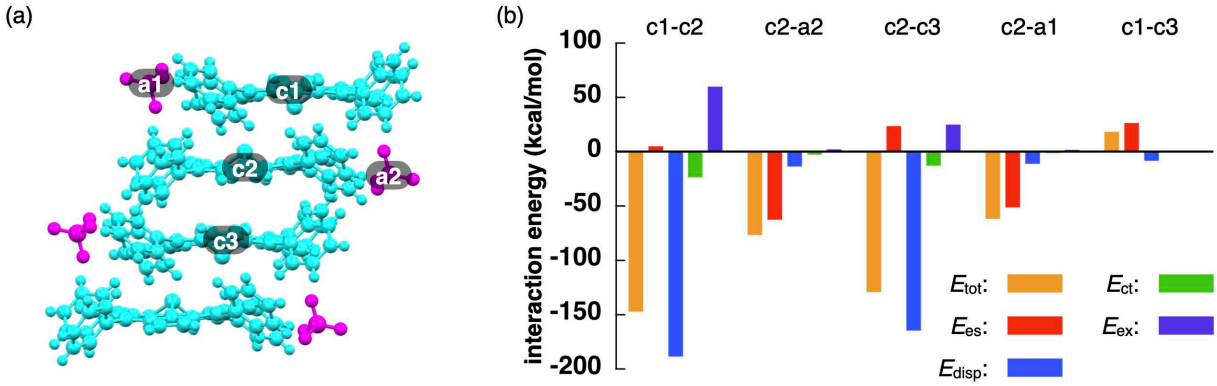

Fig. S61 Energy decomposition analysis (EDA)[S16] of **1pd**$^{+}$-BF_4^{-}: (a) single-crystal X-ray structure and (b) intermolecular interaction energies (kcal/mol) between selected ions estimated at an FMO2-MP2 using mixed basis sets including NOSeC-V-DZP with MCP with TZP for Pd.[S17–19] The labels (c1–3 and a1,2) correspond to the fragments shown in Table S2.

Table S2 Energies between selected fragments in **1pd**$^{+}$-BF_4^{-} (Fig. S61) estimated by EDA calculations[S16] based on an FMO2-MP2 using mixed basis sets including NOSeC-V-DZP with MCP with TZP for Pd.[S17–19]

fragments	total interaction energy (E_{tot}) (kcal/mol)	electrostatic interaction energy (E_{es}) (kcal/mol)	dispersion interaction energy (E_{disp}) (kcal/mol)	charge-transfer interaction energy (E_{ct+mix}) (kcal/mol)	exchange repulsion interaction energy (E_{ex}) (kcal/mol)
c1-c2	–147.190	4.859	–188.450	–23.426	59.832
c2-a2	–76.484	–62.458	–13.480	–2.542	1.996
c2-c3	–129.060	23.537	–164.640	–12.771	24.811
c2-a1	–61.634	–51.086	–10.977	–1.087	1.516
c1-c3	18.093	26.279	–8.166	–0.021	0.000

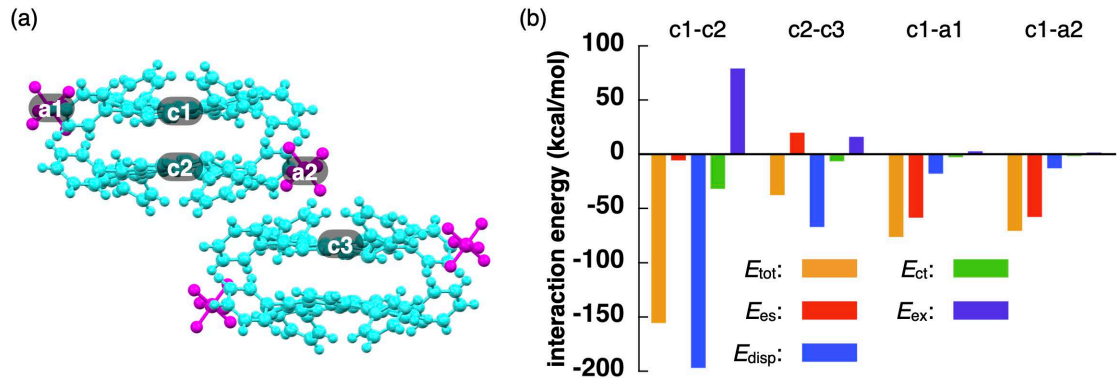

Fig. S62 EDA[S16] of **1pd**$^+$-PF_6^-: (a) single-crystal X-ray structure and (b) intermolecular interaction energies (kcal/mol) between selected ions estimated at an FMO2-MP2 using mixed basis sets including NOSeC-V-DZP with MCP with TZP for Pd.[S17–19] The labels (c1–3 and a1,2) correspond to the fragments shown in Table S3. The negative E_{es} value of c1-c2 was derived from the orientation of **1pd**$^+$.

Table S3 Energies between selected fragments in **1pd**$^+$-PF_6^- (Fig. S62) estimated by EDA calculations[S16] based on an FMO2-MP2 using mixed basis sets including NOSeC-V-DZP with MCP with TZP for Pd.[S17–19]

fragments	total interaction energy (E_{tot}) (kcal/mol)	electrostatic interaction energy (E_{es}) (kcal/mol)	dispersion interaction energy (E_{disp}) (kcal/mol)	charge-transfer interaction energy (E_{ct+mix}) (kcal/mol)	exchange repulsion interaction energy (E_{ex}) (kcal/mol)
c1-c2	–155.515	–5.585	–196.931	–31.837	78.837
c2-c3	–37.725	19.711	–66.925	–6.398	15.888
c1-a1	–76.196	–58.325	–17.870	–2.547	2.546
c1-a2	–70.731	–57.666	–12.745	–1.706	1.386

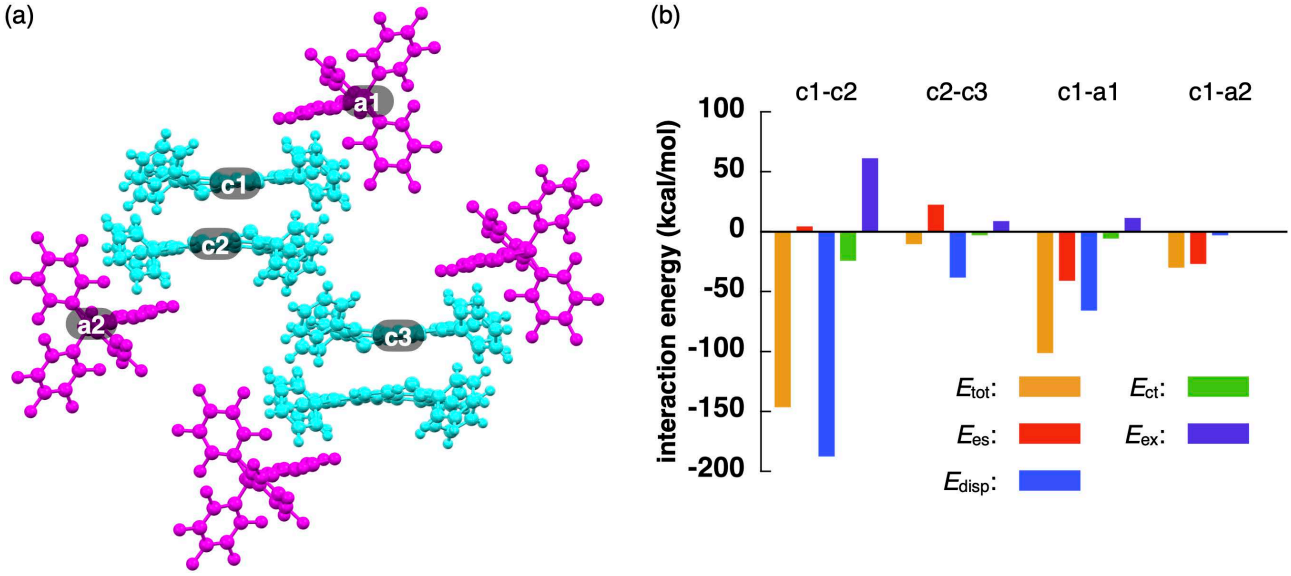

Fig. S63 EDA[S16] of **1pd**$^+$-$B(C_6F_5)_4^-$: (a) single-crystal X-ray structure and (b) intermolecular interaction energies (kcal/mol) between selected ions estimated at an FMO2-MP2 using mixed basis sets including NOSeC-V-DZP with MCP with TZP for Pd.[S17–19] The labels (c1–3 and a1,2) correspond to the fragments shown in Table S4.

Table S4 Energies between selected fragments in **1pd**$^+$-$B(C_6F_5)_4^-$ (Fig. S63) estimated by EDA calculations[S16] based on an FMO2-MP2 using mixed basis sets including NOSeC-V-DZP with MCP with TZP for Pd.[S17–19]

fragments	total interaction energy (E_{tot}) (kcal/mol)	electrostatic interaction energy (E_{es}) (kcal/mol)	dispersion interaction energy (E_{disp}) (kcal/mol)	charge-transfer interaction energy (E_{ct+mix}) (kcal/mol)	exchange repulsion interaction energy (E_{ex}) (kcal/mol)
c1-c2	–146.390	4.292	–187.533	–24.341	61.192
c2-c3	–10.329	22.371	–38.298	–2.896	8.495
c1-a1	–101.218	–40.898	–65.670	–5.841	11.191
c1-a2	–29.924	–26.893	–2.967	–0.066	0.002

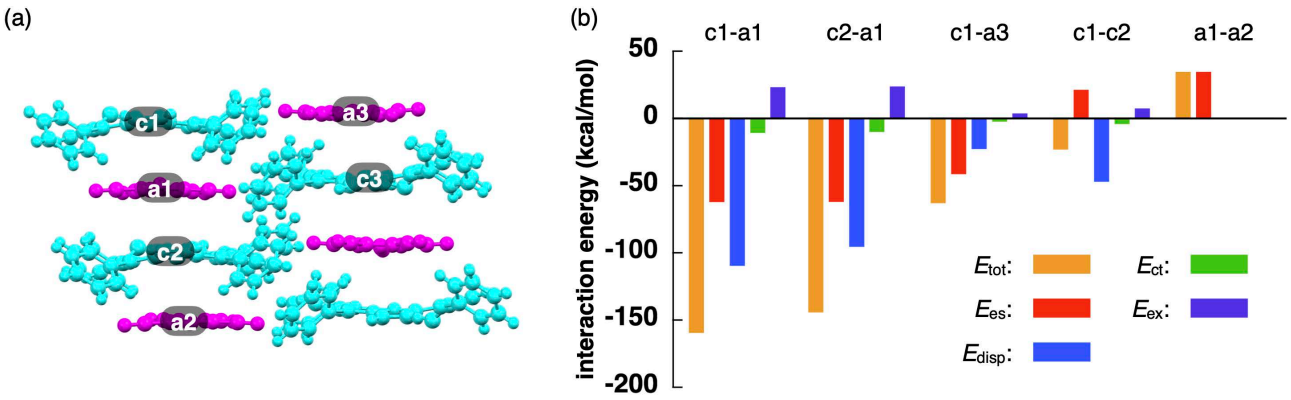

Fig. S64 EDA[S16] of **1pd**$^{+}$-PCCp^{-}: (a) single-crystal X-ray structure and (b) intermolecular interaction energies (kcal/mol) between selected ions estimated at an FMO2-MP2 using mixed basis sets including NOSeC-V-DZP with MCP with TZP for Pd.[S17–19] The labels (c1–3 and a1–3) correspond to the fragments shown in Table S5.

Table S5 Energies between selected fragments in **1pd**$^{+}$-PCCp^{-} (Fig. S64) estimated by EDA calculations[S16] based on an FMO2-MP2 using mixed basis sets including NOSeC-V-DZP with MCP with TZP for Pd.[S17–19]

fragments	total interaction energy (E_{tot}) (kcal/mol)	electrostatic interaction energy (E_{es}) (kcal/mol)	dispersion interaction energy (E_{disp}) (kcal/mol)	charge-transfer interaction energy (E_{ct+mix}) (kcal/mol)	exchange repulsion interaction energy (E_{ex}) (kcal/mol)
c1-a1	–159.430	–62.171	–109.640	–10.755	23.141
c2-a1	–144.170	–62.079	–95.547	–10.079	23.533
c1-a3	–63.000	–41.435	–22.807	–2.307	3.549
c1-c3	–33.365	18.145	–56.463	–4.660	9.614
a1-a2	34.462	34.462	0.000	0.000	0.000

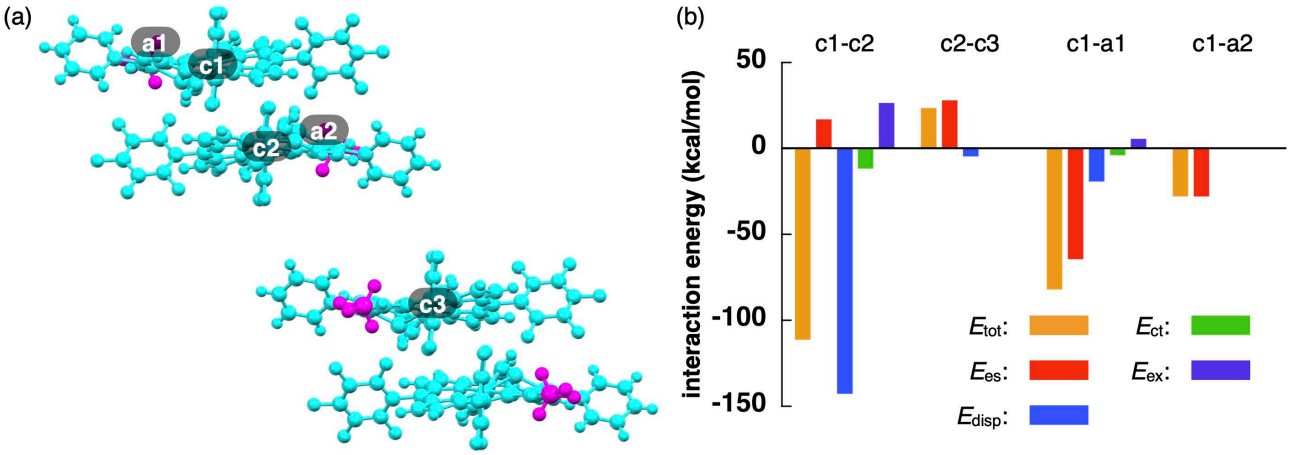

Fig. S65 EDA[S16] of **2pd**$^{+}$-BF_4^{-}: (a) single-crystal X-ray structure and (b) intermolecular interaction energies (kcal/mol) between selected ions estimated at an FMO2-MP2 using mixed basis sets including NOSeC-V-DZP with MCP with TZP for Pd.[S17–19] The labels (c1–3 and a1,2) correspond to the fragments shown in Table S6.

Table S6 Energies between selected fragments in **2pd**$^{+}$-BF_4^{-} (Fig. S65) estimated by EDA calculations[S16] based on an FMO2-MP2 using mixed basis sets including NOSeC-V-DZP with MCP with TZP for Pd.[S17–19]

fragments	total interaction energy (E_{tot}) (kcal/mol)	electrostatic interaction energy (E_{es}) (kcal/mol)	dispersion interaction energy (E_{disp}) (kcal/mol)	charge-transfer interaction energy (E_{ct+mix}) (kcal/mol)	exchange repulsion interaction energy (E_{ex}) (kcal/mol)
c1-c2	–111.26	16.804	–142.74	–11.703	26.383
c2-c3	23.352	27.925	–4.566	–0.007	0
c1-a1	–81.95	–64.443	–19.133	–3.888	5.514
c1-a2	–27.844	–27.844	0	0	0

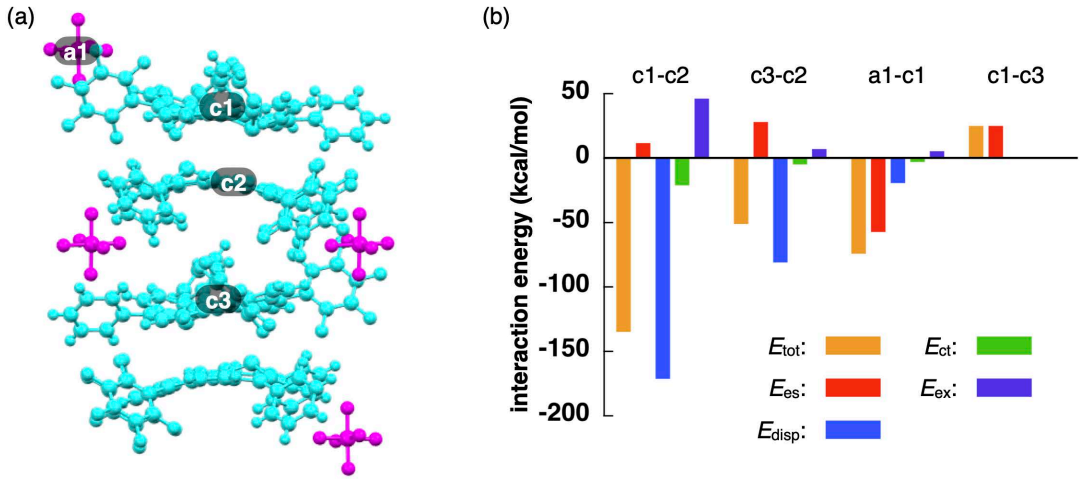

Fig. S66 EDA[S16] of **2pd**$^{+}$-PF_6^{-}: (a) single-crystal X-ray structure and (b) intermolecular interaction energies (kcal/mol) between selected ions estimated at an FMO2-MP2 using mixed basis sets including NOSeC-V-DZP with MCP with TZP for Pd.[S17–19] The labels (c1–3 and a1) correspond to the fragments shown in Table S7.

Table S7 Energies between selected fragments in **2pd**$^{+}$-PF_6^{-} (Fig. S66) estimated by EDA calculations[S16] based on an FMO2-MP2 using mixed basis sets including NOSeC-V-DZP with MCP with TZP for Pd.[S17–19]

fragments	total interaction energy (E_{tot}) (kcal/mol)	electrostatic interaction energy (E_{es}) (kcal/mol)	dispersion interaction energy (E_{disp}) (kcal/mol)	charge-transfer interaction energy (E_{ct+mix}) (kcal/mol)	exchange repulsion interaction energy (E_{ex}) (kcal/mol)
c1-c2	–134.820	11.462	–171.290	–21.045	46.050
c3-c2	–51.090	27.832	–80.915	–4.766	6.759
a1-c1	–74.191	–57.133	–19.360	–2.976	5.277
c1-c3	24.801	24.801	0.000	0.000	0.000

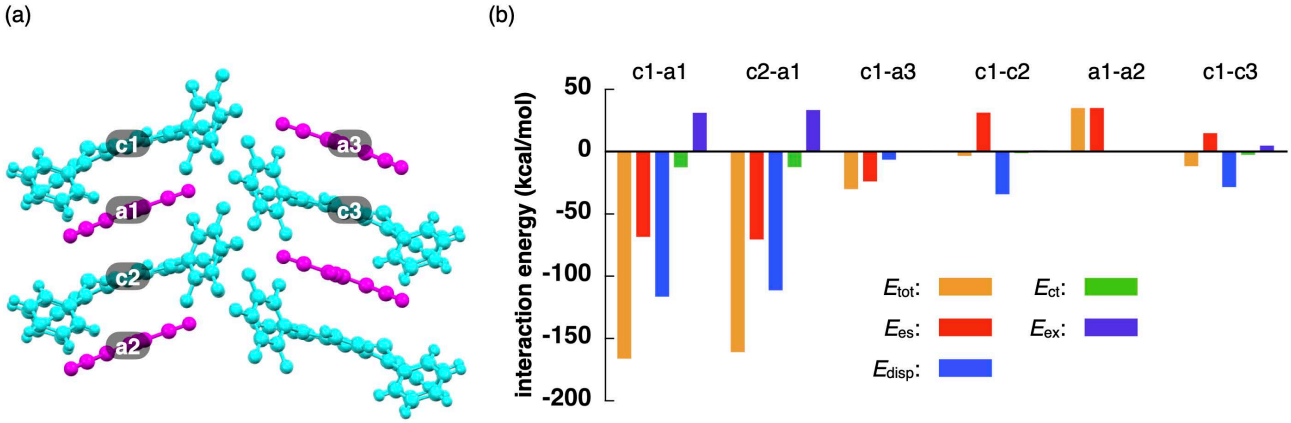

Fig. S67 EDA[S16] of **2pd**$^{+}$-$PCCp^{-}$: (a) single-crystal X-ray structure and (b) intermolecular interaction energies (kcal/mol) between selected ions estimated at an FMO2-MP2 using mixed basis sets including NOSeC-V-DZP with MCP with TZP for Pd.[S17–19] The labels (c1–3 and a1–3) correspond to the fragments shown in Table S8.

Table S8 Energies between selected fragments in **2pd**$^{+}$-$PCCp^{-}$ (Fig. S67) estimated by EDA calculations[S16] based on an FMO2-MP2 using mixed basis sets including NOSeC-V-DZP with MCP with TZP for Pd [S17–19]

fragments	total interaction energy (E_{tot}) (kcal/mol)	electrostatic interaction energy (E_{es}) (kcal/mol)	dispersion interaction energy (E_{disp}) (kcal/mol)	charge-transfer interaction energy (E_{ct+mix}) (kcal/mol)	exchange repulsion interaction energy (E_{ex}) (kcal/mol)
c1-a1	–166.090	–68.244	–116.390	–12.499	31.044
c2-a1	–160.850	–70.365	–111.290	–12.336	33.143
c1-a3	–29.954	–23.803	–6.486	–0.231	0.567
c1-c2	–3.317	31.093	–34.068	–1.120	0.778
a1-a2	34.846	34.846	0.000	0.000	0.000
c1-c3	–11.611	14.570	–28.408	–2.428	4.655

Cartesian coordination of optimized structures

Cartesian Coordination of 1pd$^+$

–2382.6872403 hartree

H,13.2120359881,27.2462002076,12.5551180935
H,11.3444731679,26.1649837913,13.7958748226
C,10.7149331083,21.1526980041,19.8141839523
C,10.3388209473,21.5867814088,21.0881571436
C,11.0595135313,21.1729500279,22.213028101
C,12.154635886,20.3166589288,22.0590546124
C,12.5246063138,19.8714887477,20.7872162204
C,11.8106635016,20.288816796,19.6514859884
H,10.1499187806,21.4733957404,18.9438050479
H,9.4842047553,22.2475347088,21.1999520797
H,10.7696561638,21.5146433552,23.2022710523
H,12.721556931,19.993670262,22.9272309175
H,13.3769236528,19.2081376551,20.671963616
H,10.9575188015,17.7080775454,19.8537885429
C,12.9570002333,22.1509829786,17.7218000355
C,13.3549058268,22.7788539955,16.5808925166
C,13.4054708079,21.7875787559,15.5323120753
C,13.657326965,22.1226777473,14.1663246601
C,13.5339110779,23.5459425394,13.7405322957
C,12.3687523316,24.2859538942,14.0148292629
C,12.2534624068,25.6093076906,13.5856662686
C,13.3014932488,26.2152534978,12.8843505862
C,14.4642196475,25.4886303902,12.6071402387
C,14.5775545864,24.1611916199,13.024939342
C,13.9281223637,21.1780819775,13.1729679986
C,13.7460199854,21.2168196322,11.7677079642
C,13.8210147455,19.9774788008,11.1448089189
H,12.8266952603,22.5863500939,18.7009301492
H,13.6129951194,23.8199437262,16.4579059524
H,11.5473570378,23.8171694045,14.5479206858
H,15.2836588034,25.9546325646,12.0681292973
H,15.4853967351,23.6031985001,12.8152966746
H,13.4627038868,22.1252322954,11.2506727102
H,13.6017849202,19.8261140169,10.0951320624
C,12.2101957225,19.8108390273,18.2893223674
C,12.7363751325,20.7613538285,17.3923254161
C,14.066361969,18.8935418572,12.0247695652
C,13.9362153417,17.5134280174,11.8497499524
C,13.9297924343,16.999594019,10.4503968214
C,14.9919389957,17.3081851112,9.5806914643
C,14.9866373983,16.8456711097,8.2632878307
C,13.9138537575,16.0819492761,7.7914573609
C,12.8475378141,15.7788601948,8.6449732196
C,12.8557221217,16.2300599292,9.9659903382
C,13.7198133304,16.5945353925,12.922358866
C,13.8158770393,15.1638007137,12.7536010179
C,13.4151853949,14.5842417135,13.9188325502
C,13.0461345175,15.6492683505,14.8231727377
C,12.4748824553,15.4435455462,16.0945046938
C,12.1898478027,14.0321532255,16.5071358441
C,11.1917080187,13.2848167498,15.8601470037
C,10.9214646106,11.972208687,16.2562854505
C,11.6525917695,11.3867126293,17.2948558498
C,12.6512432158,12.1225337216,17.9410058768
C,12.9144186767,13.4393954026,17.5547089915
C,12.138187356,16.4603109968,17.0145129681
C,11.4726488059,16.2610369955,18.283706293
C,11.3988332211,17.478561238,18.8955655576
C,12.0181600916,18.4402865622,18.0095610156
H,15.8307832599,17.8935128611,9.9456768063
H,15.820073521,17.0797995355,7.6077427556
H,13.9080797666,15.7263981642,6.765398354
H,12.0073612598,15.1943358944,8.2821255331
H,12.0197850717,16.0021482587,10.6201322858
H,14.1668013062,14.6707619872,11.8595254487
H,13.3751769091,13.5304953614,14.1495657442
H,10.6186965215,13.7368294531,15.0557903797
H,10.1410034906,11.4091181704,15.753027306
H,11.4453745802,10.3649387169,17.5988533395
H,13.2257982601,11.6738158185,18.7459847505
H,13.6921753751,14.0065657158,18.0578669036
H,11.1025564583,15.3158928405,18.6516204987
N,13.0566840329,20.5556735235,16.0657349971
N,13.2804058218,16.8633823567,14.2101518779
N,12.4240534568,17.7908802269,16.8760385804
Pd,13.2128788139,18.6677136046,15.2264541735
S,14.5053775822,19.567415915,13.5920013272

Cartesian Coordination of 1pd$^+$ in CH_2Cl_2

–2382.6872403 hartree

H,13.2120359881,27.2462002076,12.5551180935
H,11.3444731679,26.1649837913,13.7958748226
C,10.7149331083,21.1526980041,19.8141839523
C,10.3388209473,21.5867814088,21.0881571436
C,11.0595135313,21.1729500279,22.213028101
C,12.154635886,20.3166589288,22.0590546124
C,12.5246063138,19.8714887477,20.7872162204
C,11.8106635016,20.288816796,19.6514859884
H,10.1499187806,21.4733957404,18.9438050479
H,9.4842047553,22.2475347088,21.1999520797
H,10.7696561638,21.5146433552,23.2022710523
H,12.721556931,19.993670262,22.9272309175
H,13.3769236528,19.2081376551,20.671963616
H,10.9575188015,17.7080775454,19.8537885429
C,12.9570002333,22.1509829786,17.7218000355
C,13.3549058268,22.7788539955,16.5808925166
C,13.4054708079,21.7875787559,15.5323120753
C,13.657326965,22.1226777473,14.1663246601
C,13.5339110779,23.5459425394,13.7405322957
C,12.3687523316,24.2859538942,14.0148292629
C,12.2534624068,25.6093076906,13.5856662686
C,13.3014932488,26.2152534978,12.8843505862
C,14.4642196475,25.4886303902,12.6071402387
C,14.5775545864,24.1611916199,13.024939342
C,13.9281223637,21.1780819775,13.1729679986
C,13.7460199854,21.2168196322,11.7677079642
C,13.8210147455,19.9774788008,11.1448089189
H,12.8266952603,22.5863500939,18.7009301492
H,13.6129951194,23.8199437262,16.4579059524
H,11.5473570378,23.8171694045,14.5479206858
H,15.2836588034,25.9546325646,12.0681292973
H,15.4853967351,23.6031985001,12.8152966746
H,13.4627038868,22.1252322954,11.2506727102
H,13.6017849202,19.8261140169,10.0951320624
C,12.2101957225,19.8108390273,18.2893223674
C,12.7363751325,20.7613538285,17.3923254161

C,14.066361969,18.8935418572,12.0247695652
C,13.9362153417,17.5134280174,11.8497499524
C,13.9297924343,16.999594019,10.4503968214
C,14.9919389957,17.3081851112,9.5806914643
C,14.9866373983,16.8456711097,8.2632878307
C,13.9138537575,16.0819492761,7.7914573609
C,12.8475378141,15.7788601948,8.6449732196
C,12.8557221217,16.2300599292,9.9659903382
C,13.7198133304,16.5945353925,12.922358866
C,13.8158770393,15.1638007137,12.7536010179
C,13.4151853949,14.5842417135,13.9188325502
C,13.0461345175,15.6492683505,14.8231727377
C,12.4748824553,15.4435455462,16.0945046938
C,12.1898478027,14.0321532255,16.5071358441
C,11.1917080187,13.2848167498,15.8601470037
C,10.9214646106,11.972208687,16.2562854505
C,11.6525917695,11.3867126293,17.2948558498
C,12.6512432158,12.1225337216,17.9410058768
C,12.9144186767,13.4393954026,17.5547089915
C,12.138187356,16.4603109968,17.0145129681
C,11.4726488059,16.2610369955,18.283706293
C,11.3988332211,17.478561238,18.8955655576
C,12.0181600916,18.4402865622,18.0095610156
H,15.8307832599,17.8935128611,9.9456768063
H,15.820073521,17.0797995355,7.6077427556
H,13.9080797666,15.7263981642,6.765398354
H,12.0073612598,15.1943358944,8.2821255331
H,12.0197850717,16.0021482587,10.6201322858
H,14.1668013062,14.6707619872,11.8595254487
H,13.3751769091,13.5304953614,14.1495657442
H,10.6186965215,13.7368294531,15.0557903797
H,10.1410034906,11.4091181704,15.753027306
H,11.4453745802,10.3649387169,17.5988533395
H,13.2257982601,11.6738158185,18.7459847505
H,13.6921753751,14.0065657158,18.0578669036
H,11.1025564583,15.3158928405,18.6516204987
N,13.0566840329,20.5556735235,16.0657349971
N,13.2804058218,16.8633823567,14.2101518779
N,12.4240534568,17.7908802269,16.8760385804
Pd,13.2128788139,18.6677136046,15.2264541735
S,14.5053775822,19.567415915,13.5920013272

Cartesian Coordination of 1pd^{+}-Cl^{-}

–2843.0641312 hartree

C,3.6842043094,3.5316677568,0.1273925981
C,3.8451314048,4.5212306992,-0.8567042131
C,4.5193547,3.552152655,1.2568697652
C,2.6305830327,2.4773464631,-0.0233633895
C,3.0600350723,1.1505805266,-0.2256153666
C,-2.7003441303,-1.0707191616,-0.6533705167
C,-4.0493608521,-0.6017077127,-0.8655120364
C,-4.0260348647,0.7576345593,-0.8058714207
C,-2.6617526795,1.151908969,-0.535765072
C,-2.2579661097,2.4781024467,-0.285383068
C,-3.3224929555,3.5304283829,-0.2412215382
C,-4.2826308932,3.5310684312,0.7845879237
C,-5.2673108334,4.5216224372,0.8302235044
C,-5.3123219242,5.515175699,-0.1530802196
C,-4.3632469294,5.5181372671,-1.1806169079
C,-3.3700638254,4.5359652714,-1.2214519384
C,-0.9300785056,2.8985379217,-0.0529419459
C,-0.5204468002,4.2415731699,0.2964024495
C,0.8422716891,4.241876854,0.3674807699
C,1.28630324,2.898480061,0.0645534854
H,3.2078019962,4.5119068863,-1.736190857
H,4.3961132523,2.7983638283,2.0290114457
H,-4.2498805264,2.7634240733,1.5519433077
H,-5.9978723991,4.5141130674,1.6336950677
H,-6.0811524185,6.2815595369,-0.1190062432
H,-4.3941139892,6.283625664,-1.9505429886
H,-2.6364401815,4.5402648713,-2.0225052005
H,-1.1894246098,5.0696029766,0.4763850692
H,1.4884346495,5.0704697686,0.6156953422
H,-4.9016929025,-1.2388059812,-1.0467975365
H,-4.8571430108,1.4353774628,-0.9272955917
N,0.1864779556,2.1157356552,-0.1579111839
N,-1.8663383578,0.0258855197,-0.494252589
Pd,0.2020164913,0.1083227192,-0.4465825216
C,4.4449436585,0.7567775208,-0.3487150228
C,4.4750080148,-0.6034871934,-0.4072191765
C,3.1114123172,-1.0736268156,-0.3391629115
C,2.7780393435,-2.4587847799,-0.2369992574
C,3.8454370156,-3.4315139981,0.1345136649
C,4.6303166417,-3.2432338119,1.2870486973
C,5.6070018901,-4.1769304865,1.6385034344
C,5.8195733525,-5.3069365182,0.8414684374
C,5.0445098515,-5.5036133693,-0.3062904181
C,4.0592356919,-4.5772362334,-0.6536653172
C,1.4803342921,-2.9575881384,-0.3784671461
C,0.8654971189,-4.1329456893,0.1207722489
C,-0.521995291,-4.131880296,0.0444438404
C,-1.0766004876,-2.9561766301,-0.5194406077
C,-2.3813013639,-2.4559425367,-0.5156259714
C,-3.4834862142,-3.4263798507,-0.2601178776
C,-3.6172001423,-4.5646714339,-1.0771246941
C,-4.6371346336,-5.4886743164,-0.8429337408
C,-5.525341349,-5.2961577185,0.2209371262
C,-5.3896743158,-4.1748597669,1.0462940503
C,-4.3791042932,-3.2401540532,0.8094760323
H,5.342022844,-1.2393103002,-0.5057783532
H,4.4605957545,-2.3751840058,1.9165276502
H,6.1978324894,-4.0238926362,2.5367005856
H,6.5822796513,-6.0302732562,1.1142771785
H,5.2068633207,-6.376278034,-0.9319197987
H,3.4643440843,-4.7296158159,-1.5494797491
H,1.4321266967,-4.9092100493,0.6199564132
H,-1.1421469668,-4.9058481844,0.4792931153
H,-2.9329587588,-4.7121191776,-1.9078107464
H,-4.7382838944,-6.3550727677,-1.4900345962
H,-6.3160138561,-6.0172591696,0.4070919074
H,-6.0667833016,-4.0266319039,1.8820378836
H,-4.2732224962,-2.385834658,1.4741949818
H,5.2835084524,1.4354309102,-0.3869383314
N,2.2653309204,0.0234738337,-0.2664053733
S,0.2445255532,-2.024575972,-1.2163787508
C,4.8270193148,5.5058696643,-0.7175948626
C,5.6514759126,5.5216398334,0.412119417
C,5.492768222,4.5445705041,1.4001792099
H,4.9457450617,6.2592402086,-1.4908496284
H,6.4108247447,6.2902462049,0.522285632

H,6.1249460742,4.5532620389,2.2832569451
Cl,-4.4219830153,-0.854018897,3.921767496

Cartesian Coordination of $1pd^{+}$-BF_4^{-}

–2807.3421427 hartree

C,-0.7060513717,4.1449147101,0.0031464016
C,-0.9686411359,2.7669843168,-0.351668229
C,-2.2328983165,2.2290696931,-0.6777657913
C,-3.385693809,3.1836490384,-0.7318851209
C,-3.4457389289,4.1669261635,-1.7337924126
C,-4.5210825413,5.0576427634,-1.7880198997
C,-5.4831092851,4.0128577532,0.1705647301
C,-4.4155519697,3.1116563538,0.2216131132
C,-2.4972520436,0.8713403601,-0.943390817
C,-3.7963430715,0.3568775974,-1.3139460414
C,-3.6938200901,-0.9991888274,-1.36590573
C,-2.3286189317,-1.3455563715,-1.0469432699
C,-1.8989427437,-2.697037503,-0.8757215195
C,-2.927641381,-3.7611208042,-0.6943968017
C,-4.8468748372,-4.6715430901,0.4854865665
C,-4.8287254088,-5.800516111,-0.3406293236
C,-3.8572011376,-5.9150364024,-1.3408643633
C,-2.9073583749,-4.9059603888,-1.5119554254
F,-2.1908378097,0.5678822007,2.9061167518
F,-4.4843432294,0.8256074045,2.799784833
F,-3.5526521809,-1.2857113181,2.6911283679
H,3.1244672896,4.7143289009,-1.777778597
H,-1.4574793034,4.9109550742,0.1216485874
H,-2.6561876695,4.2251567302,-2.4776508069
H,-4.560007019,5.8065519781,-2.5738179473
H,-4.3738449404,2.3630377941,1.0078480499
H,-4.6723428154,0.9584183765,-1.5026906079
H,-4.4691834231,-1.7101579814,-1.608288238
H,-5.5647450827,-6.5874699442,-0.2040054693
H,-3.8390909887,-6.7870245446,-1.988070959
H,-2.158427389,-4.9937646779,-2.2938153788
N,-1.6107061617,-0.1792182968,-0.8326639058
C,-5.5413483423,4.9843426413,-0.8338700514
H,-6.374846737,5.679758939,-0.8727602037
H,-6.2686862132,3.9534618345,0.9182664797
B,-3.4327116422,0.0017239034,3.2689164863
F,-3.5120075012,-0.1063700006,4.6763561605
C,4.3172573502,-3.1089031258,0.2717180515
C,5.726959982,-5.068974135,-0.0395291009
C,6.3858280447,-4.7943907736,1.1634988663
C,6.0102910811,-3.6811828217,1.9231680808
C,4.9863964263,-2.8417073872,1.4803367136
C,5.1591433341,5.0063126999,1.513608595
H,7.1849019695,-5.4442714075,1.5077628843
H,6.5105788287,-3.468152396,2.8631751291
H,4.6899592106,-1.9872063704,2.0807040355
H,4.1764903373,3.1802974448,2.1035011287
H,5.7209097963,5.087050435,2.439591615
C,0.0528146363,-4.2016082476,-0.1635495722
C,1.4242070377,-4.0780548675,0.0209024225
C,1.9688501615,-2.851729766,-0.4365729786
C,3.2010520625,-2.2385035769,-0.1974309753
C,4.6951518701,-4.237131124,-0.4790939599
C,3.4181074103,-0.8293372323,-0.2905688681
C,4.7362195759,-0.24054218,-0.2637059233
C,4.5820748793,1.1122347016,-0.2280132423
C,3.1625710893,1.3820125628,-0.2133339779
C,2.6033326773,2.6666320931,-0.0638767455
C,3.5458960463,3.8135635652,0.1385052203
C,4.2900318611,3.9283763792,1.3243873043
C,5.3039854624,5.9761944505,0.516388294
C,4.5701010673,5.8668814759,-0.6692167092
C,3.6916010525,4.796044079,-0.8550233966
C,1.2241887357,2.9664067533,-0.0769367894
C,0.6425045228,4.2680752046,0.1705080803
C,-3.9065577658,-3.6536031833,0.3110233903
C,-0.5593106565,-3.07935563,-0.7757137404
H,-0.5274706209,-5.0289356811,0.2258570362
H,2.0173306133,-4.8007633489,0.567441643
H,4.190950479,-4.4491926236,-1.417379348
H,6.0162975441,-5.9286818022,-0.6366234449
H,5.6607194751,-0.7976964088,-0.2885836523
H,5.358043011,1.8625304117,-0.2139185729
H,5.9824877697,6.8115245583,0.6626027911
H,4.6789624443,6.6142316791,-1.4497630892
H,1.1932702145,5.1536535621,0.450013976
H,-3.9107798631,-2.7903341165,0.9696663524
H,-5.5906875787,-4.5831797121,1.2718464513
N,2.4758296224,0.1881962068,-0.2959802108
N,0.2169559866,2.0860128747,-0.3625761709
Pd,0.4319139285,0.0872272565,-0.6247418092
S,0.7233494252,-2.0327447414,-1.3746064011

Cartesian Coordination of $1pd^{+}$-PF_6^{-}

–3323.4817583 hartree

C,-1.0757152018,18.1262373916,16.7047360067
C,-0.6376700349,17.1374205233,15.8081632875
C,-0.2322405308,19.2141695865,16.9845541411
C,-2.4270146034,18.0240075862,17.343546748
C,-2.475874951,17.7915008317,18.7323674428
C,-8.6590049017,17.6205969966,18.8896007942
C,-9.7800296244,17.4748298736,17.9911666713
C,-9.3002973667,17.5525773487,16.719957819
C,-7.8735764565,17.7659784106,16.8122849347
C,-7.0390886731,18.0101660058,15.7042129605
C,-7.6865696893,18.1118881858,14.3576580579
C,-8.5425116257,19.185102215,14.0573719439
C,-9.13491734,19.280358098,12.7948979458
C,-8.8900401946,18.3034402684,11.8245023589
C,-8.0426190065,17.2301839313,12.1188743422
C,-7.4387519763,17.138015188,13.3756527282
C,-5.6383441386,18.1807502744,15.7575904933
C,-4.7875112702,18.5168679354,14.6366499356
C,-3.501497046,18.5176434536,15.0928061346
C,-3.5472515147,18.1841090319,16.5000436462
F,-7.3072880451,22.2826559673,17.1490701343
F,-9.3846725979,21.8444995077,16.1929063362
F,-8.8141094472,24.0208586585,16.7927170952
F,-10.4312097386,22.8665237247,18.0044691473
F,-8.3543935517,23.304973161,18.9597364139
F,-8.9246240058,21.1277275736,18.3616262829
H,-1.2803748316,16.2898568257,15.5882094964
H,-0.5659471781,19.9899174547,17.6674849376
H,-8.7321448183,19.9501558694,14.8043676898
H,-9.787166981,20.119719705,12.5721691274

H,-9.3553581683,18.3778904494,10.8459060172
H,-7.8500834794,16.4649873868,11.3724198067
H,-6.7827644156,16.3021482106,13.6015000974
H,-5.1322907937,18.736638879,13.6374793674
H,-2.60449946,18.7378090706,14.5336886083
H,-10.8025860722,17.3214525449,18.3015305843
H,-9.8594206582,17.4776240774,15.7998121748
N,-4.854522987,18.0143273608,16.8656097375
N,-7.5009078106,17.7566200906,18.1402511532
P,-8.8685145025,22.5748870148,17.5768997493
Pd,-5.5245259631,17.7041236396,18.7542109757
C,-1.3095379682,17.6019211411,19.5640421006
C,-1.7397051327,17.5346347625,20.8545209941
C,-3.1778312544,17.6620579048,20.8422621625
C,-3.9520973062,17.7695847403,22.0381678065
C,-3.2579717354,18.0917755672,23.3180695229
C,-2.4154388925,19.2137840558,23.4231504864
C,-1.7945643525,19.5215101739,24.6351903199
C,-1.9994550613,18.7106119969,25.7567221631
C,-2.8353500819,17.5929170536,25.6628151995
C,-3.4664556417,17.2893942571,24.4547646172
C,-5.3456237335,17.6793041807,22.0717791786
C,-6.2988757147,18.1915242046,22.9875538128
C,-7.6074872397,18.178072435,22.5215924792
C,-7.7579020261,17.6551040542,21.2128389014
C,-8.8172664972,17.726311285,20.3053311237
C,-10.1693336444,18.0276663044,20.8563446698
C,-10.7178350148,17.212030371,21.8630322678
C,-11.9776668239,17.4944648922,22.3946777306
C,-12.6981542939,18.6038999784,21.9391419977
C,-12.1540812105,19.4278742547,20.9479713649
C,-10.8996481261,19.1426890033,20.404868646
H,-1.1411110436,17.3931857776,21.7418823736
H,-2.2636448291,19.854173616,22.5597576288
H,-1.1553575031,20.3966806194,24.7041749033
H,-1.5127513917,18.949432593,26.697707703
H,-2.9954286232,16.9565546388,26.5281233518
H,-4.108856737,16.4165588796,24.3836335281
H,-6.0057558978,18.6546642793,23.9215686168
H,-8.4334305343,18.630866363,23.0560020329
H,-10.1634235742,16.3460193076,22.213107285
H,-12.3958078233,16.8486112719,23.1611893263
H,-13.6760911238,18.8263812877,22.3559749873
H,-12.703104047,20.2973786837,20.5990831542
H,-10.4717609735,19.79490635,19.6501677348
H,-0.2942313601,17.5296738981,19.2046402044
N,-3.6035100216,17.7799065036,19.5274920135
S,-6.2294607083,16.9090067665,20.7576533476
C,0.622095883,17.2308529121,15.210482569
C,1.4540694336,18.3195690454,15.4910916246
C,1.0222639524,19.3123008943,16.3765991909
H,0.9510578629,16.4543152041,14.5261005148
H,2.4307067152,18.3945559369,15.0220030282
H,1.6597457481,20.164032246,16.5950240106

Cartesian Coordination of 1pd^{+}-B(C$_6$F$_5$)$_4^{-}$

–5319.0405135 hartree

C,3.4915317915,-1.761836124,-3.7999785769
C,3.9650156698,-3.6410289861,1.5241421266
C,7.4448479177,0.8178212883,0.7744610256
C,7.7733357227,1.7393962555,-0.2092700607
F,4.3506274093,-2.1036571457,-4.7826728497
F,5.2883707104,-0.893025472,-2.6273915838
F,4.7624858331,-4.7129880492,1.3364464403
F,5.1274013515,-2.5282049038,-0.1530236519
F,8.3543948941,0.4964123505,1.7180841195
F,8.9913586927,2.31050116,-0.2372448381
F,7.106785908,2.9666640362,-2.1245702566
B,3.6099052491,-0.0512122969,-0.1437797119
C,-3.382864024,-0.2286795294,-3.3319488191
C,-3.5537204687,-0.3414807448,-4.8159971265
C,-2.5958425459,-1.0177871177,-5.5897679966
C,-2.7533733004,-1.125591157,-6.9740834572
C,-3.8741287184,-0.5703787312,-7.6000514383
C,-4.8355674292,0.0984169528,-6.8355469902
C,-4.6743770817,0.2171995631,-5.4524405468
C,-3.5017840261,-1.4187927058,-2.5820925137
C,-3.8477249691,-2.7189164861,-3.1149546657
C,-3.7869280915,-3.6071998774,-2.0810821115
C,-3.4041289739,-2.86301321,-0.900517371
C,-3.170286443,-3.4139401868,0.3779951165
C,-3.2484452125,-4.905202165,0.4997485826
C,-2.2753942216,-5.7174360139,-0.1058318045
C,-2.3444618317,-7.1085501284,0.0072580136
C,-3.3919790853,-7.7052008921,0.7163872123
C,-4.3683687178,-6.9036774173,1.3166144949
C,-4.2948360912,-5.5118484588,1.2139151801
C,-2.879739724,-2.6793310682,1.5441639341
C,-2.6153510989,-3.2770243524,2.8332697658
C,-2.4964585601,-2.2621405077,3.7325995934
C,-2.667148801,-1.0207961732,3.0148592572
C,-2.7337957512,0.2452407466,3.6726637135
C,-2.9505274686,0.2807657272,5.1475473667
C,-4.0333834472,-0.3947057882,5.7397010751
C,-4.238799922,-0.3297126401,7.1191258059
C,-3.3625963373,0.4030124132,7.9271076428
C,-2.2826490549,1.0775657162,7.3480223828
C,-2.0815755495,1.0237682717,5.9673735112
C,-2.6914297622,1.4717087638,3.0048372972
C,-3.1856265548,2.7519299483,3.3611995075
C,-3.2480788691,3.6558122434,2.3081118162
C,-2.8059853747,3.1373709759,1.0646745793
C,-2.9629117277,3.6064139406,-0.2419759674
C,-3.283373919,5.0523849353,-0.4141217878
C,-2.4426630247,6.0319625131,0.1454964822
C,-2.7441331315,7.3880671291,0.0051465921
C,-3.8958397162,7.784517232,-0.6826170169
C,-4.7436468747,6.8177239111,-1.2339461171
C,-4.4389776687,5.4613748684,-1.1048463743
C,-2.9201575201,2.7670898051,-1.3971322421
C,-2.859360532,3.294198898,-2.7400709479
C,-2.9742234472,2.2445599401,-3.5994692671
C,-3.1261742231,1.05011377,-2.8001042969
C,2.7716611859,1.33148469,0.2670708087
C,1.9780600864,2.1121167549,-0.5782164126
C,1.3918662425,3.3215452269,-0.2014009147
C,1.5914934847,3.8184985595,1.0781382253
C,2.3892798779,3.0954323246,1.9575062787
C,2.9553710801,1.8982094758,1.5351392593
C,3.1271633178,-0.7196191704,-1.5936133177

C,1.784479036,-1.0749300924,-1.7744708704
C,1.2805294917,-1.721156233,-2.8967814397
C,2.1446405131,-2.0680136548,-3.929079352
C,3.9506727815,-1.112250577,-2.6526851764
C,3.3619648845,-1.3239115208,0.9048686989
C,2.3546856432,-1.4382002623,1.8667192203
C,2.1494203079,-2.5739830623,2.6517117166
C,2.96017268,-3.6871891511,2.4840223217
C,4.1322213008,-2.4862921741,0.7687588998
C,5.1804174248,0.5093685626,-0.1542276267
C,6.1755104295,0.2370282571,0.7886821205
C,6.8151083811,2.0671169814,-1.1620697531
C,5.565405633,1.4614905113,-1.1067791656
F,1.7295658106,1.7420885688,-1.8588013889
F,0.6321747271,4.015286071,-1.0749630679
F,1.0270019806,4.980237065,1.4602471844
F,2.6027652719,3.5609405173,3.2061361355
F,3.7358505765,1.2658226139,2.4473362578
F,0.876227413,-0.7834965874,-0.8081568575
F,-0.0331565043,-2.0166331895,-2.9951471692
F,1.683344767,-2.6956256675,-5.0268601812
F,1.4793918076,-0.4274183256,2.099203866
F,1.1599639382,-2.6013769668,3.5689883481
F,2.7731957978,-4.7922813366,3.2289850176
F,5.9618514062,-0.6243659513,1.814378854
F,4.6840232582,1.8468552858,-2.0647021148
H,-1.7229887104,-1.4471507669,-5.1072562845
H,-2.0000880783,-1.6427564041,-7.5611128003
H,-3.9974730486,-0.6584950386,-8.6754639944
H,-5.7110486593,0.528278464,-7.3134212025
H,-5.4250920582,0.7341289031,-4.8616919383
H,-4.1082443932,-2.921544832,-4.142935744
H,-3.9894277897,-4.667305876,-2.1107082718
H,-1.4586245549,-5.258067496,-0.6547755366
H,-1.5797566362,-7.7236230923,-0.45791778
H,-3.4469486638,-8.7865549632,0.8005513791
H,-5.1872677389,-7.3594496795,1.865492731
H,-5.05688526,-4.8929914447,1.6787811911
H,-2.5248148646,-4.3361310611,3.0209062752
H,-2.2861415511,-2.3393490253,4.7886507733
H,-4.7224683368,-0.9559616404,5.1160700204
H,-5.0840261212,-0.848558183,7.5615141887
H,-1.5948429471,1.6427920536,7.9698214987
H,-1.2365448412,1.540654131,5.5223731652
H,-3.5792160463,2.9612288545,4.3481704479
H,-3.6943983571,4.6387960124,2.3942753863
H,-1.5410146194,5.7297216829,0.6694358115
H,-2.0777041545,8.133126472,0.4293793336
H,-5.1061583091,4.7149792874,-1.5249059445
H,-2.7212180741,4.336073699,-2.9869978272
H,-2.9515927111,2.2719189402,-4.6783055261
N,-3.0477718297,1.3878454103,-1.464456912
N,-3.2696609606,-1.5451402342,-1.2404095644
N,-2.8659680728,-1.3056185188,1.672083532
Pd,-2.8887531052,-0.024079964,0.0442719253
S,-2.0272666522,1.5903569097,1.3795506337
H,-4.1314952258,8.8393697996,-0.7880947463
H,-5.6438287691,7.1184033364,-1.7617720818
H,-3.5208241948,0.4482621912,9.0005391026

Cartesian Coordination of 1pd^{+}-PCCp^{-}

–3037.6159064 hartree

N,7.0203817745,20.7295454288,17.9645813455
H,13.1827021898,27.1624470992,12.4266272802
H,11.2950282899,25.9863073286,13.5448089393
C,10.7958747009,20.9951067788,19.7298131215
C,10.4131649573,21.4178051869,21.0059507328
C,11.1691022761,21.0523298665,22.1241569102
C,12.3070296653,20.2551134156,21.9618309472
C,12.6849173107,19.8225153962,20.6879414213
C,11.9350224347,20.1926617715,19.5590790043
H,10.1994709263,21.2752961642,18.8670535566
H,9.5236695115,22.0295926256,21.1231738884
H,10.8725851247,21.3841514336,23.1148153489
H,12.9006863901,19.9678770136,22.8247874105
H,13.5691763479,19.2036709716,20.5654803173
H,11.1419979284,17.5954627815,19.7524311631
C,12.9972693826,22.0950859922,17.6203777278
C,13.3852772248,22.7309595409,16.4804595709
C,13.503771117,21.7338258776,15.4430460711
C,13.7811923884,22.0698130434,14.0819527766
C,13.6144104324,23.485768164,13.6441925575
C,12.396533099,24.1629585479,13.8399574441
C,12.2439248196,25.4789073859,13.39859475
C,13.3033800971,26.1376364067,12.7653652057
C,14.5171955439,25.4714480619,12.5658040541
C,14.6698412113,24.1512662039,12.994543662
C,14.1187124316,21.1334864188,13.1028213089
C,13.992508605,21.1619396828,11.6908372693
C,14.1307367516,19.9235904035,11.077052987
C,8.8687113587,21.2606487226,14.5991761248
H,12.8238132783,22.5328200658,18.5917065102
H,13.5911828034,23.7827560103,16.3499886336
H,11.5638869662,23.6502959506,14.3121408274
H,15.3447297368,25.9781104681,12.0780796995
H,15.6153992441,23.6382450679,12.8444709905
H,13.7000011071,22.0588381501,11.1589688554
H,13.9566634408,19.761575049,10.020587851
N,9.0894084875,22.3891589734,14.4047231884
C,12.3487170047,19.7278310102,18.1955366451
C,12.8471242874,20.6940192714,17.300247233
C,14.3714768574,18.8498715114,11.97105191
C,14.2823858692,17.4664108108,11.7990276009
C,14.3438678434,16.9491966521,10.4016372056
C,15.4414776443,17.2676193413,9.5811755875
C,15.5014470814,16.8034610964,8.2655824843
C,14.4590021927,16.0282874826,7.7468158913
C,13.3577487139,15.7160080398,8.5512403887
C,13.300360782,16.1691796059,9.8704800367
C,14.0468885823,16.5446209269,12.8650619575
C,14.163598384,15.1150089741,12.6964998115
C,13.7309978104,14.5282473004,13.8464418642
C,13.3270519095,15.5872447762,14.7428243253
C,12.728856022,15.3703784661,15.999549844
C,12.4425231774,13.9533245363,16.3936903385
C,11.4303828764,13.2261195695,15.7459393514
C,11.1584734243,11.9076577154,16.1220943687
C,11.8995785645,11.2982906163,17.1395981399
C,12.9108851777,12.0160384645,17.7866223324
C,13.1773885911,13.3381897765,17.4205468191

C,12.3641690934,16.3777413643,16.9179337237
C,11.6959311452,16.1620506615,18.1829758836
C,11.594774883,17.3762968134,18.7970866095
C,12.1966309861,18.352868697,17.9150951394
C,8.9576316215,18.8083357055,13.9946025277
C,9.6215123727,18.9097833777,12.7480349973
C,8.6072496892,19.8906051718,14.8424443544
C,7.9527177585,19.3591465016,15.9844582452
C,7.4404614122,20.1087069322,17.0711894394
C,7.9010397,17.9482612442,15.8433717215
C,7.3285369224,17.0406737541,16.7677434632
C,8.5236671742,17.607450034,14.6139186419
C,8.6864965345,16.2984770726,14.099286439
H,16.2559233181,17.8629392345,9.9834348371
H,16.3612209752,17.0460866493,7.6480748694
H,14.5032019737,15.6715579363,6.7220293377
H,12.5400796424,15.1239871731,8.1511792613
H,12.4367369811,15.9359061357,10.4851950861
H,14.5422557533,14.6276447756,11.8106672462
H,13.6877869493,13.4734364828,14.071569254
H,10.8449166307,13.6986888563,14.9624606684
H,10.3664393287,11.3598446014,15.6199717548
H,11.6891122288,10.2726056147,17.4280050211
H,13.4921685817,11.5496463939,18.5767246966
H,13.9639291452,13.8922849975,17.9248225926
H,11.3412337951,15.2088943717,18.5453998099
N,13.1996234407,20.4924154651,15.9811348598
N,13.5682911561,16.8047814859,14.14052255
N,10.1642466894,18.9935573519,11.7192640695
N,6.8569446232,16.2943913886,17.5295876492
N,8.8258547569,15.2200202998,13.6775034977
N,12.622826548,17.7141910679,16.7828995626
Pd,13.4231358031,18.6081075008,15.1486756729
S,14.727660235,19.5425914938,13.5496929285

Cartesian Coordination of 2pd^{+}

–3375.0021169 hartree

C,9.5641910127,14.3915664442,7.4870557646
C,10.8412576634,13.7374165621,7.30572982
C,10.989869812,12.3730767247,6.9934039633
C,9.7325326009,11.5786396207,6.8076693347
C,9.0098351034,11.6217703654,5.611384086
C,7.8434729275,10.8854298776,5.4239197823
C,7.3699434855,10.0765024579,6.4542166589
C,8.0648927261,10.0110022581,7.6593517316
C,9.2296383753,10.7565346215,7.8202974183
C,12.2037370476,11.685663019,6.8252515969
C,12.3455947203,10.2868813856,6.4702501674
C,13.6768414526,10.0018735198,6.4909065957
C,14.3682134345,11.2221990274,6.8590662678
C,15.7514870635,11.3535055321,7.067838429
C,16.5783826298,10.1128394231,6.9144838492
C,16.6702514457,9.1632952567,7.9362949624
C,17.4320709797,8.0053469196,7.8053176873
C,18.1285628571,7.7730723017,6.6218764567
C,18.0585637177,8.6984445296,5.583176249
C,17.2907677342,9.8488564542,5.740572771
C,16.4362112395,12.5393759763,7.3933133785
C,17.8631137038,12.6144908101,7.6169409823
C,18.1736801731,13.926768151,7.7894708364
F,9.4432686621,12.3898575791,4.5957235527
F,7.1767411175,10.9484751449,4.2623313579
F,6.2498733325,9.3649806055,6.2867001173
F,7.6093887609,9.2351534565,8.6534170678
F,9.8752387654,10.6750432072,8.9974807978
F,16.0130789457,9.3606139102,9.0931822685
F,17.5002259467,7.1173074469,8.8074832086
F,18.8637382969,6.66439454,6.4831971023
F,18.7270304693,8.4757599097,4.4424039464
F,17.2402115134,10.7206678276,4.7174516334
H,8.6037473263,13.8974945553,7.488110162
H,11.5340634542,9.6137038027,6.2349746116
H,14.148297989,9.0540013148,6.2755671397
H,18.536612239,11.7705380031,7.6435076176
H,19.1455778679,14.352903266,7.9870327705
N,13.4462850152,12.2161244592,7.027064276
N,15.8933010822,13.799524071,7.4793273384
Pd,13.8525036218,14.1474905024,7.4972692952
C,15.7363310147,16.8596427054,7.7601668213
C,15.4270536969,18.1565932093,7.2965598214
C,14.0641081029,18.4484493568,7.2751841081
C,13.237222049,17.3947838638,7.7209463933
C,11.8548036678,17.1905419934,7.5917291216
C,11.0112468329,18.3907385897,7.3338966513
C,11.0697454485,19.4941098932,8.2056041987
C,10.2950389621,20.6294984256,7.9623853435
C,9.4655021483,20.6860096681,6.8372634339
C,9.4102018167,19.5995365791,5.9577243052
C,10.1736657245,18.4574270436,6.2046293551
C,11.2463583109,15.9045992591,7.5955020551
C,9.8130865682,15.717074821,7.6584048967
C,16.9454074591,14.6842461504,7.6848604419
C,16.9171734889,16.1065281719,7.6711580189
C,18.1854749102,16.8544885303,7.4464608649
C,19.0104815515,16.5650500537,6.343363844
C,20.1816498758,17.2928701817,6.1268048617
C,20.549572461,18.3124908666,7.0111542012
C,19.7361959131,18.607886711,8.1104214294
C,18.5576448303,17.8907728302,8.3230051675
H,16.181867871,18.8176586368,6.8891393555
H,13.6586815414,19.3579562512,6.849548572
H,11.7059050423,19.4508029869,9.084673679
H,10.3381658517,21.4676049954,8.6513498764
H,8.8675699863,21.5720047817,6.6459252958
H,8.7763951552,19.6418048458,5.0770874838
H,10.1383897455,17.6233128,5.5107126137
H,9.095391171,16.505025857,7.8294317809
H,18.7220324189,15.7850750711,5.6455457089
H,20.8033702504,17.066205654,5.2659302006
H,21.4632713048,18.8747861512,6.8435249062
H,20.019280207,19.3946778398,8.8030813592
H,17.9334024674,18.1174360642,9.1822385645
N,11.8496632752,14.6653550126,7.4160381131
S,14.270352567,16.1683693079,8.4485341028

Cartesian Coordination of 2pd^{+} in CH_2Cl_2

–3374.9451742 hartree

C,4.2441060386,0.1172047994,-0.415095261
C,2.8623920393,-0.2720043434,-0.2453047686
C,2.4377010504,-1.59652076,-0.0290631118

C,3.4999652801,-2.6500483985,0.0551942371
C,4.2488591526,-2.8416408021,1.2214778221
C,5.2346051412,-3.8220529258,1.3145662069
C,5.4920543436,-4.6420509507,0.2151841264
C,4.7635398891,-4.4762142552,-0.9633489396
C,3.7814592879,-3.4894985285,-1.0283648063
C,1.1078801028,-2.0232853787,0.1265583994
C,0.6809170689,-3.3819338243,0.3952864336
C,-0.6800455081,-3.3821184369,0.3952514815
C,-1.1073633679,-2.0235815028,0.1265234414
C,-2.4372937004,-1.5971727052,-0.0291398943
C,-3.4992773523,-2.6509864476,0.0550741407
C,-3.7805034258,-3.4905095436,-1.0284980651
C,-4.7623205204,-4.4774900588,-0.9635226947
C,-5.4908353081,-4.6435266714,0.2149820667
C,-5.2336488957,-3.8234629215,1.3143765861
C,-4.2481637755,-2.8427846736,1.2213287142
C,-2.8623318864,-0.2727694762,-0.2453927665
C,-4.2441437045,0.1160708872,-0.41523258
C,-4.275266883,1.4733648709,-0.4867842326
F,4.0171679949,-2.0671285584,2.2948494647
F,5.9298067877,-3.9803338404,2.4442906377
F,6.4327934996,-5.5819779564,0.2907246323
F,5.010287182,-5.2584299372,-2.017346803
F,3.0969455377,-3.3463656248,-2.1749398369
F,-3.0959844828,-3.3471886075,-2.175046477
F,-5.0088167267,-5.2597691836,-2.0175322024
F,-6.4313237457,-5.5837076609,0.2904837406
F,-5.9288505914,-3.981934859,2.4440741715
F,-4.0167219233,-2.0682138928,2.2947119487
H,5.0810922958,-0.5626113282,-0.474955947
H,1.3382486606,-4.2225739892,0.5622839183
H,-1.3371577128,-4.2229362677,0.5622180526
H,-5.08094615,-0.5639687105,-0.4751245669
H,-5.1384822328,2.1073848671,-0.6220706884
N,0.0001547621,-1.2337631423,-0.0047309768
N,-2.0679932118,0.850451407,-0.2606998956
Pd,-0.0001074626,0.7653367505,-0.3214329454
C,-1.2813717488,3.8280056668,-0.3339449665
C,-0.6977783574,4.9989722801,0.1984554938
C,0.6964189466,4.9991587613,0.1984756682
C,1.2803410144,3.828348043,-0.3339073366
C,2.5905545689,3.3315236531,-0.2631133066
C,3.6717150672,4.3099559124,0.0396917647
C,3.8357357001,5.4505705767,-0.7687270941
C,4.8368514585,6.3803920891,-0.4855289864
C,5.6746478729,6.1947310382,0.6187988109
C,5.5111568789,5.0721372618,1.4366476379
C,4.5207172838,4.1323709043,1.1483807827
C,2.9140197091,1.9492388416,-0.3707174368
C,4.2748683873,1.4745064452,-0.4866575561
C,-2.9145479687,1.9484601477,-0.3708051
C,-2.5914545941,3.3308311128,-0.2631899388
C,-3.6728848482,4.3089749616,0.0395845495
C,-4.5218696403,4.1311645944,1.1482508263
C,-5.5125676604,5.0706670315,1.4364899374
C,-5.6763358137,6.1932164585,0.6186356643
C,-4.8385587934,6.3791001118,-0.485669363
C,-3.8371873098,5.4495454091,-0.7688394107
H,-1.2941632017,5.7741136386,0.6643219232
H,1.2925829561,5.7744596633,0.664359252
H,3.1952524269,5.5918734986,-1.6346475046
H,4.9651578546,7.2460797014,-1.1281256471
H,6.4499141342,6.9214741591,0.8414733554
H,6.151838018,4.9297780012,2.3015519818
H,4.3885028497,3.2702480915,1.7951700534
H,5.1379184134,2.1087564544,-0.6219208265
H,-4.3894427158,3.269077746,1.7950445463
H,-6.153234265,4.928137762,2.3013770547
H,-6.4518018485,6.9197530292,0.8412886119
H,-4.9670784529,7.2447530061,-1.1282701826
H,-3.1967179858,5.5910185884,-1.6347423347
N,2.0677542542,0.8510047558,-0.260635426
S,-0.0003791368,2.8944961848,-1.1018062598

Cartesian Coordination of 2pd^{+}-Cl^{-}

–3835.3790387 hartree

C,-3.9257702081,-2.2597132816,0.1017841117
C,-4.3897700428,-3.0218230609,-0.9744312028
C,-4.6096300847,-2.3968437534,1.3136289461
C,-2.7462236745,-1.3444386796,-0.0366522435
C,-3.0182213485,0.0191448236,-0.2562710724
C,2.9772871055,1.5206061043,-0.6136174701
C,4.2745100368,0.8858358702,-0.7077822643
C,4.0859152511,-0.4542746833,-0.5898703083
C,2.6657914142,-0.671661484,-0.4155592262
C,2.0874709571,-1.9310170365,-0.1716565787
C,3.0180703497,-3.1048181539,-0.0955378893
C,3.6058723876,-3.4989826031,1.1103111185
C,4.4679896514,-4.5899183341,1.1898771476
C,4.761693337,-5.3180932692,0.0397618275
C,4.1919393749,-4.9524955231,-1.1772309729
C,3.331999199,-3.8591804267,-1.2295057086
C,0.7210505224,-2.1988312512,0.0137182704
C,0.1419377189,-3.4995120015,0.2888846444
C,-1.2089884533,-3.3356033757,0.3287882018
C,-1.4755719504,-1.9327159131,0.0757028886
H,0.6969175017,-4.4149560244,0.433030727
H,-1.9566630311,-4.0932166752,0.5129512137
H,5.2071966445,1.4100244203,-0.849562878
H,4.840028403,-1.227112911,-0.6113342337
N,-0.2858935967,-1.2822125747,-0.0875711355
N,2.0090291891,0.5344179417,-0.4671423439
Pd,-0.0548807789,0.6983867136,-0.4593592401
C,-4.3507479057,0.5707951755,-0.3654014194
C,-4.219189118,1.9196980232,-0.471846114
C,-2.8055688591,2.2259912524,-0.4375275931
C,-2.3110514576,3.5589001592,-0.3919499399
C,-3.2522475512,4.6716743365,-0.0799689295
C,-4.0574536645,4.638357679,1.0735035989
C,-4.9138286511,5.7008149385,1.3680004657
C,-4.9841241498,6.8056766367,0.512801022
C,-4.1866249616,6.8485749219,-0.6357627331
C,-3.3197779129,5.793633011,-0.9265119853
C,-0.9555447674,3.891642676,-0.5335453039
C,-0.2173032822,5.0016955824,-0.0687917424
C,1.1659271619,4.8334931339,-0.1208821159
C,1.5793569345,3.5821819212,-0.6261083599
C,2.8209765111,2.9325648973,-0.5662051846
C,4.0206684383,3.7900249694,-0.3460480995

C,4.3216588281,4.8138562798,-1.2634346659
C,5.4380794232,5.629226495,-1.0699589651
C,6.2535403088,5.4446879038,0.0521161239
C,5.9478758599,4.4419208539,0.9782544584
C,4.8406088435,3.6129023684,0.7833814361
H,-5.0058515456,2.6511548101,-0.5779936198
H,-0.6939177094,5.8577821893,0.3924010043
H,1.8677417619,5.5444965902,0.2969794912
H,-5.2671750506,-0.0006123329,-0.3613520615
N,-2.0954914837,1.0348732461,-0.338461649
S,0.169695008,2.7873672401,-1.3153893891
C,-5.4800488452,-3.8798863925,-0.85969832
C,-6.1380314677,-3.9928671359,0.3624550935
C,-5.7015847288,-3.248743143,1.4557625576
Cl,3.7628593092,1.8737077467,4.0819051413
H,-3.9951904587,3.790471448,1.7485388893
H,-5.5212966709,5.667223102,2.2673868559
H,-5.653684279,7.6294072698,0.741709665
H,-4.2391873962,7.7016944922,-1.3055046713
H,-2.7071568361,5.827507571,-1.8226596111
H,3.6920341331,4.9545250895,-2.1374460153
H,5.669850978,6.4057398848,-1.7929652641
H,7.1186678831,6.0829978932,0.2064373881
H,6.5665019148,4.306706749,1.8602886189
H,4.5917896527,2.8597163406,1.5273045305
F,-4.2118219321,-1.6947458564,2.3890014911
F,-6.3333047496,-3.3569982838,2.6337619009
F,-7.1872095934,-4.8140933209,0.4859535779
F,-5.8996974755,-4.5946484767,-1.914359916
F,-3.778283648,-2.9334959421,-2.1696528098
F,2.7970580333,-3.5312941847,-2.4202763404
F,4.4734471425,-5.6534250516,-2.2861845932
F,5.5891227142,-6.3680914824,0.1037649643
F,5.0141727297,-4.9436977284,2.3621319879
F,3.3401617069,-2.8189794039,2.2372348206

Cartesian Coordination of $2pd^{+}$-BF_4^{-}

–3799.6573281 hartree

C,9.0061928811,-0.0368904276,13.8562031931
C,10.2176375493,-1.6357317959,15.8051611803
C,10.1840492825,-0.2493378956,15.9648338877
C,9.6540182816,-2.2254922749,14.6686684199
C,9.0527476423,-1.4225788328,13.6935285854
H,10.6817954554,-2.2537936902,16.5678061471
H,9.685231511,-3.3036110217,14.5425881998
H,8.6234585226,-1.8735934133,12.8039364575
B,12.9422757647,12.9988048937,16.047000709
C,9.4069281086,10.5096607435,14.0619930345
C,8.8928083218,11.382321236,15.0249024307
C,8.8467916541,12.7588491495,14.826339271
C,9.326009783,13.2958170959,13.6348884764
C,9.8456931494,12.4547748719,12.6551696375
C,9.8815942332,11.0824641067,12.8791120525
C,9.5542499625,2.045806437,15.1697027943
C,2.3427226677,5.74064543,14.5892796104
C,7.0388123419,2.0742038679,15.0579929461
C,6.0871180432,3.0036993711,14.7761752461
C,8.3204663604,2.7446373795,15.0537345419
C,6.7664284128,4.2661994631,14.5856676272
C,12.5291019656,4.5561044564,15.3993343315
C,4.165249884,4.8623975709,12.6957263969
C,6.128194578,5.4529395792,14.1768125387
C,4.6570557222,5.3728081198,13.9009771064
C,3.7116089426,5.808392573,14.834482668
C,13.0692908985,5.8460507063,15.2815338011
C,6.7382747407,6.7043874758,13.9879518407
C,12.8448092892,8.3540964876,15.2410265526
C,9.5693178785,0.5658932276,14.9963773168
C,6.0780027207,7.9109336936,13.5286683211
C,10.7935008242,2.6798143519,15.3454250094
C,12.2785792565,7.0239492004,15.1779529696
C,12.1021426028,2.2710944369,15.0076016099
C,13.0485906414,3.2942739455,15.0372837195
C,15.1483551703,6.6019445797,14.068375285
C,9.437021484,9.0276225367,14.2841253652
C,16.7650094393,5.4506016566,16.0392678788
C,2.8020514679,4.7849821549,12.4247959224
C,16.538315429,6.6713234321,13.9607764889
C,17.3496423096,6.100434101,14.9470652037
C,1.8874344246,5.2262883257,13.3778382869
C,10.6562677706,8.4684644763,14.7081402039
C,8.2426347198,8.3286780307,14.0364512281
C,11.854608512,9.2413355632,14.9581611732
C,14.5506067722,5.9515856591,15.163885991
C,7.0031546909,8.9096613439,13.558421426
C,15.3755866237,5.3683782523,16.1436825768
F,10.3850646608,10.294574643,11.9098032518
F,13.1536636193,14.3850543855,15.8892104357
F,4.1180168535,6.3043856864,16.0165855186
F,12.0028248819,12.7716990634,17.0777519472
F,5.0223079253,4.4317964147,11.7523192462
F,10.3093813918,12.970488192,11.5064697402
F,9.2890150321,14.6179659302,13.4322954945
F,8.3464339444,13.5677268623,15.7719053486
F,12.4414118858,12.4571798654,14.833087211
F,8.4207380274,10.8930425253,16.1863792581
F,1.4634326133,6.1636643129,15.5091304705
F,2.3656530601,4.2915634128,11.2564908799
F,0.574567548,5.1558006118,13.1301280527
F,14.1632784101,12.363562721,16.3695474137
H,8.5514049649,0.5825950316,13.08941861
H,6.8923796511,1.0251562386,15.2660437034
H,5.0204619195,2.8485689747,14.7066087471
H,13.8717609829,8.5759324186,15.4884991995
H,5.0443305564,7.983345731,13.2229367039
H,12.3190026349,1.2721580592,14.6500200666
H,14.0714248993,3.1668787358,14.7051001362
H,10.6160140375,0.2041329154,16.8520203246
H,14.5239935967,7.0371344974,13.29433056
H,17.3892880454,5.0114642851,16.8115938404
H,16.9863478328,7.1703477387,13.1068907482
H,18.4306947879,6.1617521163,14.8650349583
H,11.9315877569,10.3200131123,14.9249584464
H,6.8613619479,9.9444144474,13.2821897178
H,14.9252980335,4.8726752435,16.9985742078
N,8.1142418053,4.0952754115,14.7969007348
N,8.0452514681,6.9958518338,14.2598126679
N,10.9238469727,7.1303839618,14.8836475799
Pd,9.4512643152,5.6759143945,14.8880448656
S,10.8908152498,4.3132095961,15.9934442525

Cartesian Coordination of $2pd^{+}$-PF_6^{-}

–4315.7965118 hartree

C,12.411799275,-2.3755618836,18.0407559495
C,12.7096562778,-3.6798058243,17.5903681658
C,14.0700266556,-3.9851742499,17.5746909308
C,14.9064797429,-2.9353597217,18.011476023
C,16.2915447444,-2.7456189746,17.8868225205
C,17.1226946872,-3.960750798,17.6557935092
C,17.050300672,-5.0414614591,18.554348275
C,17.8132593523,-6.1910156603,18.3422713158
C,18.6451789956,-6.2845238881,17.2214344565
C,18.7132634419,-5.2214159462,16.314666765
C,17.9611146412,-4.0652844689,16.5303768778
C,16.9132714718,-1.4666441361,17.8767643677
C,18.3489835481,-1.2946171721,17.9263840605
C,11.2234321548,-0.1889819009,17.9451550559
C,11.2387814443,-1.6111656427,17.9452784779
C,9.9636767094,-2.3515555243,17.7299802892
C,9.1437574057,-2.075462968,16.6200096434
C,7.9660894703,-2.7963117986,16.4146858737
C,7.5868973956,-3.7958769003,17.3169365449
C,8.3957890506,-4.0786287251,18.4228060906
C,9.5805604698,-3.3684041033,18.6242652707
H,11.9491422359,-4.3379106668,17.1888273016
H,14.4670750398,-4.9034026252,17.1599927413
H,16.4112821875,-4.9693417215,19.4294894925
H,17.7591816284,-7.0109121818,19.0521529747
H,19.2347110979,-7.1810240896,17.0542286704
H,19.3484124051,-5.2927071669,15.4368510975
H,18.0068052296,-3.249738609,15.8153533273
H,19.0598695211,-2.0896933516,18.0926598395
H,9.4405955521,-1.3108095531,15.9089366783
H,7.3479934229,-2.5795436088,15.54867244
H,6.6680430861,-4.3523934209,17.1581313697
H,8.1044113394,-4.850015042,19.1292938506
H,10.2016773408,-3.585519635,19.4882323187
N,16.3227973348,-0.2208394137,17.6960407578
S,13.8831211844,-1.6934321733,18.7240698488
C,18.6115625389,0.0270016481,17.7455488937
C,17.3401935717,0.6956001739,17.5752417405
C,17.2030296746,2.0621593346,17.2656654266
C,18.4656536478,2.8508485262,17.0885465073
C,19.1634566208,2.853468924,15.8773263618
C,20.3307924524,3.5901517797,15.6970342648
C,20.8304588556,4.351896422,16.7504172392
C,20.1609879339,4.3702758796,17.9714721295
C,18.9945092896,3.6260419774,18.1247134863
C,15.996224586,2.7602757511,17.0953751558
C,15.8680247297,4.1611434691,16.741249747
C,14.5404862331,4.4611098821,16.7563704969
C,13.8378808621,3.2452449274,17.1210307634
C,12.4532476766,3.1295201392,17.3231844301
C,11.6412218542,4.3809599673,17.175381072
C,11.4991919891,5.2864447173,18.2301244226
C,10.738845336,6.4455345399,18.1120621374
C,10.0979707397,6.7259430504,16.9084447399
C,10.2235992059,5.8480764701,15.8356968635
C,10.9888761444,4.6951997486,15.9801787877
C,11.7541699204,1.950079998,17.6440081602
C,10.3234899851,1.8876903629,17.8475515756
C,10.0003969237,0.5794314882,18.02756916
F,18.7052902148,2.1296191934,14.840326213
F,20.9746494481,3.5707286381,14.5208517887
F,21.9528129629,5.0622555696,16.5903959171
F,20.6430022094,5.0998146495,18.9881870449
F,18.3734888992,3.6609896644,19.3173865887
F,12.0999997982,5.0383116164,19.4097605628
F,10.619186141,7.2907819964,19.1476093754
F,9.3621892716,7.8358419794,16.7850928872
F,9.6113300941,6.1176744905,14.6742903331
F,11.0919783678,3.8658272718,14.9254952385
F,13.544993568,8.7315714139,13.1938656527
F,15.1295978968,7.7728250985,14.6044574163
F,13.1109339747,6.6820453764,14.2157240619
F,13.9732129826,9.675510756,15.2793849951
F,11.9540420759,8.586126692,14.8888111529
F,13.5393309175,7.6256736162,16.2984693495
H,19.578931344,0.5071696303,17.7301009599
H,16.6858708698,4.8271001092,16.5077777835
H,14.0810764532,5.4144818452,16.5369488078
H,9.6547688194,2.7358716627,17.8528357635
H,9.022122649,0.1629109025,18.2136465742
N,14.7482516997,2.2403085372,17.2914959388
N,12.2853533939,0.6862162638,17.745776846
P,13.5411881804,8.1824796297,14.7427621457
Pd,14.3234507846,0.3196692256,17.7751498683

Cartesian Coordination of $2pd^{+}$-$B(C_6F_5)_4^{-}$

–5319.0405135 hartree

C,3.4915317915,-1.761836124,-3.7999785769
C,3.9650156698,-3.6410289861,1.5241421266
C,7.4448479177,0.8178212883,0.7744610256
C,7.7733357227,1.7393962555,-0.2092700607
F,4.3506274093,-2.1036571457,-4.7826728497
F,5.2883707104,-0.893025472,-2.6273915838
F,4.7624858331,-4.7129880492,1.3364464403
F,5.1274013515,-2.5282049038,-0.1530236519
F,8.3543948941,0.4964123505,1.7180841195
F,8.9913586927,2.31050116,-0.2372448381
F,7.106785908,2.9666640362,-2.1245702566
B,3.6099052491,-0.0512122969,-0.1437797119
C,-3.382864024,-0.2286795294,-3.3319488191
C,-3.5537204687,-0.3414807448,-4.8159971265
C,-2.5958425459,-1.0177871177,-5.5897679966
C,-2.7533733004,-1.125591157,-6.9740834572
C,-3.8741287184,-0.5703787312,-7.6000514383
C,-4.8355674292,0.0984169528,-6.8355469902
C,-4.6743770817,0.2171995631,-5.4524405468
C,-3.5017840261,-1.4187927058,-2.5820925137
C,-3.8477249691,-2.7189164861,-3.1149546657
C,-3.7869280915,-3.6071998774,-2.0810821115
C,-3.4041289739,-2.86301321,-0.900517371
C,-3.170286443,-3.4139401868,0.3779951165
C,-3.2484452125,-4.905202165,0.4997485826
C,-2.2753942216,-5.7174360139,-0.1058318045
C,-2.3444618317,-7.1085501284,0.0072580136
C,-3.3919790853,-7.7052008921,0.7163872123
C,-4.3683687178,-6.9036774173,1.3166144949
C,-4.2948360912,-5.5118484588,1.2139151801

C,-2.879739724,-2.6793310682,1.5441639341
C,-2.6153510989,-3.2770243524,2.8332697658
C,-2.4964585601,-2.2621405077,3.7325995934
C,-2.667148801,-1.0207961732,3.0148592572
C,-2.7337957512,0.2452407466,3.6726637135
C,-2.9505274686,0.2807657272,5.1475473667
C,-4.0333834472,-0.3947057882,5.7397010751
C,-4.238799922,-0.3297126401,7.1191258059
C,-3.3625963373,0.4030124132,7.9271076428
C,-2.2826490549,1.0775657162,7.3480223828
C,-2.0815755495,1.0237682717,5.9673735112
C,-2.6914297622,1.4717087638,3.0048372972
C,-3.1856265548,2.7519299483,3.3611995075
C,-3.2480788691,3.6558122434,2.3081118162
C,-2.8059853747,3.1373709759,1.0646745793
C,-2.9629117277,3.6064139406,-0.2419759674
C,-3.283373919,5.0523849353,-0.4141217878
C,-2.4426630247,6.0319625131,0.1454964822
C,-2.7441331315,7.3880671291,0.0051465921
C,-3.8958397162,7.784517232,-0.6826170169
C,-4.7436468747,6.8177239111,-1.2339461171
C,-4.4389776687,5.4613748684,-1.1048463743
C,-2.9201575201,2.7670898051,-1.3971322421
C,-2.859360532,3.294198898,-2.7400709479
C,-2.9742234472,2.2445599401,-3.5994692671
C,-3.1261742231,1.05011377,-2.8001042969
C,2.7716611859,1.33148469,0.2670708087
C,1.9780600864,2.1121167549,-0.5782164126
C,1.3918662425,3.3215452269,-0.2014009147
C,1.5914934847,3.8184985595,1.0781382253
C,2.3892798779,3.0954323246,1.9575062787
C,2.9553710801,1.8982094758,1.5351392593
C,3.1271633178,-0.7196191704,-1.5936133177
C,1.784479036,-1.0749300924,-1.7744708704
C,1.2805294917,-1.721156233,-2.8967814397
C,2.1446405131,-2.0680136548,-3.929079352
C,3.9506727815,-1.112250577,-2.6526851764
C,3.3619648845,-1.3239115208,0.9048686989
C,2.3546856432,-1.4382002623,1.8667192203
C,2.1494203079,-2.5739830623,2.6517117166
C,2.96017268,-3.6871891511,2.4840223217
C,4.1322213008,-2.4862921741,0.7687588998
C,5.1804174248,0.5093685626,-0.1542276267
C,6.1755104295,0.2370282571,0.7886821205
C,6.8151083811,2.0671169814,-1.1620697531
C,5.565405633,1.4614905113,-1.1067791656
F,1.7295658106,1.7420885688,-1.8588013889
F,0.6321747271,4.015286071,-1.0749630679
F,1.0270019806,4.980237065,1.4602471844
F,2.6027652719,3.5609405173,3.2061361355
F,3.7358505765,1.2658226139,2.4473362578
F,0.876227413,-0.7834965874,-0.8081568575
F,-0.0331565043,-2.0166331895,-2.9951471692
F,1.683344767,-2.6956256675,-5.0268601812
F,1.4793918076,-0.4274183256,2.099203866
F,1.1599639382,-2.6013769668,3.5689883481
F,2.7731957978,-4.7922813366,3.2289850176
F,5.9618514062,-0.6243659513,1.814378854
F,4.6840232582,1.8468552858,-2.0647021148
H,-1.7229887104,-1.4471507669,-5.1072562845
H,-2.0000880783,-1.6427564041,-7.5611128003
H,-3.9974730486,-0.6584950386,-8.6754639944
H,-5.7110486593,0.528278464,-7.3134212025
H,-5.4250920582,0.7341289031,-4.8616919383
H,-4.1082443932,-2.921544832,-4.142935744
H,-3.9894277897,-4.667305876,-2.1107082718
H,-1.4586245549,-5.258067496,-0.6547755366
H,-1.5797566362,-7.7236230923,-0.45791778
H,-3.4469486638,-8.7865549632,0.8005513791
H,-5.1872677389,-7.3594496795,1.865492731
H,-5.05688526,-4.8929914447,1.6787811911
H,-2.5248148646,-4.3361310611,3.0209062752
H,-2.2861415511,-2.3393490253,4.7886507733
H,-4.7224683368,-0.9559616404,5.1160700204
H,-5.0840261212,-0.848558183,7.5615141887
H,-1.5948429471,1.6427920536,7.9698214987
H,-1.2365448412,1.540654131,5.5223731652
H,-3.5792160463,2.9612288545,4.3481704479
H,-3.6943983571,4.6387960124,2.3942753863
H,-1.5410146194,5.7297216829,0.6694358115
H,-2.0777041545,8.133126472,0.4293793336
H,-5.1061583091,4.7149792874,-1.5249059445
H,-2.7212180741,4.336073699,-2.9869978272
H,-2.9515927111,2.2719189402,-4.6783055261
N,-3.0477718297,1.3878454103,-1.464456912
N,-3.2696609606,-1.5451402342,-1.2404095644
N,-2.8659680728,-1.3056185188,1.672083532
Pd,-2.8887531052,-0.024079964,0.0442719253
S,-2.0272666522,1.5903569097,1.3795506337
H,-4.1314952258,8.8393697996,-0.7880947463
H,-5.6438287691,7.1184033364,-1.7617720818
H,-3.5208241948,0.4482621912,9.0005391026

Cartesian Coordination of 2pd^{+}-PCCp^{-}

–4029.9303782 hartree

N,-6.1872973592,-2.4032826303,3.2429742334
C,-4.151168479,-0.8183177257,3.3434321632
C,-4.2007015763,0.5998256691,3.3467408406
C,-5.2670094862,-1.6885829992,3.2897206746
C,-5.3746803926,1.3902392983,3.2971549654
N,-6.3427760146,2.038949167,3.2538774694
C,-4.2880276095,-0.8249046278,-1.2644515677
C,-5.422453687,-5.0001270316,-2.1600757825
C,-4.4868939937,-3.9727147947,-2.2925864684
C,-3.500812775,-3.7752138345,-1.3080901295
H,-1.1877082214,-5.1851014324,-1.5788493721
H,-5.1838837976,1.1385505447,-0.9257074935
H,-6.1689943257,-5.1510554551,-2.9340361899
H,-4.5049406132,-3.3334765043,-3.1704295418
C,-3.484603318,-4.6148912372,-0.1788779266
C,-4.4302514954,-5.6329052359,-0.0440062485
C,-5.3974065416,-5.8312900486,-1.0349645818
H,-5.1097577945,-1.441526785,-0.9216782051
H,-2.749497739,-4.4541568125,0.6037140416
H,-4.4149709616,-6.2647866315,0.8387793712
H,-6.1300555877,-6.6257586468,-0.9287976776
C,-5.7000310364,4.6687374052,-2.1770787418
H,-6.453555017,4.7738199287,-2.9518543648
C,-4.7473098527,5.3645787389,-0.0626766964
C,-5.7236959502,5.5036069648,-1.054688866

H,-4.769023741,5.9991673393,0.8180303839
H,-6.5010317491,6.2548142663,-0.9514343192
C,-2.868211537,1.0850679652,3.4079796797
C,-2.7881213574,-1.2098151284,3.402735227
C,-0.5816002083,0.0157350313,3.5142486755
C,-1.9952862104,-0.0334146055,3.4442838209
C,-3.7444087685,4.4023944104,-0.1938022899
C,-2.3060805704,-2.5412740394,3.4118309934
C,-2.4796823992,2.4466940798,3.4227603467
H,-3.0017553419,4.2871154015,0.589666704
N,0.5822039915,0.0561003892,3.5732403871
N,-1.912974666,-3.6391965856,3.4120439378
N,-2.162871227,3.5690017171,3.4274224125
C,-2.6646959154,2.5087627971,-1.4627961698
C,-1.1279099209,-2.9532503912,-1.3399707028
C,-2.5161992198,-2.6666007265,-1.4546687408
C,2.6147146341,1.1790083609,-0.2727095734
C,3.9791216102,-0.5690794258,0.1731709705
C,-1.2951274764,2.8748039602,-1.3489010312
C,3.3703561752,-3.4063501836,-0.2354068222
C,4.3065761238,-3.7330451822,-1.2206114357
C,-0.605158034,-4.3022108774,-1.3639633375
C,2.1713862529,2.4948605195,-0.485101845
C,2.6778428973,-1.0334196547,-0.2679295902
C,5.3762359742,-5.3386833473,0.2155178296
C,3.9403321355,0.7914778364,0.1701863606
C,3.1716575706,3.5871113832,-0.2511597944
C,0.7233690308,-4.2333479218,-1.0851941139
C,-4.3280847604,0.5690775813,-1.2666691953
C,3.4740487151,-4.081483636,0.9846289267
C,-0.8504372694,4.2513882543,-1.3770128705
C,1.0444846456,-2.8382853008,-0.8777645928
C,4.4596707784,-5.0366751754,1.2196065696
C,5.300222182,-4.6853031368,-1.0119230769
C,4.0901840442,3.9584380879,-1.2372576618
C,3.2363098967,4.2745214663,0.9646769016
C,-3.1057096558,1.1847544045,-1.6121235242
C,5.0300161391,4.9647906354,-1.033234326
C,-3.0323197212,-1.3705190364,-1.6081015649
C,5.0682863826,5.6289007117,0.1901999538
C,0.8805927718,2.885705658,-0.8876755641
C,4.1679179296,5.2835456614,1.1949508889
C,0.4799952138,4.2595187485,-1.0988941649
C,2.3103911036,-2.373199601,-0.475175943
C,-3.7114642804,3.5594563504,-1.3202048466
C,-4.7066586328,3.696606276,-2.3058034535
F,4.2584076779,-3.120888333,-2.4179974892
F,4.0776144758,3.3371125294,-2.4308305186
F,4.5331892125,-5.6642409318,2.4022356804
F,2.6069598564,-3.8106934114,1.9744560776
F,6.1808418009,-4.9764675496,-1.9811818108
F,6.3273011833,-6.2554434573,0.4290493462
F,4.2051172537,5.92145947,2.3737358811
F,5.8949955278,5.2976228376,-2.0031600661
F,2.3838802193,3.9627651649,1.9551946034
F,5.9675678239,6.5975029173,0.3991670172
H,4.809971836,-1.2011385407,0.450752146
H,4.7338066079,1.4709643218,0.4450961881
H,1.4243896267,-5.0526797364,-1.0247944224
H,-1.4826311447,5.0988888826,-1.5940529433
H,1.132794103,5.1179522997,-1.0411435687
H,-4.6872327065,3.0544974164,-3.1815243415
N,-0.0826288827,-2.0761627751,-1.0736010687
N,-0.2012862408,2.0598027932,-1.0802032342
N,1.8814130248,0.0504726987,-0.504351115
Pd,-0.0506438727,-0.0055897584,-1.1207512095
S,-2.0294272935,-0.0639864592,-2.2288014772

[S13 (Complete ref. 10)] *Gaussian 16*, Revision C.01, M. J. Frisch, G. W. Trucks, H. B. Schlegel, G. E. Scuseria, M. A. Robb, J. R. Cheeseman, G. Scalmani, V. Barone, G. A. Petersson, H. Nakatsuji, X. Li, M. Caricato, A. V. Marenich, J. Bloino, B. G. Janesko, R. Gomperts, B. Mennucci, H. P. Hratchian, J. V. Ortiz, A. F. Izmaylov, J. L. Sonnenberg, D. Williams-Young, F. Ding, F. Lipparini, F. Egidi, J. Goings, B. Peng, A. Petrone, T. Henderson, D. Ranasinghe, V. G. Zakrzewski, J. Gao, N. Rega, G. Zheng, W. Liang, M. Hada, M. Ehara, K. Toyota, R. Fukuda, J. Hasegawa, M. Ishida, T. Nakajima, Y. Honda, O. Kitao, H. Nakai, T. Vreven, K. Throssell, J. A. Montgomery, Jr., J. E. Peralta, F. Ogliaro, M. J. Bearpark, J. J. Heyd, E. N. Brothers, K. N. Kudin, V. N. Staroverov, T. A. Keith, R. Kobayashi, J. Normand, K. Raghavachari, A. P. Rendell, J. C. Burant, S. S. Iyengar, J. Tomasi, M. Cossi, J. M. Millam, M. Klene, C. Adamo, R. Cammi, J. W. Ochterski, R. L. Martin, K. Morokuma, O. Farkas, J. B. Foresman and D. J. Fox, Gaussian, Inc., Wallingford CT, 2016.

[S14] Z. Chen, C. S. Wannere, C. Corminboeuf, R. Puchta and P. v. R. Schleyer, *Chem. Rev.*, 2005, **105**, 3842–3888.

[S15] R. Herges and D. Geuenich, *J. Phys. Chem. A*, 2001, **105**, 3214–3220.

[S16] M. J. S. Phipps, T. Fox, C. S. Tautermann and C.-K. Skylaris, *Chem. Soc. Rev.*, 2015, **44**, 3177–3211.

[S17] Articles for *GAMESS*: (a) M. W. Schmidt, K. K. Baldridge, J. A. Boatz, S. T. Elbert, M. S. Gordon, J. H. Jensen, S. Koseki, N. Matsunaga, K. A. Nguyen, S. J. Su, T. L. Windus, M. Dupuis and J. A. Montgomery, *J. Comput. Chem.*, 1993, **14**, 1347−1363; (b) M. S. Gordon and M. W. Schmidt, in *Theory and Applications of Computational Chemistry: the first forty years*, eds. C. E. Dykstra, G. Frenking, K. S. Kim and G. E. Scuseria, Elsevier, 2005, pp.1167–1189.

[S18] Report for FMO: K. Kitaura, E. Ikeo, T. Asada, T. Nakano and M. Uebayasi, *Chem. Phys. Lett.*, 1999, **313**, 701–706.

[S19] Report for pair interaction energy decomposition analysis (PIEDA): D. G. Fedorov and K. Kitaura, *J. Comput. Chem.*, 2007, **28**, 222–237.

4. Solution-state properties

Electrochemical analysis. Cyclic voltammograms (CVs) were measured under Ar atmosphere in CH_2Cl_2 solutions containing the sample and $TBAPF_6$ or TBACl (0.1 M) as a supporting electrolyte using an ALS/CH Instruments 619E electrochemical analyzer with a glassy-carbon disk working electrode (3-mm diameter), an $Ag/AgNO_3$ (0.010 M) reference electrode, and a Pt counter electrode.

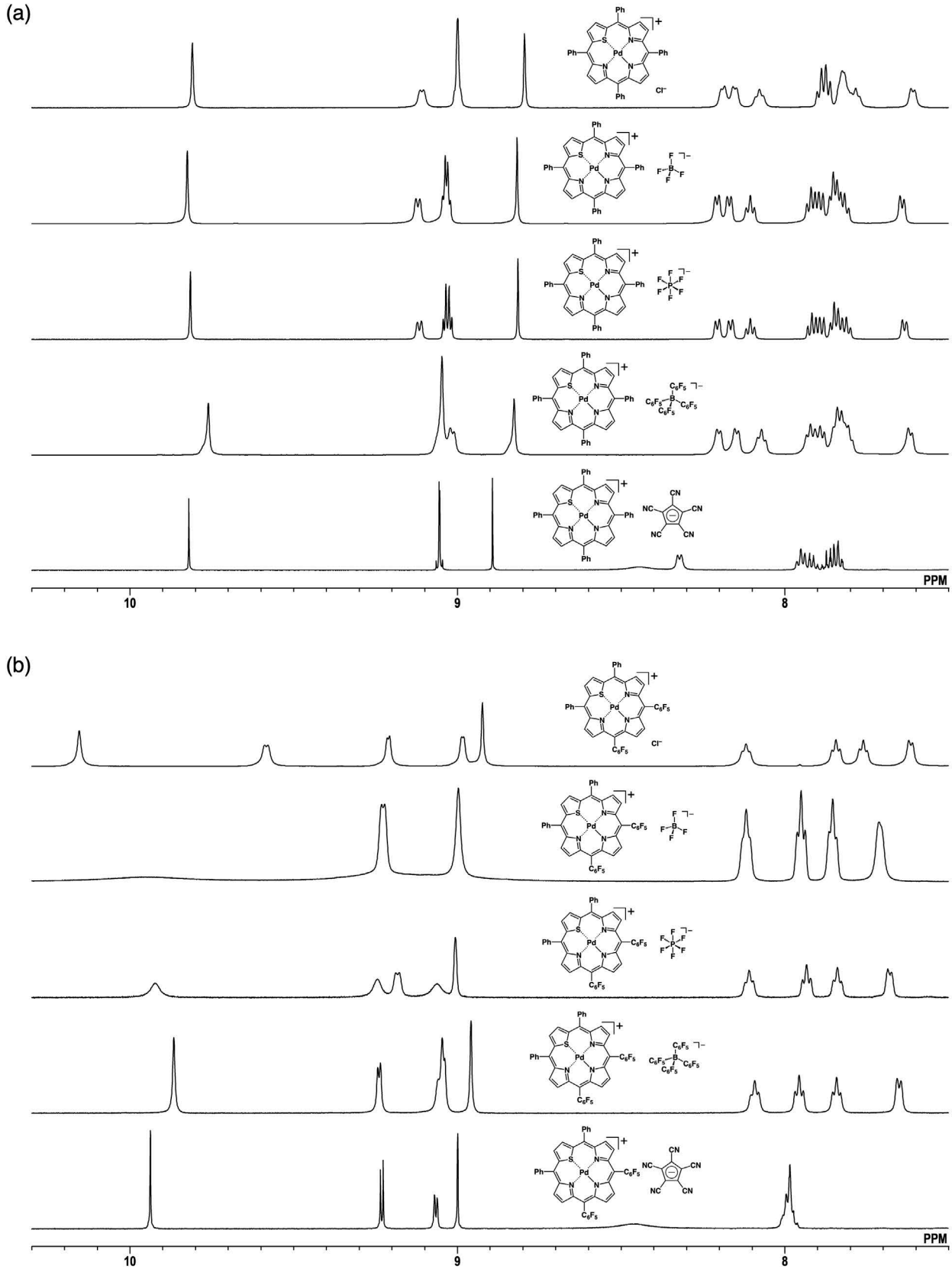

Fig. S68 Summarized ^{1}H NMR spectra of (a) **1pd**$^{+}$-X^{-} and (b) **2pd**$^{+}$-X^{-} (X^{-} = Cl^{-}, BF_4^{-}, PF_6^{-}, $B(C_6F_5)_4^{-}$ (30 mM, –60 °C for each), $PCCp^{-}$ (1 mM, 20 °C)) in $CDCl_3$ (600 MHz) (Fig. S1–9). The differences of signals in these spectra are related with the interactions between the cations and anions in solution (Fig. S69–76).

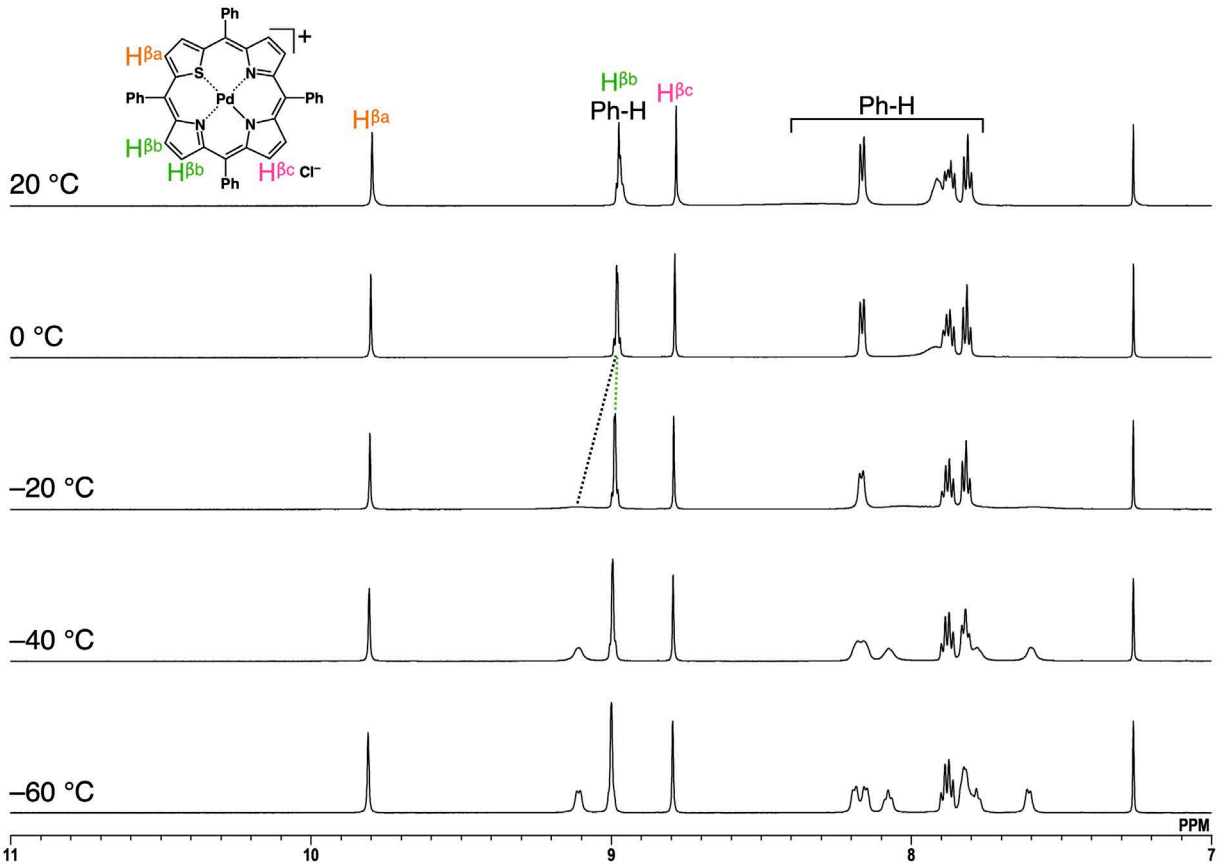

Fig. S69 VT-^{1}H NMR spectra of **1pd**$^+$-Cl$^-$ from 20 to –60 °C in $CDCl_3$ (30 mM). Broad signals were exhibited at higher temperature (Fig. S69–76) due to i) fast chemical exchange between ion-pairing and ion-unpairing states and ii) rotation of phenyl groups.

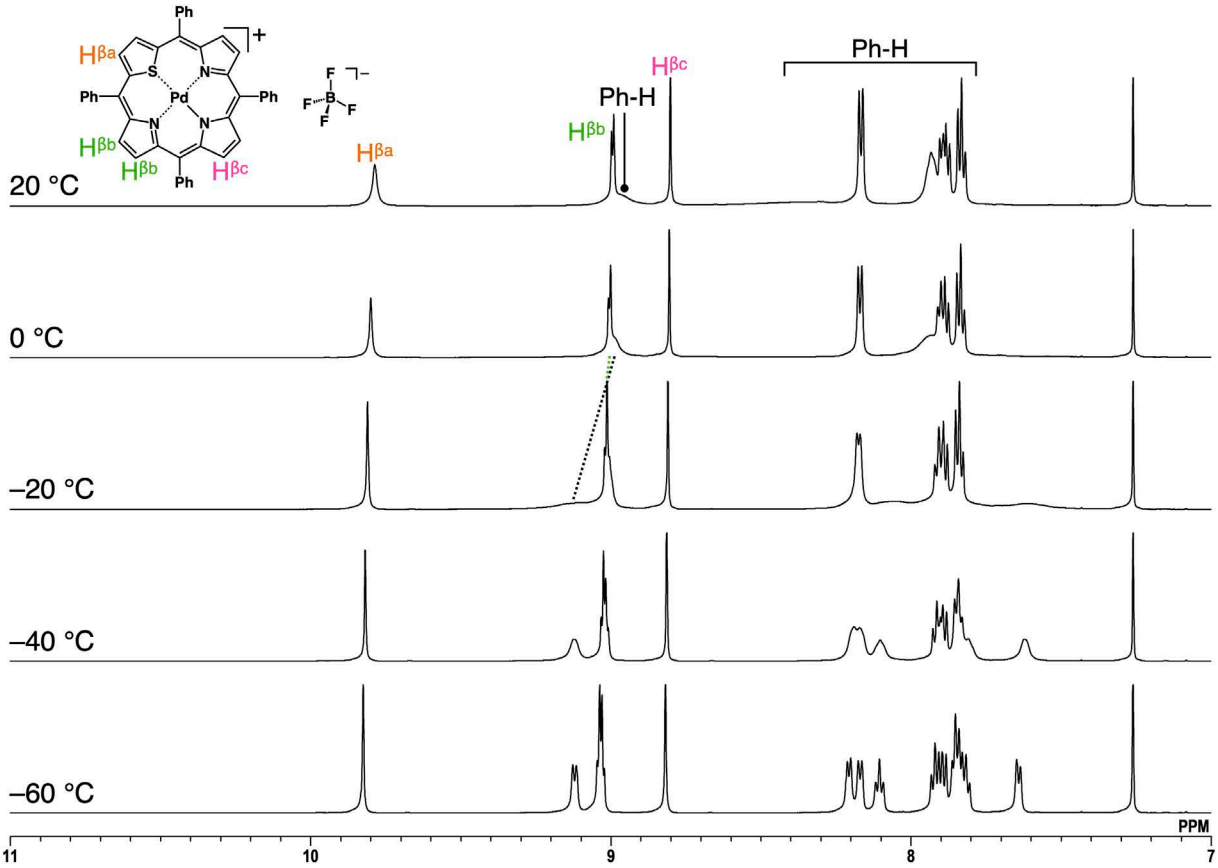

Fig. S70 VT-^{1}H NMR spectra of **1pd**$^{+}$-BF_4^- from 20 to –60 °C in $CDCl_3$ (30 mM).

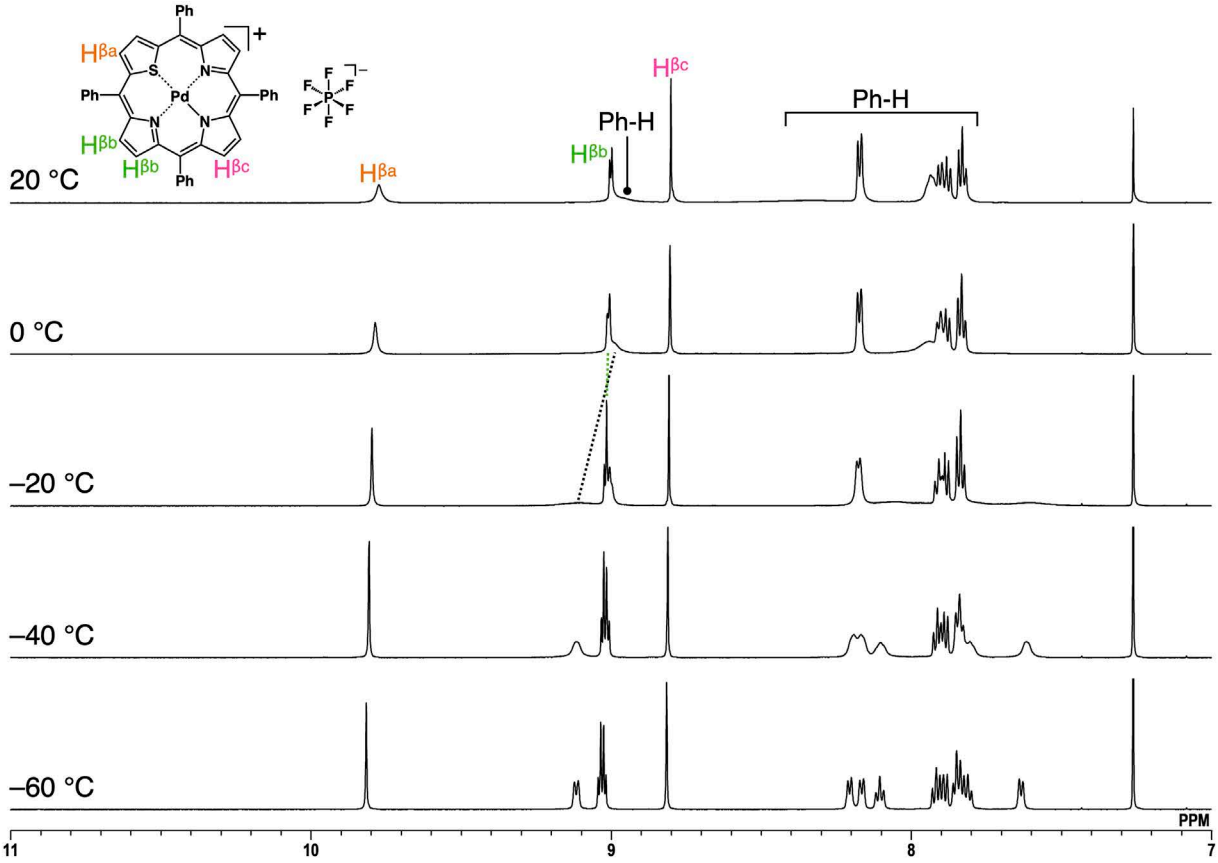

Fig. S71 VT-^{1}H NMR spectra of **1pd**$^{+}$-PF_6^- from 20 to –60 °C in $CDCl_3$ (30 mM).

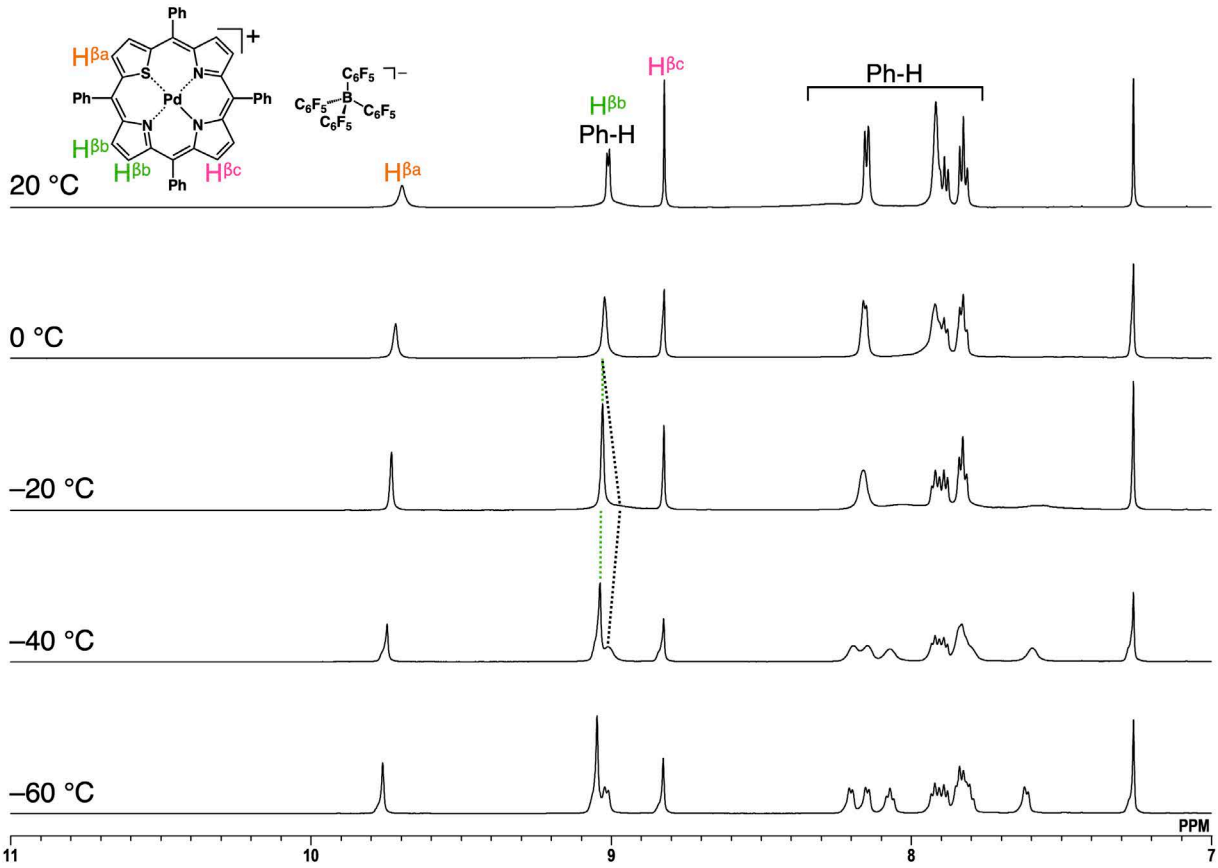

Fig. S72 VT-^{1}H NMR spectra of **1pd**$^{+}$-B(C_6F_5)$_4^-$ from 20 to –60 °C in $CDCl_3$ (30 mM).

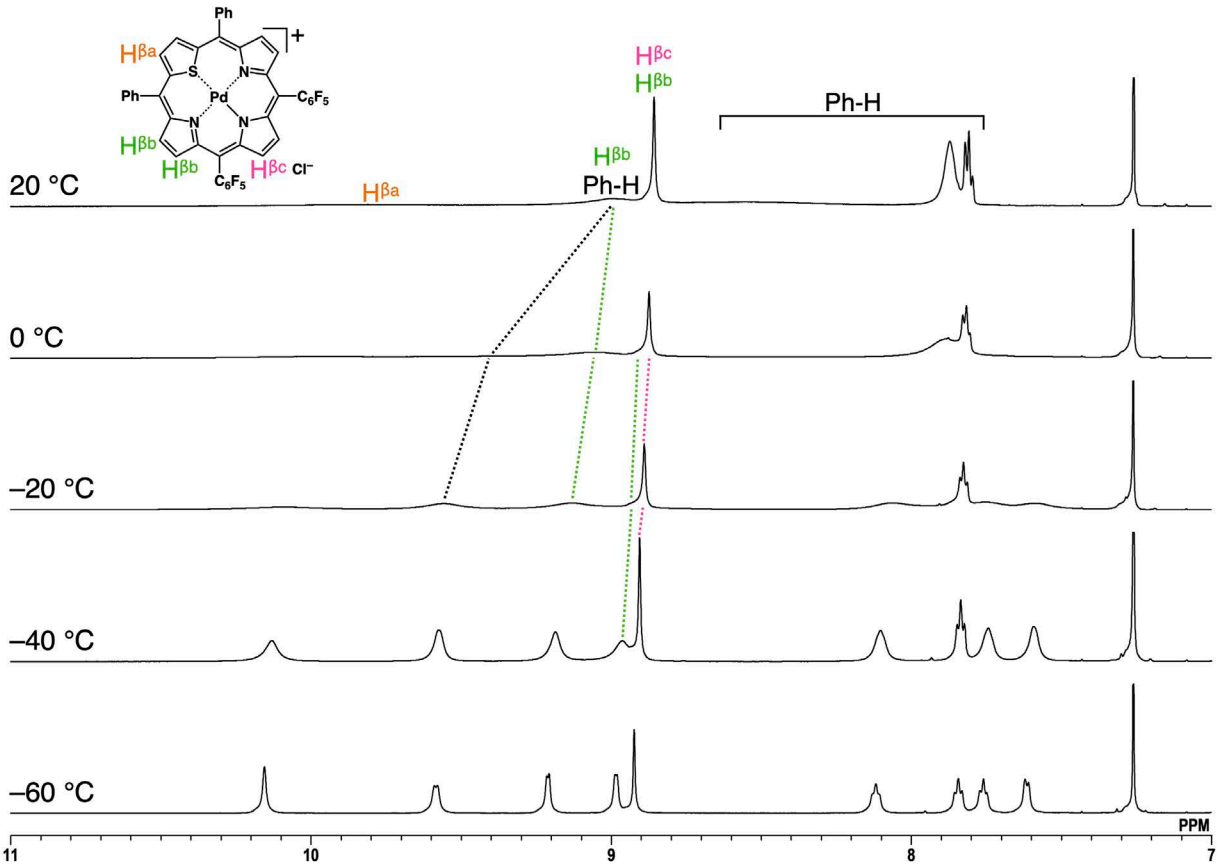

Fig. S73 VT-^{1}H NMR spectra of **2pd**$^{+}$-Cl^{-} from 20 to –60 °C in $CDCl_3$ (30 mM).

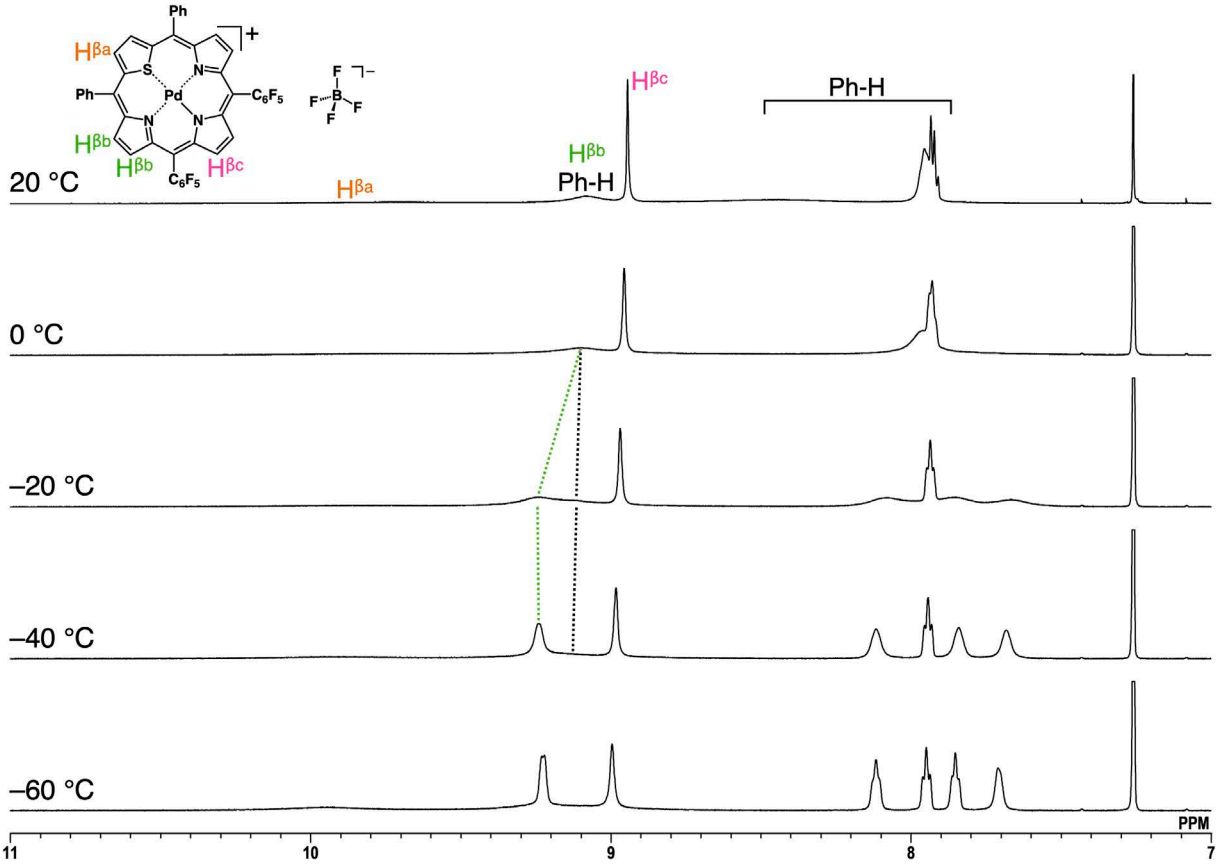

Fig. S74 VT-^{1}H NMR spectra of **2pd**$^{+}$-BF_4^- from 20 to –60 °C in $CDCl_3$ (30 mM).

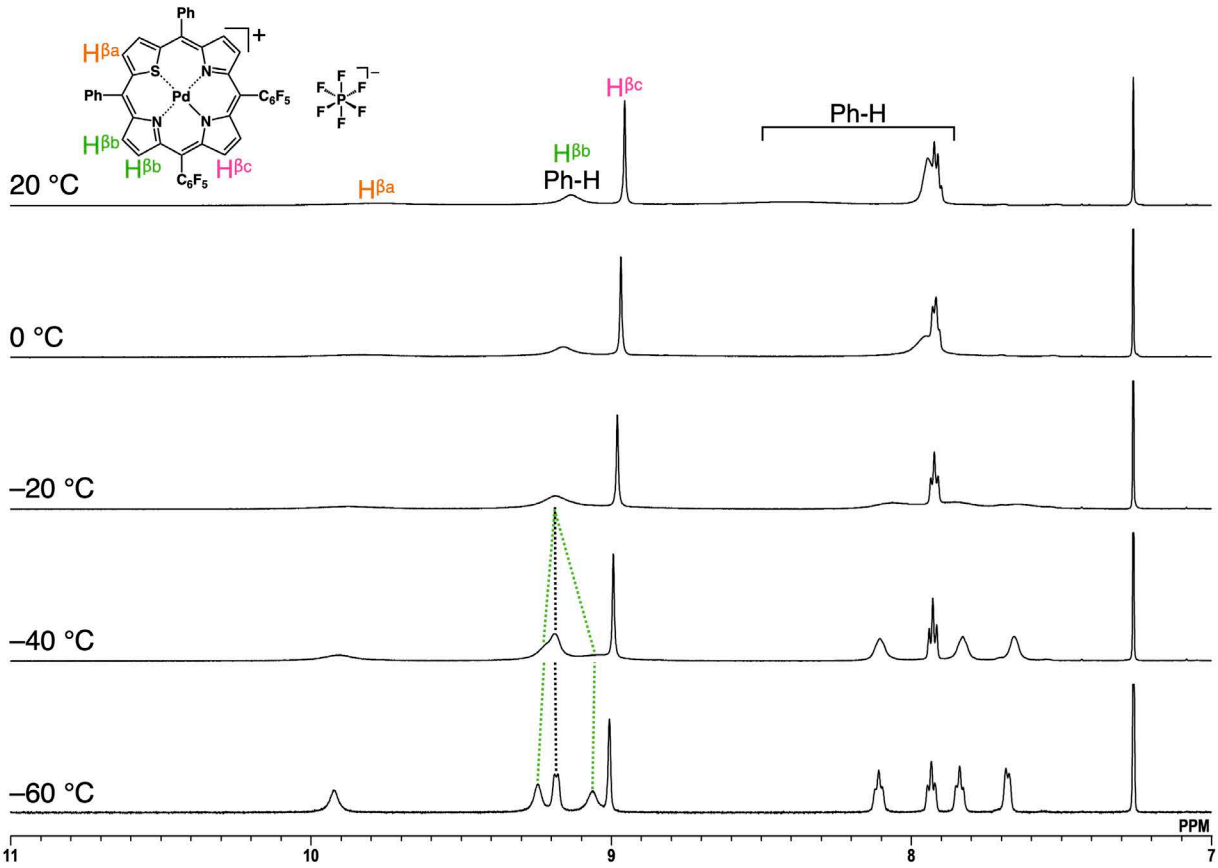

Fig. S75 VT-^{1}H NMR spectra of **2pd**$^{+}$-PF_6^- from 20 to –60 °C in $CDCl_3$ (30 mM).

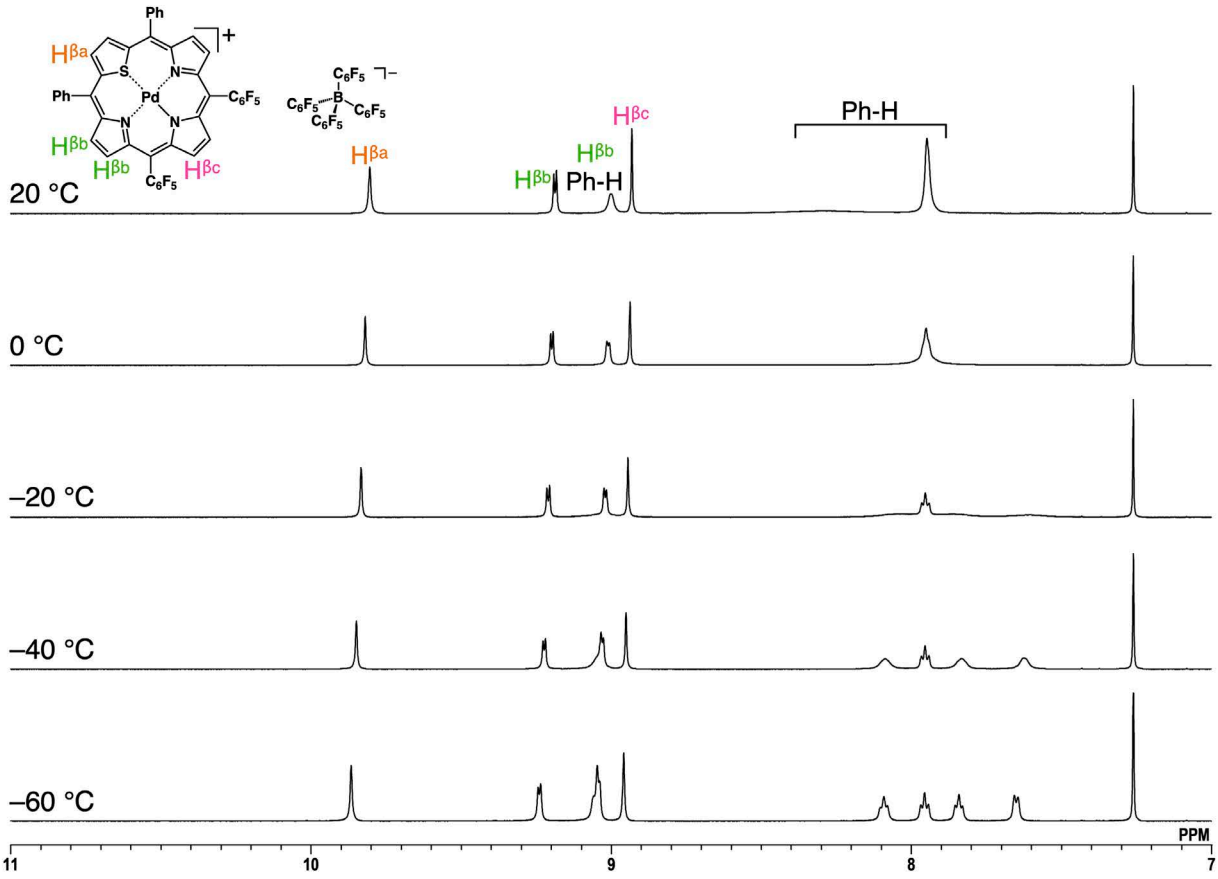

Fig. S76 VT-^{1}H NMR spectra of **2pd**$^{+}$-B(C_6F_5)$_4^-$ from 20 to –60 °C in $CDCl_3$ (30 mM).

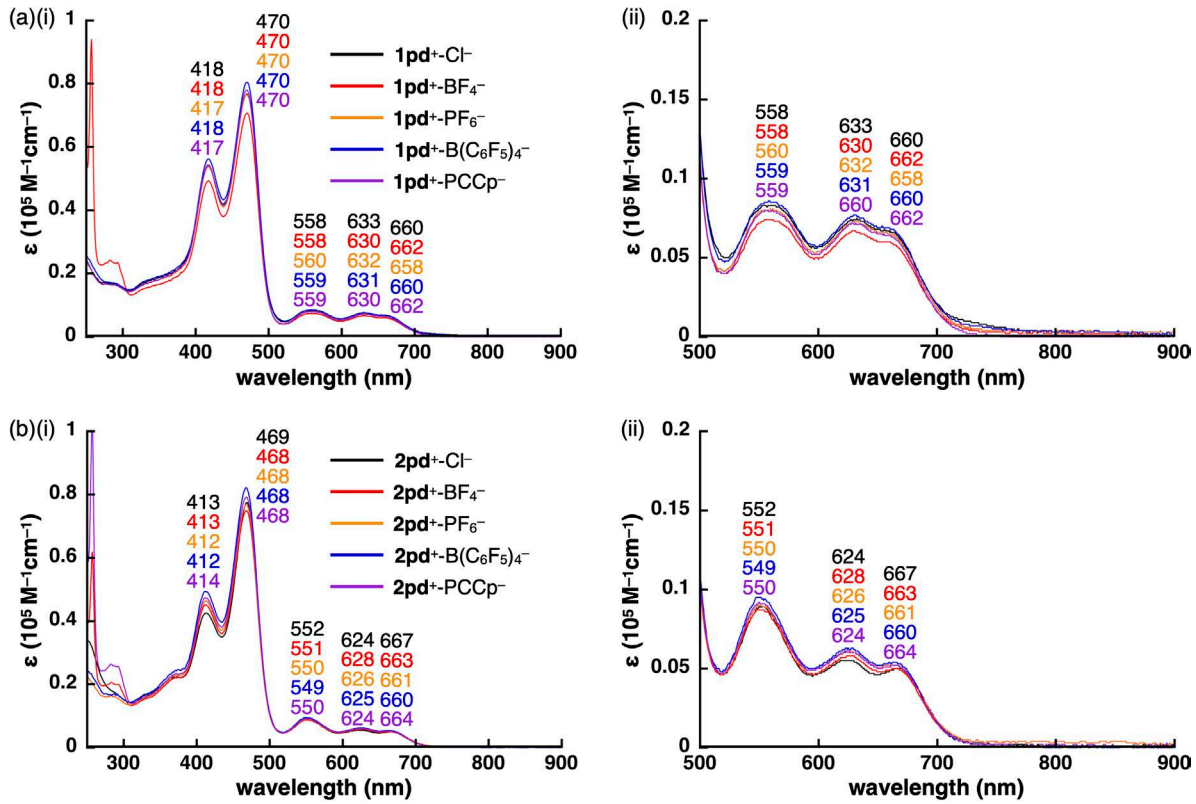

Fig. S77 UV/vis absorption spectra of (a) **1pd**$^{+}$-X^{-} and (b) **2pd**$^{+}$-X^{-} (X^{-} = Cl^{-}, BF_4^-, PF_6^-, B(C_6F_5)$_4^-$, PCCp^{-}) in CH_2Cl_2 (1×10^{-5} M) as (i) wide-range and (ii) enlarged versions. **2pd**$^{+}$-X^{-} show blue-shifted Soret and Q bands due to the C_6F_5 groups.

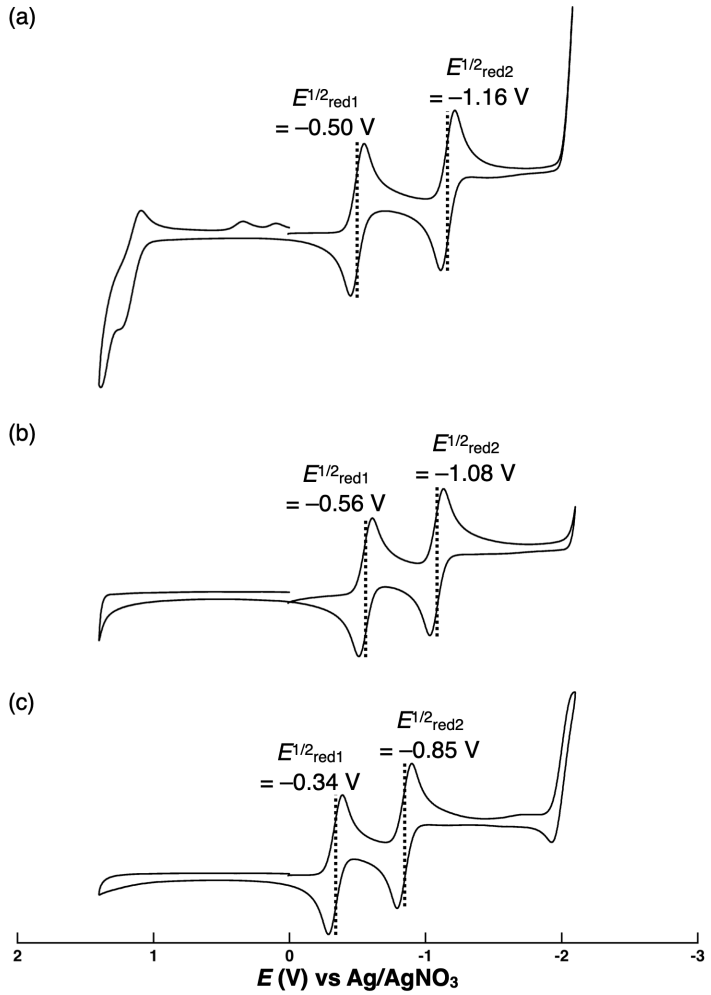

Fig. S78 Cyclic voltammograms (CVs) of (a) **1ni**$^+$-PF_6^-, (b) **1pd**$^+$-PF_6^- and (c) **2pd**$^+$-PF_6^- in CH_2Cl_2 (1.0 mM) containing $TBAPF_6$ (0.1 M) as an electrolyte under Ar atmosphere at a scan rate of 100 mV/s. The small peaks at 0–0.5 V in (a) have not been clearly assigned.

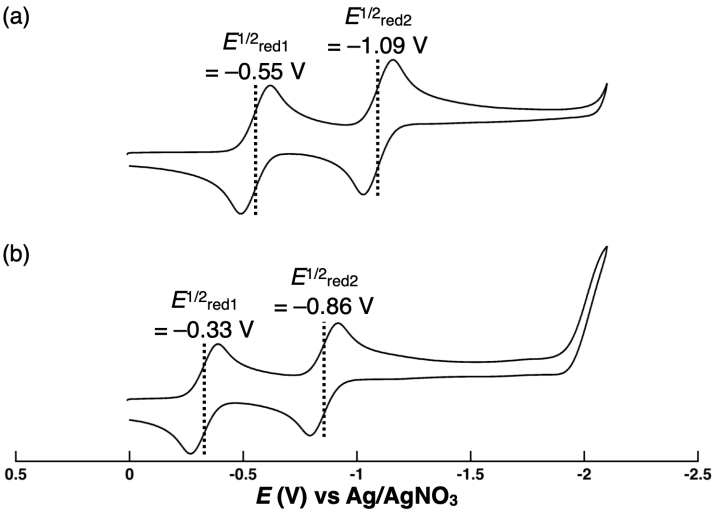

Fig. S79 CVs of (a) **1pd**$^+$-Cl^- and (b) **2pd**$^+$-Cl^- in CH_2Cl_2 (1.0 mM) containing TBACl (0.1 M) as an electrolyte under Ar atmosphere at a scan rate of 100 mV/s. The Cl^- ion pairs showed no significant differences in reduction potentials compared to PF_6^- ion pairs (Fig. S78), suggesting the absence of axial coordination.

5. Electric conductivities of ion pairs

Method for Time-Resolved Microwave Conductivity and Electric Conductivity measurements. All the single/poly-crystals of the compounds were placed onto quartz substrates (for quantitative analysis) and/or columnar quarts rods (8 mmϕ for anisotropic measurements), and overcoated by Cytop®. The overcoated crystals were dried and evaluated in vacuo for 30 min prior to the measurement at 25 °C. Crystals on the quartz plate or rods were inserted into a TE-102 mode microwave cavity at Q-value of 2500 (quartz plates) or of 1300 (quartz rods), and were fixed at the position of electric field maximum. Excitation of the crystals was carried out through the quartz at 355 nm by 3rd harmonic generation from a Spectra-Physics INDI Nd:YAG laser. The power of probing microwave was set at 3 mW. The excitation light intensity (I_0) through the crystal and quartz was monitored by an Ophir VEGA power meter with a PE-25 head. Microwave reflection signals (P_R and $\Delta P_R(t)$) from the cavity were evolved through a Schottky diode, amplified, and monitored by a Tektronics TDS3054 digital oscilloscope. Inside of the cavity was filled with dry N_2, and the measurements were performed at 25 °C. The evolved microwave reflection signal from the diode reflecting the power of microwave was converted into pseudo transient conductivity ($\phi\Sigma\mu$) as,

$$\phi\sum\mu(t)=\frac{\Delta P_R(t)}{eI_0AF_LP_R},$$

where e, A, and F_L are elementary charge, sensitivity factor, and filling factor, respectively. The latter two were estimated by numerical calculation from the overlap of excitation light absorption profile in the sample and electric field strength distribution in the cavity.

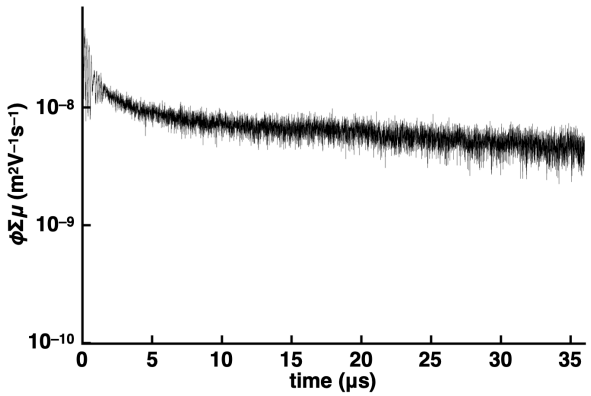

Fig. S80 FP-TRMC photoconductivity transients recorded for the crystalline-state **1pd**$^+$-BF_4^- upon excitation at 355 nm, 1.8×10^{16} photons cm^{-2} pulse^{-1}. A crystal of the compound was fixed onto quartz substrate and overcoated with Cytop® thin film, back-excited with the excitation light pulses. Sensitivity factor was calculated via numerical calculation with the geometry of homogeneous thin film at 22 μm thick; calibrated light transmittance of a polycrystalline film (Transmittance > 0.98).

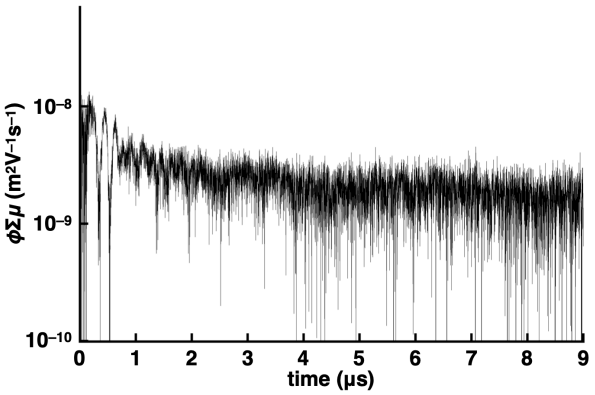

Fig. S81 FP-TRMC photoconductivity transients recorded for the crystalline-state **1pd**$^+$-PF_6^- upon excitation at 355 nm, 9.1×10^{15} photons cm^{-2} pulse^{-1}. A crystal of the compound was fixed onto quartz substrate and overcoated with Cytop® thin film, back-excited with the excitation light pulses. Sensitivity factor was calculated via numerical calculation with the geometry of homogeneous thin film at 18 μm thick; calibrated light transmittance of a polycrystalline film (Transmittance > 0.98).